

**PLASTIC SHRINKAGE CRACKING OF CONCRETE  
WITH MINERAL ADMIXTURES AND ITS  
MITIGATION**

*A THESIS*

*submitted by*

**MOGHUL SIRAJUDDIN**

*for the award of the degree*

*of*

**MASTER OF SCIENCE**



**BUILDING TECHNOLOGY AND CONSTRUCTION MANAGEMENT DIVISION**

**DEPARTMENT OF CIVIL ENGINEERING**

**INDIAN INSTITUTE OF TECHNOLOGY MADRAS**

**MAY 2016**

**In the name of Allah, most benevolent, ever-merciful.**

## THESIS CERTIFICATE

This is to certify that the thesis titled **PLASTIC SHRINKAGE CRACKING OF CONCRETE WITH MINERAL ADMIXTURES AND ITS MITIGATION**, submitted by **Moghul Sirajuddin**, to the Indian Institute of Technology Madras, for the award of the degree of **Master of Science**, is a bonafide record of the research work carried out by him under my supervision. The contents of this thesis, in full or in parts, have not been submitted to any other Institute or University for the award of any degree or diploma.

**Prof. Ravindra Gettu**  
Research Guide  
Professor  
Dept. of Civil Engineering  
IIT-Madras, 600 036

Place: Chennai

Date:

## ACKNOWLEDGEMENTS

I take this opportunity to express my heartfelt gratitude and respect towards my research supervisor **Dr. Ravindra Gettu**, Professor, Department of Civil Engineering for his guidance and encouragement without which this work would have not been fruitful. I am deeply grateful to him, for his whole-hearted support which has played a big role from the commencement to completion of this project, and the knowledge I have acquired beyond this project in the process.

A special thanks to Assistant Professor **Radhakrishna G. Pillai** for his motivation at every stage of my research which rendered to carry out a systematic work.

I express my sincere thanks to Professor **A. Meher Prasad**, Head of the Department, Civil Engineering and Professor **K. Ananthanarayanan**, Head of the Laboratory, Building Technology and Construction Management Division, for extending all the facilities to carry out this work.

I would like to express my gratitude towards the general test committee members Professors **Manu Santhanam** and **Srinivasan Chandrasekaran** for their critical evaluation and suggestions during the meetings. I also thank all the faculty members of BTCM division for their encouragement.

I express my heartfelt thanks to the team of Ultra Thermo Scientific for the fabrication and regular maintenance of the environment chamber. I also acknowledge BASF, Chryso, W.R. Grace, Bekaert, Dolphin, Reliance Industry Limited and Owens Corning for generously donating the materials.

I have a great pleasure to thank my friend Ramya, who helped me with in this thesis. My hearty regards to Sunitha K. Nayar and Sujatha Jose for their training and help in carrying out flexural test. Also I thank all the laboratory staff of construction materials and fellow research scholars for their constant support and timely help in every aspect of the work.

My stay in the institute was made memorable by the friends Bhagya, Venkatesh, Ram, Aysha, Bankesh, Nanda, Madhu, Jamsheer, Vikram, Khaleel, Imran, Mekala, Deva, Vinay, Srikanth, Jai, Giri, Ajay, Sai Kiran, Ananth, Pavan, Bhavesh, Sandeep, Azhar, Abul, Stefie, Anila, Sheetal, Murgan, Sakthivel, Suryabala, Manjari, Ashwetha, Ashwathy, Sreelatha, Megha, Shanka, Staff members of BTCM division, Staff

members of department workshop, Staff members of Krishna hostel and Administration. My sincere thanks to each of them.

Last, and certainly not the least, I wish to thank my beloved family and well-wishers for their ceaseless love, support and motivation, which has helped me through these years.

**-Moghul Sirajuddin**

## ABSTRACT

**KEYWORDS:** Plastic shrinkage cracking, supplementary cementitious materials, fibres, shrinkage reducing admixtures, curing compounds

In recent years, there has been a rapid increase in the use of supplementary cementitious materials for high performance and durable concrete. Supplementary cementitious materials being finer and less reactive than cement, when added to the concrete, increase the water demand and reduce bleeding capacity and early strength gain of concrete. In addition, this also increases the menisci of capillaries on the surface of concrete if the rate of evaporation exceeds the rate of bleeding, thereby, making concrete susceptible to plastic shrinkage in hot and dry environmental conditions. Furthermore, if chemical admixtures are used to compensate the above deficiencies, these may retard hydration and make concrete more vulnerable for plastic shrinkage cracking. Plastic shrinkage cracking remains a serious concern in large surface area/volume applications as water can easily evaporate from large surfaces of concrete, and may impair durability of the concrete structure.

The present study has two objectives: firstly, to investigate the influence of supplementary cementitious materials on plastic shrinkage cracking; secondly, to control plastic shrinkage cracks using fibres and shrinkage reducing admixture. Two supplementary cementitious materials – Fly ash (class F) and Granulated blast furnace slag are analysed; both replace ordinary portland cement at 15% and 30%, by weight. Fibres, shrinkage reducing admixtures and curing compounds are evaluated for their influence on plastic shrinkage cracking. The binder content and water binder ratio are fixed as 340 kg/m<sup>3</sup> and 0.55, respectively, for the entire study.

The restrained plastic shrinkage test according to ASTM C1579-13 is performed subjecting the fresh concrete to a wind velocity of 4 m/s and 35% relative humidity at 42°C for 24 hours. Crack length, width and initiation time, the setting time of concrete and one day compressive strength were assessed to evaluate the influence of supplementary cementitious materials on plastic shrinkage. For the assessment of the efficacy of the fibres, shrinkage reducing admixtures and curing compounds, the crack reduction ratio was determined and used as the parameter.

Results indicate that the addition of supplementary cementitious materials in concrete increases the potential for plastic shrinkage cracking with an increase in their replacement dosage. The incorporation of fly ash and slag at a cement replacement level of 15%, increased the crack area from 100 mm<sup>2</sup> (in the control mix) to 120 mm<sup>2</sup> and 225 mm<sup>2</sup>, respectively. At 30% replacement of fly ash and slag, the crack area further increased to 140 mm<sup>2</sup> and 400 mm<sup>2</sup>, respectively. Further, the use of blended cements with fly ash and slag (i.e., PPC and PSC, respectively) resulted in much higher crack areas. Similarly, the crack length, mean crack width and maximum crack width also increased significantly with the replacement of ordinary portland cement with SCMs and with the use of blended cements.

The incorporation of shrinkage reducing components in concrete had a substantial influence in controlling plastic shrinkage cracking. The use of fibres at the manufacturer-recommended dosages completely eliminated cracking in the control mix and that with 30% fly ash. In case of the concrete with 30% slag, the polypropylene, polyester and steel fibres eliminated cracking at the recommended dosages while the dosages of glass and polyacrylonitrile fibres had to be increased. The incorporation of shrinkage reducing admixtures (SRAs) contributed significantly in controlling plastic shrinkage cracking. At a dosage of 1%, the positive effect of the SRA was reflected in the reduction in crack area by 40-65%. At a SRA dosage of 2%, two products completely eliminated cracking while the other two reduced cracking by about 60%. Furthermore, the application of curing compounds on the surface of concrete was found to be useful in controlling cracking by lowering the rate of evaporation. Among the four curing compounds tested, the acrylic-based products eliminated cracking while the other two curing compounds, which were water- and wax-based, reduced cracking only by 29% and 44%, respectively. Therefore, fibres, shrinkage reducing admixtures and curing compounds have been found to be viable for mitigating plastic shrinkage cracking in concretes with supplementary cementitious materials.

# TABLE OF CONTENTS

Title	Page No.
<b>ACKNOWLEDGEMENTS .....</b>	<b>i</b>
<b>ABSTRACT .....</b>	<b>iii</b>
<b>TABLE OF CONTENTS .....</b>	<b>v</b>
<b>LIST OF TABLES.....</b>	<b>x</b>
<b>LIST OF FIGURES.....</b>	<b>xii</b>
<b>ABBREVIATIONS.....</b>	<b>xv</b>
<b>NOTATIONS.....</b>	<b>xvi</b>
<b>CHAPTER1 INTRODUCTION</b>	
1.1 Introduction.....	1
1.2 Significance of research .....	2
1.3 Objectives .....	2
1.4 Scope of the study .....	2
1.5 Thesis organization .....	3
<b>CHAPTER2 LITERATURE REVIEW</b>	
2.1 Introduction.....	4
2.2 Plastic shrinkage cracking mechanism.....	4
2.2.1 Evaporation.....	4
2.2.2 Plastic settlement.....	6
2.3 Quantitative determination of tensile capillary pressure.....	7
2.4 Test methods used to quantify plastic shrinkage .....	8
2.4.1 Unrestrained plastic shrinkage tests .....	9
2.4.2 Restrained plastic shrinkage tests .....	10
2.5 Influence of low volume fibres on plastic shrinkage cracking.....	13

2.6	Influence of environment conditions on plastic shrinkage .....	15
2.7	Influence of mineral admixture on plastic shrinkage .....	20
2.8	Influence of chemical admixtures on plastic shrinkage .....	22
2.8.1	Influence of shrinkage reducing admixtures .....	22
2.8.2	Influence of superplasticizers .....	23
2.8.3	Influence of retarders .....	24
2.8.4	Influence of accelerators.....	24
2.9	Influence of mix proportions on plastic shrinkage.....	24
2.10	Influence of curing compounds on plastic shrinkage cracking.....	25

### **CHAPTER3 EXPERIMENTAL PROGRAM AND METHODOLOGY**

3.1	Introduction.....	27
3.2	Materials .....	27
3.2.1	Cements .....	27
3.2.2	Supplementary cementitious materials.....	29
3.2.3	Aggregates .....	29
3.2.4	Chemical admixtures.....	30
3.2.4.3	Fibres .....	31
3.2.5	Curing compounds .....	31
3.3	Mix proportion.....	32
3.4	Mixing procedure .....	32
3.5	Assessment of plastic shrinkage cracking potential.....	33
3.5.1	Environmental chamber .....	34
3.5.2	Test configuration .....	34
3.5.3	Crack microscope.....	36
3.6	Test procedure.....	36
3.7	Fresh properties of concrete - experimental methods .....	38
3.8	Experimental methods for hardened properties of concrete.....	38

3.8.1	Compressive strength .....	38
3.8.2	Flexural toughness .....	39
3.9	Summary.....	41

**CHAPTER4 INFLUENCE OF SUPPLEMENTARY  
CEMENTITIOUSMATERIALS ON THE PLASTIC  
SHRINKAGE CRACKING OF CONCRETE**

4.1	Introduction.....	42
4.2	Fresh and hardened properties of concrete .....	43
4.2.1	Workability.....	43
4.2.2	Fresh unit weight.....	43
4.2.3	Final setting times .....	44
4.2.4	Compressive strength .....	45
4.3	Plastic shrinkage results .....	47
4.3.1	Influence of blended cements on plastic shrinkage cracking .....	51
4.3.2	Influence of fly ash on plastic shrinkage cracking.....	53
4.3.3	Influence of slag on plastic shrinkage cracking.....	55
4.3.4	Influence of superplasticizer on plastic shrinkage .....	57
4.4	Evaporation rates.....	60
4.5	Capillary pressure.....	61
4.6	Discussion.....	62
4.7	Summary.....	63

**CHAPTER5 INFLUENCE OF FIBRES ON PLASTIC SHRINKAGE  
CRACKING OF CONCRETE**

5.1	Introduction.....	64
5.2	Assessment of the fibre performance in fresh and hardened concrete.....	64
5.2.1	Workability and fresh unit weight .....	65
5.2.2	Compressive strength .....	65

5.2.3	Flexural response .....	66
5.3	Influence of fibres in mitigating plastic shrinkage cracking in the control mix .....	69
5.3.1	Performance of fibres .....	69
5.3.2	Evaporation rates.....	69
5.4	Influence of fibres in mitigating plastic shrinkage cracking in mixes with 30% replacement of cement by SCMs .....	71
5.4.1	Performance of fibres .....	71
5.4.2	Evaporation rates.....	73
5.5	Influence of fibres in mitigating plastic shrinkage cracking at higher dosages .....	74
5.6	Discussion.....	75
5.7	Summary.....	75

**CHAPTER6 MITIGATION OF PLASTIC SHRINKAGE CRACKING USING SHRINKAGE REDUCING ADMIXTURES**

6.1	Introduction.....	77
6.2	Fresh and Hardened Properties of Concrete .....	77
6.2.1	Workability.....	77
6.2.2	Fresh unit weight.....	78
6.2.3	Compressive Strength .....	78
6.3	Evaporation rates.....	80
6.4	Influence of shrinkage reducing admixtures on plastic shrinkage cracking..	81
6.5	Discussion.....	82
6.6	Summary.....	83

**CHAPTER7 MITIGATION OF PLASTIC SHRINKAGE CRACKING USING CURING COMPOUNDS**

7.1	Introduction.....	84
7.2	Experimental procedure.....	85

7.3	Evaporation rates.....	86
7.4	Influence of curing compounds on plastic shrinkage cracking.....	87
7.5	Discussion.....	87
7.6	Summary.....	89

**CHAPTER8 CONCLUSIONS AND SCOPE FOR FURTHER STUDIES**

8.1	Introduction.....	90
8.2	General conclusions .....	90
8.3	Specific conclusions .....	90
8.3.1	Workability.....	90
8.3.2	Fresh unit weight.....	91
8.3.3	Compressive strength .....	91
8.3.4	Flexural response .....	92
8.3.5	Influence of SCMs on plastic shrinkage cracking .....	92
8.3.6	Mitigation of cracking using shrinkage reducing components.....	93
8.4	Scope for further studies.....	94

**REFERENCES.....96**

**APPENDIX A DESIGN AND PERFORMANCE ASSESSMENT OF THE ENVIRONMENTAL CHAMBER**

A.1.	Introduction.....	<del>105</del> <sup>105</sup>
A.2.	First design of the climatic chamber .....	<del>105</del> <sup>105</sup>
A.3.	Problems encountered with the first design.....	<del>107</del> <sup>107</sup>
A.4.	Modified design of the chamber .....	<del>108</del> <sup>108</sup>
A.5.	Performance evaluation of the chamber .....	<del>110</del> <sup>110</sup>

## LIST OF TABLES

Title	Page No.
Table 2.1: Unrestrained plastic shrinkage specimens .....	9
Table 2.2: Restrained plastic shrinkage tests with ring shaped specimens .....	10
Table 2.3: Restrained plastic shrinkage slab tests on specimens .....	11
Table 2.4: Restrained plastic shrinkage test using prism specimens .....	12
Table 2.5: Fibres and their dosage used .....	15
Table 3.1: Physical properties of cements used in the study .....	28
Table 3.2: Chemical composition of cements used in the study .....	28
Table 3.3: Properties of fly ash and slag .....	29
Table 3.4: Properties of the aggregates used .....	29
Table 3.5: Properties of fibres specified by the suppliers.....	31
Table 3.6: Dosages of fibres .....	31
Table 3.7: Mix proportion of concrete mixes .....	32
Table 4.1: Fresh properties of concrete .....	43
Table 4.2: Final setting times: average and standard deviation .....	45
Table 4.3: Compressive strengths at various ages .....	47
Table 4.4: Summary of test results.....	51
Table 4.5: Maximum capillary for various concretes.....	61
Table 5.1: Experimental matrix for investigation with control mix.....	64
Table 5.2: Compressive strengths of fibre reinforced concrete at various ages .....	66
Table 5.3: Toughness parameters of various fibres .....	69
Table 5.4: Experimental matrix for investigation with SCM mixes .....	71
Table 5.5: Summary of the results .....	72
Table 5.6: Experimental matrix for investigation at higher dosage of fibres .....	74
Table 6.1: Superplasticizer dosage and unit weight.....	78

Table 6.2: Compressive strength results.....	79
Table 6.3: Summary of test results.....	82
Table 7.1: Summary of test results.....	87

## LIST OF FIGURES

Title	Page no.
Figure 2.1: Schematic diagrams of plastic shrinkage: (a) Concrete when placed, (b) Bleeding of water to the surface, (c) Surface evaporation and menisci between solid particles, and (d) Discontinuous water and plastic shrinkage.....	5
Figure 2.2: Plastic settlement cracking due to internal restraint.....	7
Figure 2.3: Plastic cracking due to variation in depth of concrete.....	7
Figure 2.4: Principal radii of liquid surface (Combrinck 2012).....	8
Figure 2.5: Menzel's Nomograph (Menzel 1954).....	18
Figure 2.6: Nomograph (ACI 305.1-06).....	19
Figure 2.7: Surface tension and SRA concentration (Rongbing and Jain 2005).....	22
Figure 3.1: Particle size analysis of cements and mineral admixtures.....	28
Figure 3.2: Sieve analysis of aggregates.....	30
Figure 3.4: Plastic shrinkage mould.....	35
Figure 3.5: (a) Crack microscope and (b) Graticule.....	36
Figure 3.6: Measurement of crack width and length.....	37
Figure 3.7: Closer view of marked thread.....	37
Figure 3.8: Compression test setup (a) testing machine and (b) Close-up view.....	39
Figure 3.9: Third point loading test configuration.....	40
Figure 4.1: Paste content in various mixes.....	44
Figure 4.2: Final setting time of concretes.....	44
Figure 4.3: Compressive strength development for three different cements.....	46
Figure 4.4: Compressive strength development for fly ash concretes.....	46
Figure 4.5: Compressive strength development for slag concretes.....	47
Figure 4.6: Plastic shrinkage cracking in CM.....	48
Figure 4.7: Plastic shrinkage cracking in PPC.....	48

Figure 4.8: Plastic shrinkage cracking in PSC .....	49
Figure 4.9: Plastic shrinkage cracking in FA15 .....	49
Figure 4.10: Plastic shrinkage cracking in FA30 .....	50
Figure 4.11: Plastic shrinkage cracking in SG15 .....	50
Figure 4.12: Plastic shrinkage cracking in SG30 .....	51
Figure 4.13: Crack area of concretes with different cements .....	52
Figure 4.14: Crack length of concretes with different cements .....	52
Figure 4.15: Crack width of concretes with three different cements .....	53
Figure 4.16: Crack initiation time of concretes with three different cements .....	53
Figure 4.17: Crack area of concretes at different replacement levels of fly ash.....	54
Figure 4.18: Crack length of concretes at different replacement levels of fly ash .....	54
Figure 4.19: Crack width of concretes at different replacement levels of fly ash .....	55
Figure 4.20: Crack initiation of concretes at different replacement levels of fly ash ..	55
Figure 4.21: Crack area of concretes at different replacement levels of slag.....	56
Figure 4.22: Crack length of concretes at different replacement levels of slag.....	56
Figure 4.23: Crack width of concretes at different replacement levels of slag .....	57
Figure 4.24: Crack initiation of concretes at different replacement levels of slag .....	57
Figure 4.25: Crack area of concretes with and without superplasticizer.....	58
Figure 4.26: Crack length of concretes with and without superplasticizer .....	58
Figure 4.27: Maximum crack width of concretes with and without superplasticizer ..	59
Figure 4.28: Mean crack width of concretes with and without superplasticizer .....	59
Figure 4.29: Crack initiation time of concretes with and without superplasticizer .....	60
Figure 4.30: Cumulative rate of evaporation of various concretes .....	60
Figure 5.1: Compressive strength of various fibres with control mix.....	66
Figure 5.2: Typical load deflection curves of various fibre reinforced concretes .....	67
Figure 5.3: Typical load deflection curves up to 300 micron deflection.....	67
Figure 5.4: Cumulative rate of evaporation of various fibres with control mix .....	70

Figure 5.5: Cumulative rate of evaporation of different concretes .....	70
Figure 5.6: Plastic shrinkage crack in SG30-PAN.....	72
Figure 5.7: Plastic shrinkage crack in SG30-GLS .....	73
Figure 5.8: Cumulative rate of evaporation of concretes with and without fibres.....	73
Figure 5.9: Cumulative rate of evaporation of concrete with different fibre dosages .	74
Figure 6.1: Compressive strengths of concrete with SRAs .....	79
Figure 6.2: Evaporation rates of SG30 with various SRAs .....	80
Figure 6.3: Evaporation rates of SG30 with various SRAs .....	81
Figure 7.1: Cumulative rate of evaporation of SG30 with various curing compounds	86
Figure 7.2: Plastic shrinkage test with curing compounds: (a) MR, (b) AR, (c) WA and (d) WX .....	88

## ABBREVIATIONS

SCM	Supplementary Cementitious Material
GGBS	Ground Granulated Blast Furnace Slag
SRA	Shrinkage Reducing Admixture
NRMCA	National Ready Mix Concrete Association
OPC	Ordinary Portland Cement
PPC	Portland Pozzolana Cement
PSC	Portland Slag Cement
IS	Indian Standard
ACI	American Concrete Institute
ASTM	American Society for Testing Materials
LVDTs	Linear Variable Displacement Transducers
JSCE	Japan Society of Civil Engineers
SMF	Sulphonated Melamine Formaldehyde
SNF	Sulphonated Naphthalene Formaldehyde
PCE	Polycarboxylate Ether

## NOTATIONS

$P_c$	Capillary Pressure
$P_{max}$	Maximum Capillary Pressure
$f_{ct}$	Flexural Strength
$f_{e,n}$	Equivalent Flexural Strength
$P_{e,n}$	Average Load
$R_{e,n}$	Equivalent Flexural Strength Ratio

# CHAPTER 1

## INTRODUCTION

### 1.1 Introduction

Supplementary cementitious materials (SCMs) are being extensively used in concrete either as a replacement for portland cement or in blended cements. The use of materials, such as fly ash and ground granulated blast furnace slag (GGBS), in concrete is promoted for producing better performance, as well as for environmental concerns (i.e., reduction of carbon footprint of cement and better exploitation of the clinker). Incorporation of these materials into concrete usually modifies its properties in both fresh and hardened states. Generally, in the fresh state, SCMs retard the setting of concrete, and reduce bleeding and early-age strength (Johari et al. 2011). When concrete is used in structures with extensive surface areas, such as pavements, slabs, bridge decks, tunnel linings, etc., there is a serious concern for plastic shrinkage cracking, especially in hot and dry conditions (Dias 2003). Such premature surface cracks may accelerate the ingress of harmful agents, and impair the durability, serviceability and aesthetics of the structures. Consequently, controlling this premature cracking at a minimum cost is crucial for developing longer-lasting structures.

The incorporation of short synthetic fibres in concrete has been a highly effective technique for minimizing or preventing plastic shrinkage cracking (Balaguru 1994; Berke & Dallaire 1994; Soroushian & Ravanbakhsh 1999; Wang et al. 2002; Banthia & Gupta 2006). Some of the commonly used synthetic fibres are nylon, polyester, glass, polypropylene, cellulose, etc., at volume fractions below 0.2% (Naaman et al. 2005; Sivakumar & Santhanam 2007; Pelisser et al. 2010). However, the mechanism involved in low volume fibre reinforced concrete in controlling plastic shrinkage cracking is not clearly understood. Another viable solution for tackling plastic shrinkage cracking is by reducing the surface tension of the water through the incorporation of a shrinkage reducing admixture (SRA). Extensive studies have been conducted on the effects of using SRAs on hardened concrete (e.g., Folliard & Berke 1997; Roncero et al. 2003; Gettu & Roncero 2005) while studies on its influence on plastic shrinkage are limited (Lura et al. 2007; Mora et al. 2009; Saliba et al. 2011;

Leemann et al. 2014). Furthermore, curing compounds are used especially in hot and dry climatic conditions to keep concrete saturated and to assist hydration. These compounds, when applied to the fresh exposed surfaces, form a thin protective membrane and inhibit the loss of mix water through evaporation. This reduction in the evaporation of water was found to contribute in controlling plastic shrinkage cracking.

## **1.2 Significance of research**

Supplementary cementitious materials are advantageous for improving the performance and durability of concrete, as well as for decreasing the clinker consumption. However, plastic shrinkage cracking is often an undesired consequence of SCM usage. Since data on the influence of SCMs and blended cements on plastic shrinkage cracking is meagre, this study aims at assessing the influence of fly ash, slag, portland pozzolana cement and portland slag cement. Furthermore, the efficiency of fibres, shrinkage reducing admixtures and curing compounds are also evaluated in order to provide solutions for mitigating plastic shrinkage cracking.

## **1.3 Objectives**

The main objectives of this study are the following:

- Study of the influence of supplementary replacement materials (fly ash and slag), used to replace cement, on plastic shrinkage cracking
- Evaluation of the effect of fibres, shrinkage reducing admixtures and curing compounds in reducing plastic shrinkage cracking.

## **1.4 Scope of the study**

- Normal strength M30 concrete with water-to-binder ratio of 0.55 and binder content of 340 kg/m<sup>3</sup> was selected as the reference for the study.
- Four types of synthetic fibres (polyacrylonitrile, polypropylene, glass and polyester) and hooked-ended steel fibres were investigated for their efficiency in mitigating plastic shrinkage cracking.
- Four shrinkage reducing admixtures and curing compounds were also assessed for their efficacy in controlling plastic shrinkage cracking.

## 1.5 Thesis organization

This thesis is organized into eight chapters as follows:

**Chapter 1** gives an overall introduction to the research, discusses the significance of the research, objectives and scope of research, and also outlines the organization of the thesis.

In **Chapter 2**, a comprehensive literature review is carried out regarding the mechanism of plastic shrinkage, and different test methods adopted to quantify plastic shrinkage and the factors affecting plastic shrinkage are discussed. It also includes a summary of the review.

**Chapter** presents the details of the materials used, concrete mix proportions, mixing procedure and experimental program used for the study.

**Chapter 4** focuses on the effect of the supplementary cementitious materials and blended cement on plastic shrinkage cracking of concrete.

**Chapter 5** presents the influence of different types of fibres in mitigating plastic shrinkage cracking.

In **Chapters 6** and **7**, commercially available shrinkage reducing admixtures and curing compounds are evaluated for their efficiency in controlling plastic shrinkage cracking, respectively.

**Chapter 8** summarizes the key findings of the entire study and also gives recommendations for further studies.

Details of the environmental chamber design and its performance are given in Appendix A.

## CHAPTER 2

### LITERATURE REVIEW

#### 2.1 Introduction

In this chapter, a comprehensive review of previous research studies conducted on plastic shrinkage is presented. Firstly, the mechanisms that lead to plastic shrinkage cracking are reviewed. Secondly, in-depth analysis of the different test methods used by several authors to quantify plastic shrinkage is summarized. Finally, several factors that can influence and contribute to plastic shrinkage are presented.

#### 2.2 Plastic shrinkage cracking mechanism

The mechanisms that contribute to plastic shrinkage are evaporation and plastic settlement. Capillary forces resulting from the rapid evaporation of water from the surface of concrete are widely accepted to be the prime cause for plastic shrinkage cracking. Additionally, plastic settlement is also recognised to be a driving force for plastic shrinkage cracks. This section provides an insight on how evaporation of water from the surface and plastic settlement can lead to cracking of concrete in plastic state.

##### 2.2.1 Evaporation

After concrete is placed in the form, it is compacted to remove entrapped air. As a consequence, aggregates could move down and water bleeds to the surface forming a film on the surface. Even if it is not vibrated (i.e., in self compacting concrete), concrete undergoes some settlement due to gravity and bleed water rises (Wittmann 1976). The rate and quantity of bleed water that rises to the surface depends on mix proportions, concrete depth and compaction effort (Almusallam et al. 1998). At this stage, spaces between the particles of concrete are filled with water as shown in Figure 2.1(b). The rate of evaporation from the surface of concrete will be equal to evaporation rate of water in the same environmental condition.

In hot and arid weather conditions, the water at the surface of the concrete evaporates and is compensated by bleed water rising to the surface. When the rate of evaporation exceeds the bleeding rate, all the bleed water at the surface evaporates as

shown in Figure 2.1(c). The inability of the bleed water to replace the evaporated water is the principal cause for plastic shrinkage (Lerch 1957). Disappearance of sheen at concrete surface indicates that rate of evaporation has exceeded rate of bleeding. Duration and rate of bleeding, temperature, wind velocity and relative humidity influence the time required to attain this condition (Soroushian & Ravanbakhsh 1999).

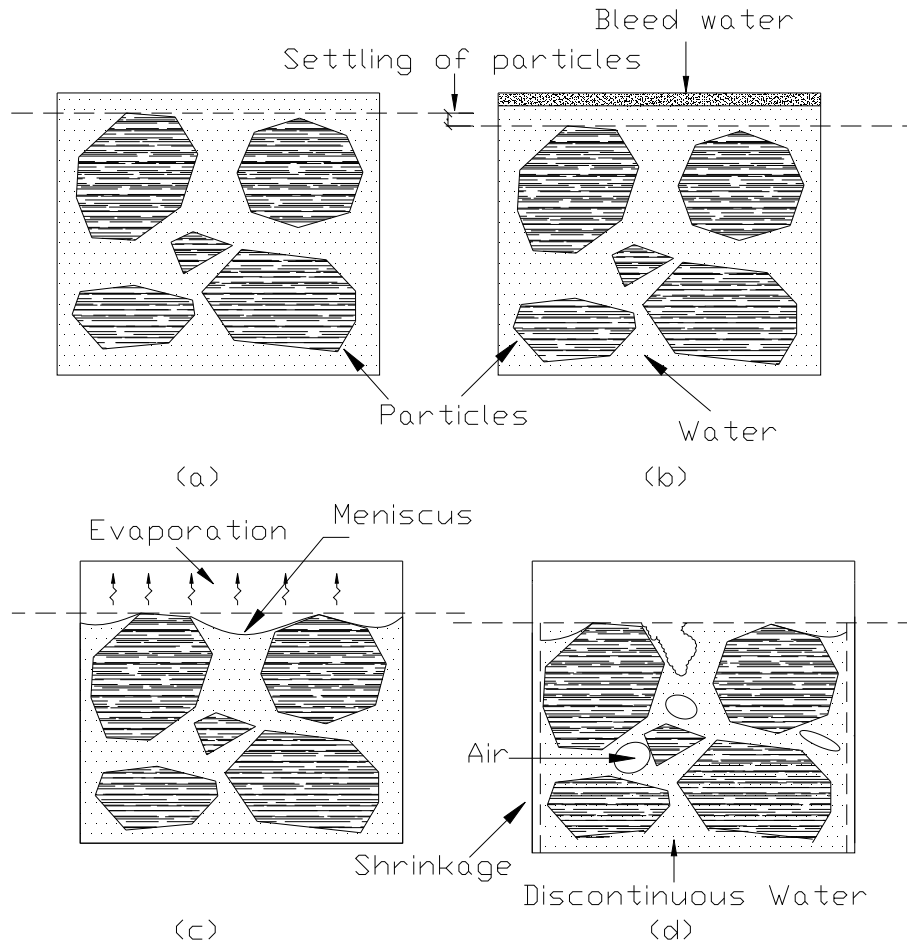


Figure 2.1: Schematic diagrams of plastic shrinkage: (a) Concrete when placed, (b) Bleeding of water to the surface, (c) Surface evaporation and menisci between solid particles, and (d) Discontinuous water and plastic shrinkage

Further evaporation of water from the concrete surface leads to a complex system of menisci on the concrete surface due to capillary action (Figure 2.1(c)). This generates tensile capillary pressure within the liquid phase. Hence, an attractive force exists between solid particles of concrete that are separated by a liquid filled

capillary. This attractive force reduces the mean distance between the solid particles of the concrete and results in contraction.

As the solid particles move closer, the radii of the menisci decrease continuously resulting in increase of tensile capillary pressure that can reach a maximum called “break-through pressure”. At this critical pressure, the mean radii of menisci are too small to interconnect all the spaces between the solid particles at the surface. Hence, air enters the pore system and water rearranges to form discrete zones (Figure 2.1(d)). Once water rearranges, there is no longer any capillary effect. The risk of plastic shrinkage cracking is assumed to reach its maximum when air starts to penetrate into the pore system as the drained pores are the weakest points in the system. The force of attraction between the particles in the air penetrated region is comparatively less than in the water filled regions (Slowik et al. 2008).

Plastic shrinkage alone at the early stage does not lead to cracking, as it is just a uniform contraction in the material. It is restraint that develops tensile stresses in fresh concrete. At this stage, concrete is still plastic and has not gained enough strength to resist these stresses, and the localization of strains at weak zones (i.e. at air filled regions) leads to cracking on the surface of concrete (Slowik et al. 2008).

### **2.2.2 Plastic settlement**

Another mechanism that is associated with plastic shrinkage is plastic settlement. After concrete is placed, solids settle and bleed water rises to the surface of the concrete. If there is no restraint, settling leads to slight lowering of the surface of the concrete and the uniform settlement does not lead to plastic cracking. In case the settlement is locally restrained (by reinforcing bars, large aggregates and ducts), the concrete adjacent to the restraint continues to settle. However, the concrete on the restraint does not settle as much. Such non-uniformity in settlement induces tensile stresses and leads to cracking over the restraining element (Weyers et al. 1982). Figure 2.2 illustrates the cracking due to plastic settlement on the restraint elements. The settlement that occurs due to settling of solids is proportional to depth of the concrete. Hence, whenever there is a sudden change in depth of a section (e.g., beam-slab joints), settlement at that section will also be different. This differential settlement also results in tensile stresses and consequently cracking at the surface. Plastic settlement cracks can be easily distinguished as the pattern reflects the

restraining element (Qi et al. 2003). Figure 2.3 shows the plastic cracks due to variation in depth of concrete.

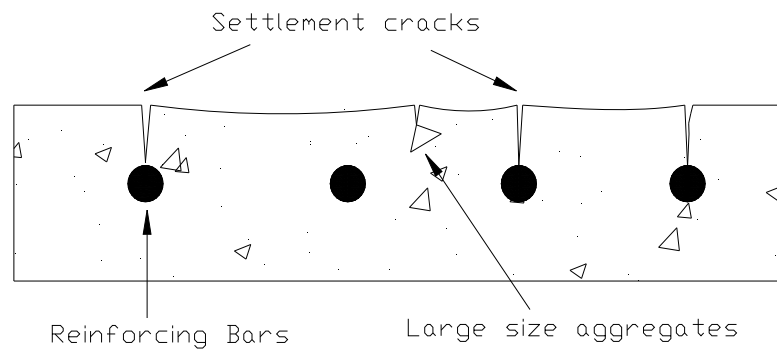


Figure 2.2: Plastic settlement cracking due to internal restraint

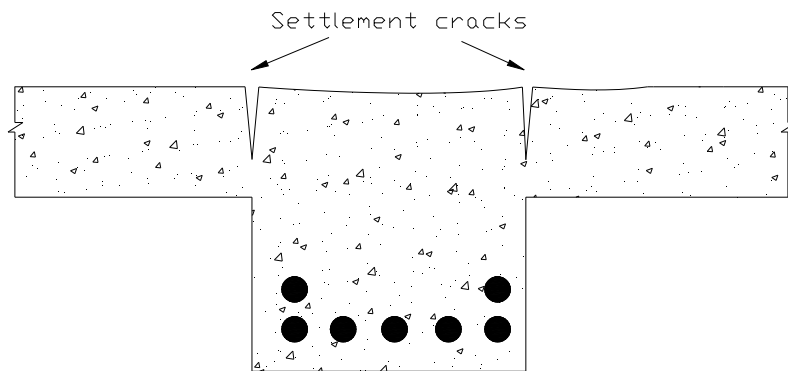


Figure 2.3: Plastic cracking due to variation in depth of concrete

### 2.3 Quantitative determination of tensile capillary pressure

Tensile capillary pressure developed in the liquid phase due to formation of menisci at the surface of concrete can be determined by using the Young-Laplace equation (Wittmann 1976):

$$P_c = \gamma \left( \frac{1}{R_1} + \frac{1}{R_2} \right) \quad 2.1$$

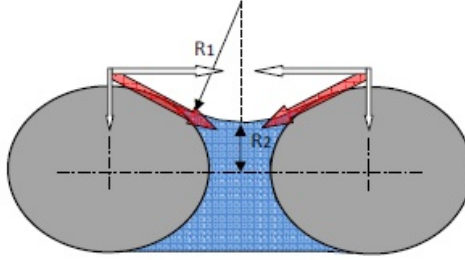


Figure 2.4: Principal radii of liquid surface (Combrinck 2012)

In the above equation,  $\gamma$  is the surface tension of the fluid (N/m), and  $R_1$  and  $R_2$  are two principal radii of curvature of the surface of the liquid; Figure 2.4 explains the terms  $R_1$  and  $R_2$ . The equation indicates that capillary pressure  $P_c$  is inversely proportional to radii of curvature of the liquid surfaces. Hence, with the progress of evaporation, the radii of menisci decrease continuously resulting in the increase of capillary pressure. In addition, capillary pressure is directly proportional to the surface tension of water. Therefore, capillary pressure developed in a cementitious matrix can be reduced by decreasing the surface tension. This is basically the principle behind the action of shrinkage reducing admixtures.

Capillary pressure developed also depends on the fineness of the particles in the system. Powers developed an expression for determining the maximum capillary pressure for cement-based composites relating surface area of cement and water cement ratio (Cohen et al. 1990):

$$P_{max} = 0.001 \frac{\gamma S}{w/c} \quad 2.2$$

where  $P_{max}$  – maximum capillary pressure (MPa),  $\gamma$  – surface tension of water (N/m),  $S$  – surface area of binder ( $m^2/kg$ ),  $w/c$  – water-cement ratio by mass. From the equation, it is clear that maximum capillary pressure developed in a cement composite is proportional to fineness of the binder in composites.

## 2.4 Test methods used to quantify plastic shrinkage

For assessing the performance of concrete against plastic shrinkage cracking several laboratory-scale test techniques were developed. All these techniques had to overcome the challenges of producing plastic shrinkage cracks with appreciable realistic restraint conditions. Based on the method of restraint, tests are classified as unrestrained plastic shrinkage and restrained plastic shrinkage tests.

#### 2.4.1 Unrestrained plastic shrinkage tests

In unrestrained plastic shrinkage tests, the main principle is to measure the strain in plastic state either by embedded studs or by measuring the movement of free head of the specimen. Linear variable displacement transducer or extensometers were generally used to measure the strains. In case of prisms, one end would be fixed and other free end would be used to measure strains whereas in slabs, strains would be measured on all the sides (Al-Amoudi et al. 2006; Wongtanakitcharoen & Naaman 2006). Yet no standard method exists to estimate unrestrained plastic shrinkage. All the unrestrained tests used in the literature are summarised in the Table 2.1.

Table 2.1: Unrestrained plastic shrinkage specimens

Reference	Specimen	Environmental conditions	Method of measuring strain
Paillere et al. (1989)	Concrete 1500 × 120 × 85 mm	Temperature: Not mentioned RH: Not mentioned Wind: Not mentioned	One head of the specimen was fixed and shrinkage was measured on the other head
Mangat and Azari (1990)	Concrete 100 (diameter) × 200 (height) mm	Temperature: Not mentioned RH: Not mentioned Wind: Not mentioned	By optically monitoring a movement of the spherical ball placed on plastic concrete
Sanjuan and Moragues (1994)	Concrete 1200 × 150 × 20 mm	Temperature: 40 °C RH: Not mentioned Wind: 0.5 m/s	Extensometer was used to measure early age shrinkage strain
Bloom and Bentur (1995)	Concrete 1000 × 40 × 40 mm	Temperature: 40 °C RH: 45 % Wind: Not mentioned	One head of the specimen was fixed with fixed grip and shrinkage was measured at the free head
Al-Amoudi et al. (2006)	Concrete 1000 × 1000 × 30 mm	Temperature: 45 °C RH: 35 % Wind: 4.2 m/s	Strains were measured using LVDTs on all the sides of the slab
Wongtanakitcharoen and Naaman (2006)	Concrete 1000 × 100 × 60 mm	Temperature: 35 - 40 °C RH: 22.5 % Wind: 2 m/s	Free end of the steel mould was used to measure the strains using LVDT
Newlands et al. (2008)	Concrete 380 × 110 × 50 mm	Temperature: 40 °C RH: 10 % Wind: 2 m/s	Free end of the mould was used to measure strains

## 2.4.2 Restrained plastic shrinkage tests

Restrained plastic shrinkage tests focus on measuring the crack properties (crack, length and width) and initiating time of cracks formed on the surface due to restraint. Restrained tests can be classified based on geometry as ring, prism and slab specimens. Different methods of restraints were used to induce plastic cracks. Firstly, hardware cloth of 12.7 mm along periphery at a distance from edge was used and later it was modified to metal lath (Kraai 1985; Shaeles & Hover 1988). Cracks due to these restraints were random and it was difficult to quantify the crack areas. Secondly, to localise and induce single crack, a stress riser and two end restraints were used at the bottom (Berke & Dallaire 1994; Balaguru 1994). Thirdly, rigidly fixed steel stud bolts along the edges were used to restrain the concrete from the sides (Yokayama et al. 1994). Finally, in order to increase degree of restraint, a combination of stress riser and steel threaded bolts were used to restrain the base and sides, respectively (Mora et al. 2002). All the restrained plastic shrinkage tests used in the literature are summarised in the Tables 2.2, 2.3 and 2.4 based on their shape as ring, slab and prism shaped specimens, respectively.

Table 2.2: Restrained plastic shrinkage tests with ring shaped specimens

Reference	Specimen	Environmental conditions	Method of restraint
Dahl (1989)	Annular ring Mortar and concrete 580 (outer diam.) × 280 (inner diam.) × 80 (height) mm	Temperature: 20 °C RH: 40 % Wind: 4 m/s	12 steel ribs welded to the inner side of the outer ring provide restraint
Padron & Zollo (1990)	Ring at centre of square slab Mortar Slab: 300 × 300 × 12.6 mm Ring: 114 mm (diam.) Concrete Slab: 300 × 300 × 25.4 mm Ring: 140 mm	Temperature: 31 °C RH: 50 % Wind: 2.8 m/s (Mortar) 6.1 m/s (Concrete)	Ring at the centre of the slab provides the restraint and causes radial cracking
Filho & Sanjuan (1999)	Ring with a cube core Mortar Ring: 150 (diam.) × 50 (height) mm Cube: 70 mm	Temperature: 40 °C RH: Not mentioned Wind: 0.5 m/s	The cube at the centre and five steel bars of 6 mm diameter positioned at mid height provides the restraint

Table 2.3: Restrained plastic shrinkage slab tests on specimens

Reference	Specimen	Environmental conditions	Method of restraint
Ravina &Shalon (1968)	Concrete 650 × 800 × 70 mm	Temperature: Not mentioned RH: Not mentioned Wind: Not mentioned	Rigidly fixed barbed wire along the periphery
Kraai (1985)	Concrete 1200 × 1200 × 20 mm Mortar 910 × 610 × 20 mm	Temperature: Not mentioned RH: Not mentioned Wind: 4.8 to 5.4 m/s	Hardware cloth strip of 12.7 mm (height) along the periphery at 19.07 mm from the edge
Shaeles & Hover (1988)	Mortar Slab 910 × 610 × 20 mm	Temperature: 25 – 35 °C RH: 10 to 25 % Wind: 3.1 to 3.6 m/s	Metal lath attached to the inner side perimeter provides edge restraint, i.e. wire mesh in case of Kraai's is replaced by metal lath
Cohen et al. (1989)	Mortar and Paste 50 × 50 × 5 mm	Temperature: 40 °C RH: Not controlled Wind: 0.8 m/s	Ultra-fine water proof sand paper was used along the periphery
Balaguru (1994)	Concrete 900 × 900 × 50 mm	Temperature: 22 °C RH: 50 % Wind: 14.2 m/s	Hardware cloth of 50 mm width placed at a depth of 25 mm
Berke & Dallaire (1994)	Concrete 560 × 356 × 100 mm	Temperature: 22 °C RH: 50 % Wind: 14.2 m/s	Restrains were provided using two triangular risers of 32 mm high along 356 mm width and riser of 63 mm high in the middle to induce crack
Yokoyama et al. (1994)	Concrete 600 × 600 × 50 mm	Temperature: 30 °C RH: 60 % Wind: 8.3 m/s	Restraint was provided by steel stud bolts on all the sides
Almusallam et al. (1998)	Concrete 450 × 450 × 20 mm	Temperature: 45 °C RH: 50 % Wind: 4.2 m/s	Not mentioned
Mora et al. (2001)	Concrete 800 × 800 × 100 mm	Temperature: 44 °C RH: 25 % Wind: 11.1 m/s	Restrained by threaded steel bolts on all the sides
Wang et al. (2002)	Paste 100 × 100 × 8 mm	Temperature: 40 °C RH: 18 % Wind: 0.8 to 1.4 m/s	Bottom was restrained by fine sand paper
Qi et al. (2003)	Concrete 508 × 254 × 76 mm	Temperature: 38 °C RH: 50 % Wind: 6.7 m/s	Restrains were provided using two triangular risers of 25.4 mm high along 254 mm width and another riser of 47.6 mm high in the middle to induce crack

ASTM C1579	Concrete 560 × 355 × 100 mm	Temperature: 36±3 °C RH: 30 ± 10 % Wind: > 4.7 m/s	Restrains were provided using two triangular risers of 32 mm high along 355 mm width and a stress riser of 63.5 mm high in the middle
Turcry & Loukili (2006)	Concrete 400 × 200 × 70 mm	Temperature: 20 °C RH: 50 % Wind: 5 m/s	Restrains were provided using two triangular risers of 35 mm high along 200 mm width and a stress riser of 55 mm high in the middle
Ghoddousi et al. (2007)	Concrete 900 × 600 × 100 mm	Temperature: 40 °C RH: 20 % Wind: 3.3 m/s	Six equal triangular risers were used to provide restraint from the base
Sivakumar & Santhanam (2007)	Concrete 500 × 250 × 75 mm	Temperature: 35 °C RH: 40 % Wind: 6 m/s	Stress riser of 55 mm and base restraints of 35 mm were used to provide restraint
He & Peng (2011)	Concrete 600 × 600 × 63 mm	Temperature: 35 °C RH: 40 % Wind: 6 m/s	14 threaded screws of 8 mm diameter and 100 mm length were fixed to each edge to provide restraint
Combrinck & Boshoff (2012)	Concrete Unique configuration	Temperature: 40 °C RH: 20 % Wind: 0.6 m/s	Triangular riser was used to provide restraint
Boshoff et al. (2012)	Concrete 600 × 200 × 100 mm	Temperature: 50 °C RH: 10 % Wind: 19.4 m/s	Restraint was provided by risers and in addition two round steel bars were used to increase restraint

Table 2.4: Restrained plastic shrinkage tests using prism specimens

Reference	Specimen	Environmental conditions	Method of restraint
Banthia et al. (1993)	Concrete 500 × 40 × 40 mm	Temperature: 38 °C RH: 5 % Wind: Not mentioned	Triple bar anchor was used to provide restraint
Banthia et al. (1996)	Concrete 1010 × 100 × 100 mm	Temperature: 38 °C RH: 5 % Wind: Not mentioned	Restraint was provided by 1010 × 100 × 40 mm substrate with 20 mm aggregates protruding on the surface.
Mora et al. (2001)	Concrete 600 × 150 × 150 mm	Temperature: 44 °C RH: 25 % Wind: 11.1 m/s	Restraint was provided by stress riser at centre and anchor bolts on the sides

Mora et al. (2003)	Concrete 600 × 150 × 150 mm	Temperature: 44 °C RH: 25 % Wind: 11.1 m/s	Configuration of Mora et al (2001) was modified with addition anchor bars to increase restraint
Naaman et al. (2005)	Concrete 1016 × 76.2 × 38.1 mm	Temperature: 35 - 40 °C RH: 22.5 % Wind: Not mentioned	Notched surface substrate was used to provide restraint
Banthia & Gupta (2006)	Concrete 375 × 100 × 60 mm	Temperature: 50 °C RH: 5 % Wind: Not mentioned	Substrate of 325 × 95 × 40 mm with hemispherical protuberance was used to provide restraint
Nabil et al. (2011)	Concrete 400 × 100 × 50 mm	Temperature: 50 °C RH: 10 % Wind: 2.8 m/s	Substrate of 365 × 65 × 50 mm with notched surface was used to provide restraint

## 2.5 Influence of low volume fibres on plastic shrinkage cracking

The use of low volumes of fibres in concrete is an effective technique to mitigate plastic shrinkage cracking. Randomly distributed fibres act as secondary reinforcement and control inherent plastic shrinkage cracking. Yet the mechanism responsible for improved performance is still not clear. The following are some of reasons from the literature for the improved performance of low volume fibre reinforced concrete in reducing plastic shrinkage cracking:

- Fibres increase the tortuosity of bleed channels and block bleed channels, thereby reducing the accumulation of the bleed water on the surface. The bleed water is expected to accumulate underneath the fibres, leading to a porous interface between fibres and cement paste. This porous interface introduces an additional group of larger diameter pores. As a result, capillary pressure reduces and provides a partial benefit in reducing plastic shrinkage cracking (Wang et al. 2002).
- At early ages, the elastic modulus of fibre is higher than cementitious matrix, so the cementitious matrix with fibres offers relatively higher resistance and helps control crack development (Filho & Sanjuán 1999).
- Addition of fibres reduces settling capacity of fresh concrete. Thereby, fibre reinforced concrete is expected to settle uniformly and have less differential settlements that could lead to plastic cracking (Qi et al. 2003).

- Fibres increase strain capacity of the concrete. Hence, fibre reinforced concrete can accommodate larger strains at early ages (Najm & Balaguru 2003).
- Fibres trap water in the mix and reduce overall early age shrinkage, and are expected to produce more intact material and less cracking (Gupta et al. 2006).
- After cracking (or microcracking), fibres transfer stresses across crack openings and arrest further cracking by bridging. So, the intensity of cracking decreases (Soroshian et al. 1995).

Different types of fibres have been used to mitigate plastic shrinkage cracking. Some of the fibres with their corresponding dosages used to mitigate plastic shrinkage cracking are summarised in Table 2.5. Investigations with all these fibres reported that the effectiveness of the fibres to reduce crack area and maximum crack width increases with an increase in fibre volume fraction (Banthia et al. 1996; Sanjuán & Moragues 1997; Qi et al. 2003; Naaman et al. 2005; Boghossian & Wegner 2008). This is due to the fact that the number of fibres participating in resisting the crack propagation increases. Thus, higher dosages of fibres effectively reduce plastic shrinkage cracking but can be uneconomical. The volume of fibres required for dramatic reduction in maximum crack width and crack area depends on the type of fibre being used and sensitivity of the concrete for plastic shrinkage cracking.

The geometry of fibre is an important factor for the selection of fibres to mitigate cracks due to plastic shrinkage. Longer fibres are more effective in controlling plastic shrinkage cracking. Long fibres relatively develop better bond with the cementitious matrix and transfer stresses effectively across a crack. On the other hand, short fibres may get pulled out of matrix even at low stress levels (Najm & Balaguru 2003; Balaguru 1994). Furthermore, fine denier fibres are more effective than coarse denier fibres. Fine denier fibres relatively have more surface area to bond with the cementitious matrix; consequently, transfer greater tensile stresses to the fibre. Also, for a given volume fraction, fine denier fibres will be higher in number, and more fibres cross a given section. Hence, for a given volume fraction, fine denier fibres reduce the stress concentration and improve the resistance to crack propagation (Wang et al. 2002; Banthia & Gupta 2006; Naaman et al. 2005).

Therefore, long and fine denier fibres, i.e. fibres with high aspect ratio (length to diameter), are relatively better in controlling plastic shrinkage cracking.

Table 2.5: Fibres and their dosage used

Fibre material	Length(mm)	Volume fraction (%)	Reference
Acrylic	10	0.05-0.10	Padron & Zollo (1990)
Carbon	6	0.05-0.40	Naaman et al (2005)
Cellulose	12	0.10-0.20	Banthia & Gupta (2007)
Flax	10	0.10-0.30	Boghossian & Wegner (2008)
Glass	6	0.12-0.50	Sivakumar & Santhanam (2007)
High density polyethylene	38	0.05-0.40	Naaman et al (2006)
Nylon	13	0.05-0.10	Pelisser et al (2010)
Polyacrylonitrile	12	0.05-0.15	Zhuo et al (2011)
Poly ethylene-terephthalate	15	0.05-0.10	Pelisser et al (2010)
Polyolefin	19	0.10-0.70	Banthia & Yan (2000)
Poly vinyl alcohol	12	0.05-0.40	Naaman et al. (2005)
Polyester	12	0.12-0.50	Sivakumar & Santhanam (2007)
Polypropylene (Fibrillated)	19	0.05-0.40	Bayasi & McIntyre (2003)
Polypropylene (Monofilament)	12	0.05-0.30	Berke & Dallaire (1994)
Sisal	25	0.10-0.20	Filho & Sanjuán (1999)
Steel (hooked)	30	0.50-1.50	Eren & Marar (2010)

The form of the fibre also influences plastic shrinkage cracking. Fibrillated fibres are more effective in combating plastic shrinkage cracking over monofilament fibres. The fibre fibrillations provide an effective anchorage to overcome the weak adhesion between fibres and matrix and reduces intensity of cracking (Wang et al. 2002; Qi et al. 2003). In addition, fibrillated fibres increase tensile strain capacity and reduce coarse aggregate settlement. These additional features also contribute to reducing plastic shrinkage cracking (Bayasi & McIntyre 2003).

## 2.6 Influence of environment conditions on plastic shrinkage

Plastic shrinkage cracking is extremely influenced by evaporative potential of the site microclimate. Evaporation of bleed water from the surface of concrete is a function of air temperature, relative humidity, wind velocity and concrete surface

temperature. Initiation of surface drying depends on rate of evaporation, hence a method to evaluate evaporation rate based on site climatic conditions is essential. The nomograph of ACI 305.1-06, “Hot Weather Concreting”, provides a graphical technique to estimate evaporation rate from the concrete surface; for finding the rate of evaporation using this nomograph, wind speed at 510 mm (20 in.) height, and relative humidity and air temperature data at 4-6 ft. (1.2 to 1.8 m) above the evaporating surface (ACI 305.1-06) are needed. High air temperature, low humidity and high wind velocity in combination are conducive for high rate of evaporation from the surface of concrete. Hence, chances of plastic shrinkage cracking are significantly high at these conditions.

John Dolton derived an expression for predicting rate of evaporation from the surface of water bodies. From Dolton’s expression, Menzel developed an equation for estimating evaporation rate over the concrete surface (Menzel 1954):

$$W = 0.44 (e_o - e_a) (0.253 + 0.096V) \quad 2.3$$

where,

W - weight (lb) of water evaporated per square foot of surface per hour, lb/ft<sup>2</sup>/hr

e<sub>o</sub> - pressure of saturated vapour pressure at the temperature of the evaporating surface, psi

e<sub>a</sub> - vapour pressure of air, psi

V - average horizontal wind speed measured at a level about 20 in. higher the evaporating surface, mph.

From the above equation, a nomograph was also developed by Menzel for easy prediction of rate of evaporation depending on the site climatic conditions; see Figure 2.5. This nomograph was based on the difference in saturated vapour pressure and vapour pressure of air. Hence, vapour pressures had to be measured for predicting rate of evaporation. Bloem resolved this difficulty by replacing vapour pressures with relative humidity and concrete temperature as equivalent variables. Bloem’s nomograph is shown in Figure 2.6 (Uno 1998), which evaluates the evaporative potential of the environment, and not the rate of evaporation from the surface of concrete; the difference between the two may be small when the concrete surface is covered with bleed water (Hover 2006).

In the literature, the most quoted critical rate of evaporation is  $1 \text{ kg/m}^2/\text{hr}$  ( $0.2 \text{ lb/ft}^2/\text{hr}$ ). This critical value for evaporation rate was first quoted by National Ready Mix Concrete Association (NRMCA) in 1960. The value originated from the research carried out by Powers. In his research, he observed that bleeding rates of various concretes varied from  $1.15$  to  $4.1 \text{ kg/m}^2/\text{hr}$ . Hence, it was assumed that concrete would crack when evaporation rate exceeds the lower bound value (i.e.,  $1.15 \text{ kg/m}^2/\text{hr}$ ). Keeping this in view, NRMCA suggested a critical evaporation rate of  $1 \text{ kg/m}^2/\text{hr}$ , above which precautions should be taken. ACI 305 also suggests the same value while the Canadian and Australian codes denote  $0.75$  and  $0.5 \text{ kg/m}^2/\text{hr}$ , respectively, as critical evaporation rates. Critical evaporation rates are not the same for all the concretes, and depend on their bleeding capacity. In modern concretes with silica fume, plastic shrinkage cracks were observed even at  $0.25 \text{ kg/m}^2/\text{hr}$  ( $0.05 \text{ lb/ft}^2/\text{hr}$ ) (Uno 1998). Irrespective of the critical evaporation rate mentioned in the standards, precautionary measures may be needed depending on the characteristics of concrete and climatic conditions.

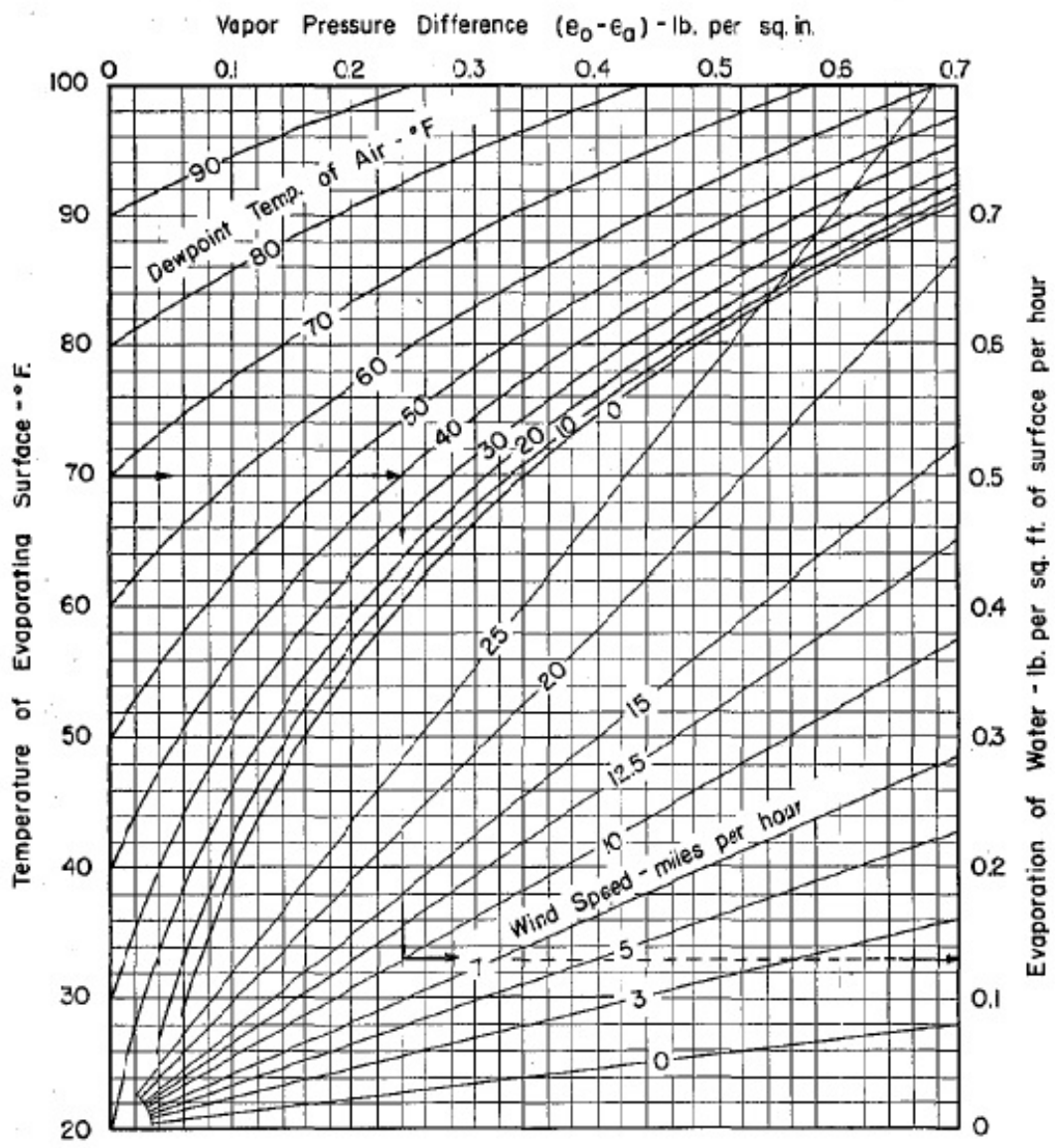


Figure 2.5: Menzel's Nomograph (Menzel 1954)

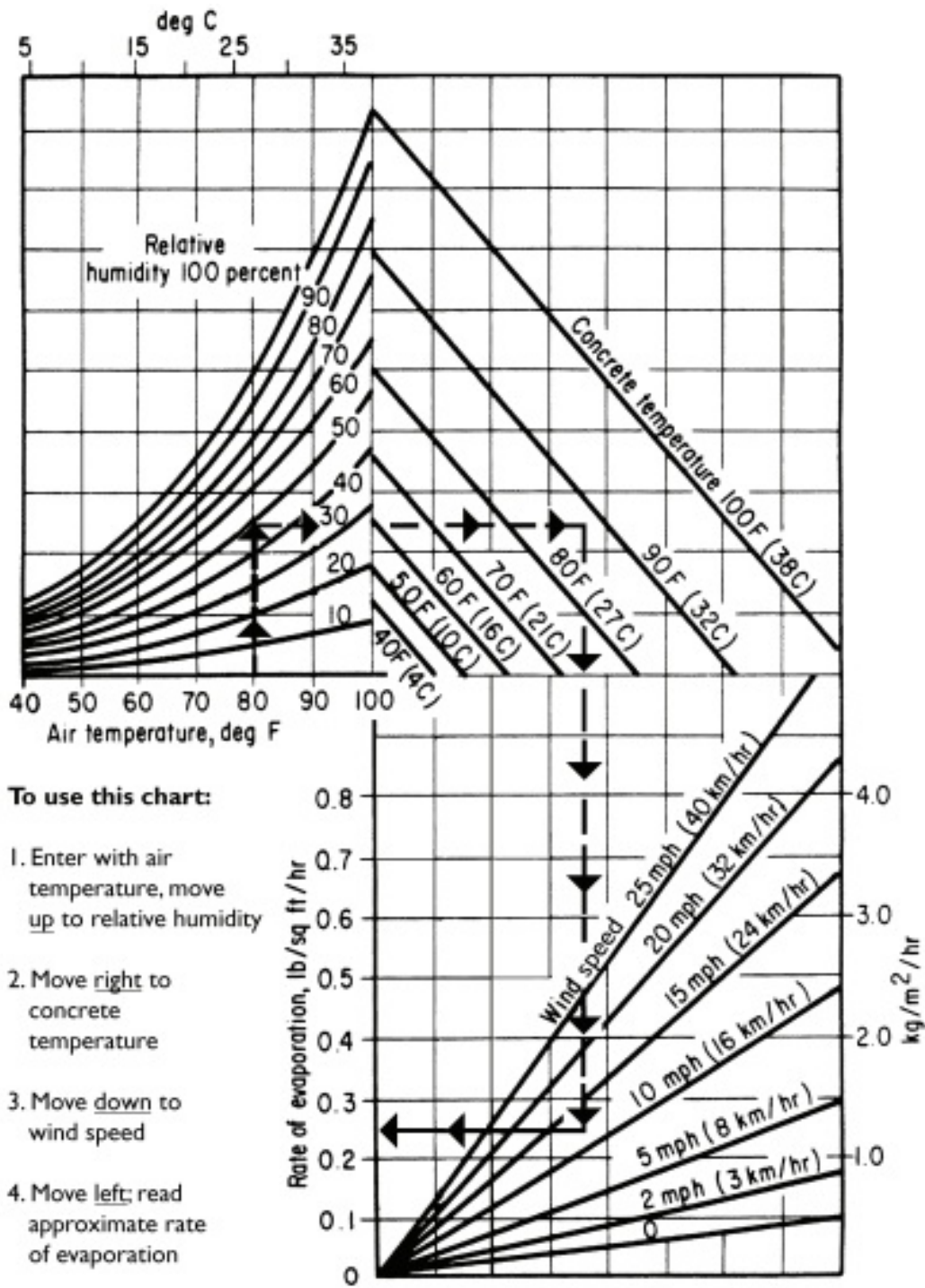


Figure 2.6: Nomograph (ACI 305.1-06)

Uno proposed simpler equations for accurate determination of rate of evaporation of water from the surface of concrete by modifying Menzel's formula. He suggested that vapour pressures in the Menzel's formula be calculated using expressions of the World Meteorological Organization. The expression is:

$$e_s = 0.61 \exp \frac{17.3 T}{(237.3+T)} \quad 2.4$$

where,

$e_s$  - saturated vapour pressure, kPa, and

$T$  - temperature, °C

By substituting temperature of air and concrete in the above expression, vapour pressures of air and concrete are obtained, respectively. These are to be substituted in the modified Menzel's formula, as shown below, to obtain the rate of evaporation from the surface of concrete.

$$E = 0.313 (e_{so} - r.e_{sa})(0.253 + 0.06 V) \quad 2.5$$

where,

$E$  - evaporation rate, kg/m<sup>2</sup>/hr

$e_{so}$  - vapour pressure at concrete surface, kPa, from the above expression

$e_{sa}$  - vapour pressure at air, kPa, from the above expression

$r$  - (relative humidity, %)/100

$V$  - wind velocity, km/hr

Samman et al. (1994) studied the influence of normal and high strength concrete on plastic shrinkage cracking. From their research, Uno (1988) derived an expression for critical rate of evaporation in relation with strength of concrete:

$$E_{max} = 1.6 - 0.016f_c \quad 2.6$$

where,

$E_{max}$  - maximum allowable evaporation rate, kg/m<sup>2</sup>/hr

$f_c$  - strength of concrete, MPa

## 2.7 Influence of mineral admixtures on plastic shrinkage

The use of supplementary cementitious materials (SCMs) like fly ash (Class C and Class F) and ground granulated blast furnace slag (GGBS) has increased to enhance

the performance and durability of concrete. SCMs when blended with ordinary portland cement contribute to protect against chemical attack, carbonation and chloride induced corrosion. On the other hand, they have some adverse effects on the performance of concrete; partial replacement of these SCMs are known to decrease rate of strength gain and increase setting time of concrete (ACI 232.2R-03; ACI 233R-03). In addition, fineness of SCMs being higher than ordinary portland cement, the replacement of OPC with the SCM increases the water requirement for wetting the particles and hence reduces bleeding capacity of concrete (Uno 1998). Furthermore, from Powers' expression for maximum pressure, maximum capillary pressure is directly proportional to surface area of the binder. Thus, maximum capillary pressure also increases. All these adverse effects exacerbate the risk of plastic shrinkage cracking when concrete with SCMs is used for large surface area applications, especially in hot and dry weather conditions.

Unfortunately, literature available on the influence of flyash and GGBS on plastic shrinkage is meagre. In a study of the influence of mix proportion and environment on plastic shrinkage, Dias (2003) observed an increase in plastic shrinkage cracking with an increase in the partial replacement of cement by fly ash (Class F). Moreover, Bantia and Gupta (2009) also reported the same with partial replacement of fly ash (Class C) up to a certain threshold value of replacement. However, these results are contrary to the findings of Wang et al. (2002), in a study with paste, that the slower hydration due to partial replacement of cement by fly ash (Class F) leads to higher porosity that reduced capillary pressure in the paste and consequently the plastic shrinkage cracking.

Concretes with silica fume are highly prone to plastic shrinkage cracking, mainly due to its high fineness. Fineness of silica fume is in the range of 13,000-30,000 m<sup>2</sup>/kg while the fineness of fly ash and GGBS are in the range of 300-400 m<sup>2</sup>/kg and 400-600 m<sup>2</sup>/kg, respectively. Such high fineness of silica fume significantly increases the capillary menisci on the surface of concrete and in turn increases the maximum capillary pressure. Replacement of 0 to 15% of silica fume increases maximum capillary pressure from 0.02 to 4 MPa, which is 200-fold compared to ordinary concrete. Additionally, silica fume significantly reduces bleeding in fresh concrete by blocking the pores in plastic state and increases the tendency of plastic shrinkage cracking. In case of concretes with silica fume, plastic

shrinkage cracks were observed even at evaporation rates of 0.2 kg/m<sup>2</sup>/hr (Bayasi & McIntyre 2003; Al-Amoudi et al. 2004; Ghoddousi et al. 2007). Hence, it becomes mandatory to take precautionary measures like fogging, wind breaks, using evaporation retarders to eliminate plastic shrinkage cracking.

## 2.8 Influence of chemical admixtures on plastic shrinkage

### 2.8.1 Influence of shrinkage reducing admixtures

Shrinkage reducing admixtures are being used in the concrete industry to improve shrinkage performance of the concrete. These are organic polymers classified as surfactants that can reduce surface free energy of liquid-solid interface (surface tension). Hence, their usage in concrete reduces the surface tension of the pore solution in the capillary pores (Bentz et al. 2001). The reduction in surface tension lowers the maximum capillary pressure developed in a cementitious matrix. This mechanism can also be inferred from the Equation 1.2. It can be observed that the maximum capillary pressure ( $P_{max}$ ) decreases with a decrease in surface tension ( $\gamma$ ). As a result, the pull on the walls of the pores decreases, thus reducing the resultant shrinkage strain. Figure 2.7 shows the variation of surface tension of the solution with the concentration of shrinkage reducing admixture in water. It can be observed that with addition of 2% of shrinkage reducing admixture surface tension reduced by 30% (Rongbing and Jian 2005).

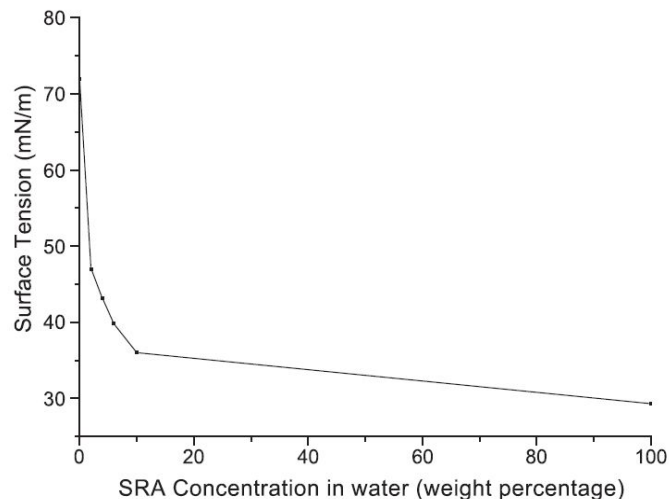


Figure 2.7: Surface tension and SRA concentration (Rongbing and Jian 2005)

Primarily, shrinkage reducing admixtures have been used mainly to reduce drying and autogenous shrinkage. Free and restrained shrinkage tests have shown

shrinkage reducing admixtures to be very effective in reducing both volumetric instability and restrained cracking (Shah et al. 1993; Weiss et al. 1998). Later researchers determined that, in addition to reducing surface tension of pore solution, shrinkage reducing admixtures are also capable of reducing evaporation, settlement capacity of fresh concrete and delaying the onset of maximum capillary pressure (Mora et al. 2001; Lura et al. 2006). All these additional benefits contributed to a reduction in plastic shrinkage and the potential for cracking due to plastic shrinkage. Many researchers (Shah et al. 1993; Mora et al. 2003; Xie et al. 2011; Rongbing & Jian 2005) have used shrinkage reducing admixtures as an alternative to fibres for mitigate plastic shrinkage cracking. Shrinkage reducing admixtures were found to be effective in reducing crack areas and maximum crack widths on par with synthetic fibres (Lura et al. 2007). The only disadvantage with shrinkage reducing admixture is that they can slightly reduce compressive strength of concrete (Roncero et al. 2003; Saliba et al. 2011).

### **2.8.2 Influence of superplasticizers**

Superplasticizers also known as high range water reducers are high molecular surfactants with long hydrocarbon chains. These long chains get adsorbed on the surface of the cement particles and impart strong electronegative charge between the particles of cement by lowering the surface tension of the surrounding water. Consequently, this improves the fluidity of concrete (Mehta & Monteiro 2006). Superplasticizers are used for three different purposes or in combination:

- To increase workability for a given water demand and therefore enhances placing characteristics of concrete;
- To reduce water cement ratio for a given workability and cement content thus resulting in higher strength and improved durability;
- To reduce cement content for a given workability and strength so as to save cement.

Hence, these advantages make it possible to produce high performance concrete with low water cement ratio and high workability. Most widely used superplasticizers are sulphonated melamine formaldehyde (SMF), sulphonated naphthalene formaldehyde (SNF) and polycarboxylate ether (PCE).

The use of SCMs increases water demand and reduces workability of concrete. Superplasticizers are invariably added with supplementary cementitious materials to

compensate these deficiencies and to extend slump retention for a given water binder ratio. In the plastic state, superplasticizers may reduce the surface tension of water, which contributes to controlling plastic shrinkage cracking. Hence, superplasticizers either prolong the onset or resist plastic shrinkage cracking. The effectiveness of the superplasticizer in controlling plastic shrinkage depends on its capacity to reduce the surface tension of water (Cabrera et al. 1992; Al-Amoudi et al. 2006). However, at higher dosages, superplasticizers retard the rate of cement hydration and prolong setting time of concrete. Hence, at higher dosages, superplasticizer can decrease the early gain in strength of concrete and aggravate the potential for plastic shrinkage cracking.

### **2.8.3 Influence of retarders**

Retarders are set-retarding admixtures used to delay the setting of concrete by inhibiting the initial rate of hydration of cement. These are primarily used at high temperatures to offset the accelerating effect and to extend workable time of concrete. Retarders extend the setting time by forming a thin film over the cement particles and thus impeding the dissolution of ions and reaction with water. The formation of hydrates and silicates reduces the influence of retarders and then the process becomes normal. This effect extends the plastic stage of concrete and retards early gain in strength, and is likely to increase the plastic shrinkage (Dias 2003; Leemann et al. 2014).

### **2.8.4 Influence of accelerators**

Accelerators are a class of chemical admixtures that accelerate early strength development of concrete. These are primarily used to offset the retardation effects due to low temperatures and for rapid removal of form work is. Accelerators act as catalysts in the reaction of hydration of calcium silicates. Accelerators reduce bleeding and setting time, as well as help in attaining early strength at a faster rate. Consequently, concretes with accelerators are expected to crack early and experience lower plastic shrinkage cracking (Leemann et al. 2014).

## **2.9 Influence of mix proportions on plastic shrinkage**

The mix composition of concrete, mainly the binder content and water-to-binder ratio, significantly affects the plastic shrinkage. With the increase in binder content, the

paste volume fraction increases. The paste content being the only fraction of concrete that shrinks, its increase leads to a higher risk of cracking (Dias 2003). On the other hand, the decrease in water-to-binder ratio (i.e. with increase in grade of concrete) reduces both the amount and rate of bleeding capacity of concrete. Subsequently, the critical rate of evaporation, at which the concrete starts to crack, decreases. It is also observed that the concretes of higher grade crack earlier than low grade concrete (Samman et al. 1996). In case supplementary cementitious materials are used, the bleeding rate and critical rate of evaporation further reduce and the concrete becomes highly sensitive to plastic shrinkage cracking (Qi et al. 2003).

The volume fraction of aggregate in concrete also influences the severity of plastic shrinkage cracking. The aggregates in concrete provide dimensional stability by resisting the shrinkage strain of paste. Hence, reduction in aggregate volume fraction can increase shrinkage strain, and consequently the risk of plastic shrinkage cracking (Shaeles & Hover 1988; Almusallam et al. 1998).

## **2.10 Influence of curing compounds on plastic shrinkage cracking**

Curing compounds are liquid membrane-forming compounds that are sprayed on the surface of freshly placed concrete to prevent the rapid loss of mix water. In hot and dry weather conditions, curing compounds are judged to be more practical, feasible and economical, especially for the construction of structures with large surface areas, like canal linings, pavements, and high-rise buildings. Some of the advantages of using a curing compound relative to conventional moist curing methods are: 1) elimination of the follow-up or supervision by single operation, 2) ease of application, 3) lower cost, if water is not available and has to be trucked. Moreover, curing compounds eliminate the difficulty of assessing the right time to apply conventional curing methods. Curing compounds are generally applied as soon as the finishing process has been completed or immediately after the water sheen disappears. Due to these advantages, the use of curing compounds for curing has increased in particular for applications involving large surface areas. As a result of the considerable demand, a variety of curing compounds are available in the market. Based on the chemical composition, these are categorised as wax emulsions, acrylic emulsions, chlorinated rubber based compounds, hydrocarbon resins and polyvinyl acetate based compounds (Guide for curing of cement concrete pavements, U.S. Department of Transportation 2006).

In the literature, curing compounds are mostly used as alternative means for curing of concrete. Most of the studies report their effect on strength and durability of concrete while studies on their influence on controlling plastic shrinkage cracking are meagre. The efficiency of a curing compound is highly variable and can reduce considerably with increase in temperature. In an investigation with 16 different curing compounds, it has been reported that the efficiency of curing compounds in reducing evaporation varied from 25% to 89%, and low efficiencies of below 47% were observed for 70% of the curing compounds investigated. The highest efficiency of 89% was obtained for a hydrocarbon resin based curing compound at temperature of 25°C and a relative humidity of 50%, but its efficiency reduced to 67% at temperature of 60°C and a relative humidity of 30% (Fattuhi 1986).

Curing compounds were effective in reducing plastic shrinkage strain compared to conventional methods of curing (Al-Gahtani 2010, Maslehuddin et al. 2013). The use of curing compounds has been reported to be the highly effective technique for mitigating early age cracking, specifically for construction of cement concrete pavements (Peyton 2006). The Indian Roads Congress also recommends the use of these compounds for construction of rigid pavements (IRC SP: 62-2014).

## **CHAPTER 3**

### **EXPERIMENTAL PROGRAM AND METHODOLOGY**

#### **3.1 Introduction**

An experimental programme has been designed to evaluate the influence of supplementary cementitious materials (SCM) on plastic shrinkage cracking obtained from the prime sources of South India. Additionally, further tests are done to assess the efficiency of shrinkage reducing components (i.e., fibres and SRAs) for providing better solutions for mitigating plastic shrinkage cracking. The program includes a series of experiments to fundamentally understand the effect of additives (SCM, fibres and SRAs) in the concrete. The emphasis was mainly on the plastic shrinkage crack dimensions and crack initiation time, in addition to the workability and compressive strength.

This chapter presents the details of the materials and experimental program used for the study. It includes an exhaustive description of the materials used in the study, followed by the concrete mix proportions and mixing procedure. The specifications of the equipment and procedure used to carry out the plastic shrinkage test are also described.

#### **3.2 Materials**

The materials that were used for producing concrete and to mitigate plastic shrinkage cracks are reported with their specifications in this section.

##### **3.2.1 Cements**

Commercially available 53 grade ordinary portland cement (OPC) conforming to IS 12269 was used in the control mix and the mixtures with supplementary cementitious materials. Two commercially available blended cements, namely portland pozzolana cement (PPC) and portland slag cement (PSC), conforming to IS 1489: Part 1 and IS 455, respectively, were also used for comparison. The physical properties and chemical composition of the cements are provided in Tables 3.1 and

3.2, respectively. The particle size distribution of the cements determined by the laser diffraction method is shown Figure 3.1.

Table 3.1: Physical properties of cements used in the study

Cement	Specific gravity	Blaine's fineness (m <sup>2</sup> /kg)	Setting time	
			Initial (min.)	Final (min.)
OPC	3.13	340	185	240
PPC	3.02	367	195	255
PSC	3.06	344	205	265

Table 3.2: Chemical composition of cements used in the study

Composition	OPC	PPC	PSC
	(% by mass)		
Calcium oxide (CaO)	62.16	50.23	53.52
Silica (SiO <sub>2</sub> )	20.95	29.50	30.02
Alumina (Al <sub>2</sub> O <sub>3</sub> )	5.14	9.28	6.46
Iron oxide (Fe <sub>2</sub> O <sub>3</sub> )	3.06	3.90	5.49
Magnesia (MgO)	1.33	1.65	2.70
Sulphur anhydrite (SO <sub>3</sub> )	3.08	2.72	-
Chloride (Cl)	0.009	0.003	-

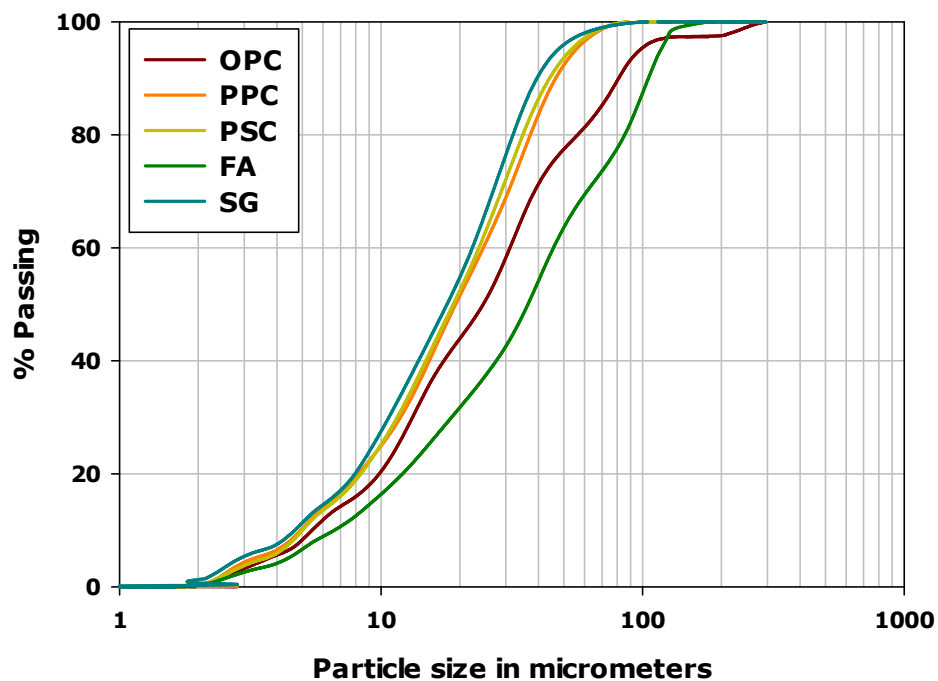


Figure 3.1: Particle size analysis of cements and mineral admixtures

### 3.2.2 Supplementary cementitious materials

Class F fly ash (FA) and ground granulated blast furnace slag or slag (SG) were used as supplementary cementitious materials for partial replacement of cement. Fly ash and slag conforming to IS 3812: Part 1 and IS 12089, respectively, were used in the study. The fly ash was obtained from the North Madras Power Plant, Chennai, while slag was obtained from the Jindal Steel Works (JSW). The Blaine's specific surface area, specific gravity and oxide composition of the mineral admixtures are provided in Table 3.3. The particle size distributions of the mineral admixtures determined by laser diffraction are also given in Figure 3.1.

Table 3.3: Properties of fly ash and slag

Materials	Slag	Fly ash
Specific gravity	2.88	2.22
Blaine's fineness (m <sup>2</sup> /kg)	410	275
Oxide composition		
Calcium oxide (CaO)	31.46	1.28
Silica (SiO <sub>2</sub> )	32.38	59.32
Alumina (Al <sub>2</sub> O <sub>3</sub> )	21.06	29.95
Iron oxide (Fe <sub>2</sub> O <sub>3</sub> )	1.87	4.32
Magnesia (MgO)	8.57	0.61
Sodium oxide (Na <sub>2</sub> O)	0.36	0.16
Potassium oxide (K <sub>2</sub> O)	0.88	1.44

### 3.2.3 Aggregates

The coarse aggregates used are from crushed granite, which complies with the grading requirements of IS 383-1970. Two different size fractions of 20–10 mm and 10–4.75 mm were used in the proportions of 65:35. The properties of the aggregates used are provided in Table 3.4. Locally available river sand conforming to Zone 2 of IS 383 was used as the fine aggregates. The coefficient of absorption and specific gravity of sand used in the study are shown in Table 3.4 while the sieve analysis results are shown in Figure 3.2.

Table 3.4: Properties of the aggregates used

Aggregates	Specific gravity	Coefficient of absorption (%)
Coarse aggregate (20 – 10 mm)	2.78	0.41
Coarse aggregate (10 – 4.75 mm)	2.76	0.43
Fine aggregate (0 – 4.75 mm)	2.63	0.72

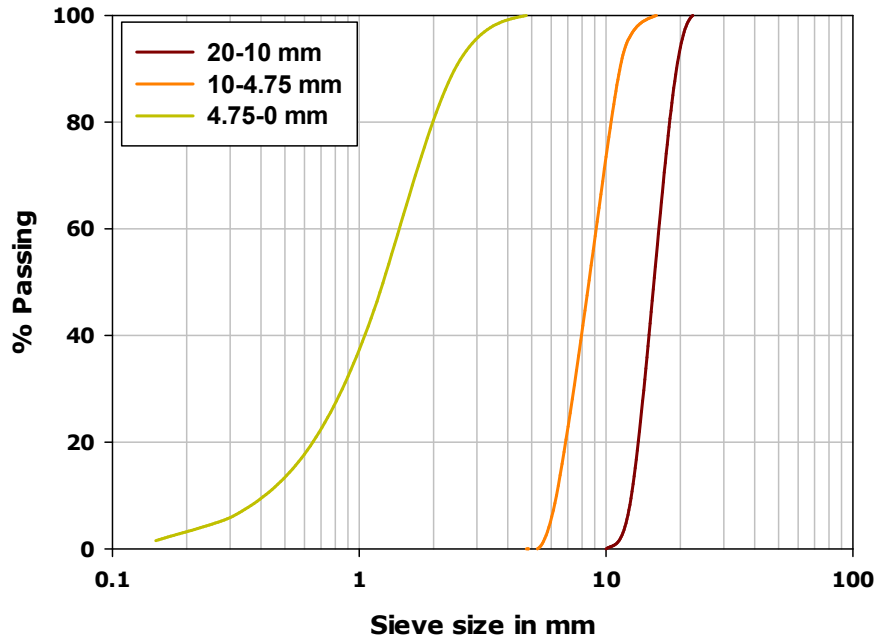


Figure 3.2: Sieve analysis of aggregates

### 3.2.4 Chemical admixtures

#### 3.2.4.1 Superplasticizer

A sulphonated naphthalene formaldehyde based superplasticizer was used to enhance the workability of the concrete. It was supplied by W.R Grace, with the brand name Daracem® 811; the product complies with BS 5075: Part 3. The specific gravity and active solid content of superplasticizer, as specified by the supplier, are 1.17 and 44.5%, respectively. The superplasticizer was incorporated at the dosage required to attain a slump of 100 – 120 mm in all the mixes, except the cases indicated later where references mixes are needed for assessing the effect of incorporating the superplasticizer.

#### 3.2.4.2 Shrinkage reducing admixture

Four shrinkage reducing admixtures, all supplied as liquids, were used in the study, and are denoted as BM, BT, GE and CS. They are expected to act by reducing the surface tension and, thereby, the capillary stresses induced by drying, and are not expected to have any expansive agents. These are incorporated at dosages of 1% and 2% with respect to the binder content, by weight, and an equivalent weight of water is removed.

### 3.2.4.3 Fibres

Four types of synthetic fibres and hooked-ended steel fibres were investigated for their efficiency in mitigating plastic shrinkage cracking. The synthetic fibres were polyacrylonitrile (PAN), polypropylene (PP), glass (GS) and polyester (PE). Some of the properties of the fibres are listed in Table 3.5. Synthetic fibres were incorporated at the dosage recommended by the supplier while the steel fibres were incorporated at a dosage of 10 kg/m<sup>3</sup>, which is the minimum dosage used in most applications. Additionally, a higher dosage was used in the cases of PAN and GS fibres. The dosages used are given in Table 3.6.

Table 3.5: Properties of fibres specified by the suppliers

Fibre	Length (mm)	Diameter (µm)	Tensile strength (GPa)	Elastic modulus (GPa)	Failure strain (%)	Specific gravity
Polyacrylonitrile	12	14.4	0.69	12.0	20	1.17
Polypropylene	12	20	0.55	6.8	25	0.92
Glass	12	14	1.70	72.0	2.4	2.68
Polyester	12	20	0.50	>5.0	20	1.34
Steel (hooked)	35	500	1.34	200.0	3.5	7.78

Table 3.6: Dosages of fibres

Fibre	Mass (kg)	V <sub>f</sub> (%)
Polyacrylonitrile	0.45, 1.20	0.04, 0.10
Polypropylene	0.90	0.10
Glass	0.60, 1.20	0.02, 0.04
Polyester	0.90	0.07
Steel	10.0	0.13

### 3.2.5 Curing compounds

Four generic curing compounds, namely wax-, acrylic resin-, water- and methacrylate resin-based, were assessed for their effect on plastic shrinkage cracking, and are denoted as WX, AR, WA and MR, respectively. The compounds comply with the requirements of ASTM C309-11. Among these compounds, three were white-pigmented (WX, AR and WA) while the other compound (MR) was a clear or

translucent without any dye. All the compounds were applied at a rate of 5 m<sup>2</sup> per litre, which is a common dosage specified by most suppliers.

### 3.3 Mix proportion

Normal strength concrete with water-to-binder ratio of 0.55 and binder content of 340 kg/m<sup>3</sup> were selected for the study. The ingredients are mix proportioned as per the guidelines of IS 10262: 2009 for attaining a characteristic strength of 30 MPa. The proportions of the control mix are shown in Table 3.7. Fly ash and slag are incorporated into this mix, at replacement levels of 15% and 30% by weight of cement. Additionally, for assessing blended cement performance, portland slag cement and portland pozzolana cement were used instead of the ordinary portland cement. For compensating the increase in volume of binder due to the difference in densities of the SCMs from cement, the total aggregate content was altered based on absolute volume calculations. However, the relative proportions of the different aggregate fractions were maintained constant. The mix proportions of all the concretes are provided in Table 3.7. Note that the aggregates are taken to be in the saturated surface dry condition.

Table 3.7: Mix proportion of concrete mixes

Constituents	Control Mix	Fly ash Mixes			Slag Mixes		
	CM	FA15	FA30	PPC	SG15	SG30	PSC
Cement	340	289	238	340	289	238	340
Mineral admixture	0	51	102	0	51	102	0
Coarse aggregate (20-10 mm)	703	696	689	698	702	700	701
Coarse aggregate (10-4.75 mm)	377	374	370	375	377	376	376
Fine aggregate	796	788	780	790	794	792	794
Water	187	187	187	187	187	187	187

### 3.4 Mixing procedure

Prior to mixing, the surface moisture of the aggregates (20 – 10 mm, 10 – 4.75 mm and fine aggregate) were determined by using a microwave oven; 250 grams of air-

dried sample was taken in a porcelain bowl and placed inside the microwave oven for 3 minutes at high power and its mass loss was calculated. The corresponding moisture correction was made in the mixing water to maintain the water-cement ratio.

Concrete was mixed in a rotary pan mixer of 40 litres (0.04 m<sup>3</sup>) capacity. Prior to the addition of materials, the surface of the pan and blades were moistened with water. The materials were added in the following sequence: first, the coarse aggregates (20 – 10 mm and 10 – 4.75) were added and followed by fine aggregate. The aggregates were dry mixed for two minutes. Then 20% of the mixing water was slowly introduced and allowed to mix for another minute. At the end of three minutes, the mix was allowed to rest for two minutes to allow for water absorption by the aggregates. After the rest period, the binder was added and mixed for two minutes. The remaining 80% of mixing water and superplasticizer (in mixes with the superplasticizer) were slowly introduced into the pan in motion and allowed to mix finally for three more minutes. The entire mixing process was for a period of 10 minutes. In mixes with shrinkage reducing admixtures, the admixture was combined with the remaining 80% mixing water and introduced. In cases of fibre reinforced concrete mixes, fibres were added in the last minute of mixing. Fibres were slowly added manually for ensuring uniform distribution. During the process of mixing, the side walls and bottom of the pan were scraped with a trowel to prevent loss of mortar and to attain a homogeneous mix. After the completion of mixing, the fresh properties of the concrete, namely slump and density were determined. Thereafter, the fresh concrete was placed in the oiled plastic shrinkage mould and vibrated on a table vibrator for 10 seconds. The excess concrete was removed with an aluminium straight-edge in the direction perpendicular to the stress riser. Finally, the surface was troweled to get a gelatinous surface and shifted to the environmental chamber. Simultaneously, 15 cubes of 100 mm were cast for each of the concrete mixtures to determine compressive strength and 9 prisms of 150 × 150 × 700 mm were cast for the control mix and the mixtures with fibres for flexure toughness determination.

### **3.5 Assessment of plastic shrinkage cracking potential**

Plastic shrinkage cracking of the concrete mixtures was evaluated as per ASTM C1579-2013. According to the Standard, the concrete has to be filled in the plastic shrinkage mould and exposed to controlled hot and dry conditions to induce

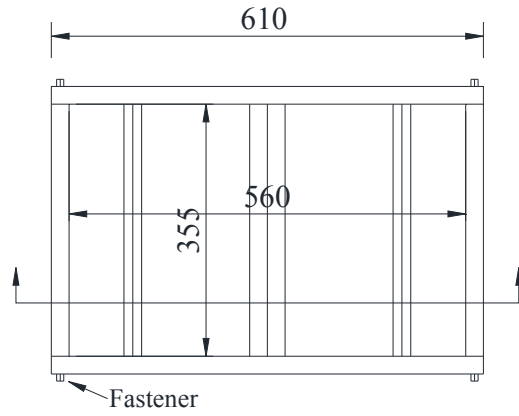
plastic shrinkage cracking. The cracks were quantified and compared between the mixtures. The details of the test chamber used for attaining hot and dry conditions, the test configuration and crack microscope used in the study are discussed in this section.

### **3.5.1 Environmental chamber**

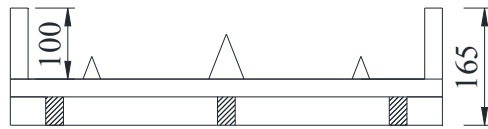
The evaporative potential of the atmosphere surrounding the concrete is an important parameter for causing plastic shrinkage cracking. The ASTM C1579 – 13 Standard prescribes a minimum evaporation rate of 1 kg/hr/m<sup>2</sup> (from a free water surface) for the test. Such high rates of evaporation are possible only at a high temperature, low relative humidity and high wind speed. For stimulating appropriate conditions, an environmental chamber was specially designed. The internal dimensions of the chamber are 77 × 100 × 50 cm. The operating range of temperature is from ambient temperature to 50°C and the relative humidity range is from 30% to 60%. Besides controlling temperature and humidity, the chamber is built with a horizontal blower to circulate air uniformly over the surface of the specimen and to produce a high rate of evaporation from the concrete surface. The blower is capable of generating air velocities ranging from 0.5 to 5 m/s. With these environmental conditions, the chamber was able to generate conditions conducive to plastic shrinkage cracking. The design details and performance evaluation of the test chamber are discussed in detail in Appendix A.

### **3.5.2 Test configuration**

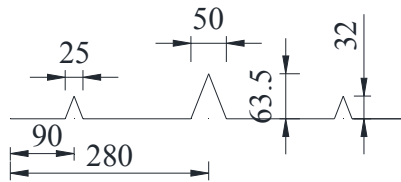
The plastic shrinkage mould for the study was fabricated as per the ASTM Standard using acrylic sheets. The mould has the internal dimensions of 560 mm length, 355 mm width, and 100 mm depth. It has two end restraints of 32 ± 1 mm high placed at 90 ± 2 mm inwards from either ends to restrain the concrete. Additionally, a stress riser of 63.5 ± 1 mm high is placed at the centre to induce cracking. Drawings of the mould and the image of fabricated mould are shown in Figures 3.3 and 3.4, respectively.



PLAN



SECTION



DIMENSIONS OF STRESS RISER

All dimensions are in mm

Figure 3.3: Plastic shrinkage test configuration



Figure 3.3: Plastic shrinkage mould

### 3.5.3 Crack microscope

A crack microscope is a handheld instrument for measuring crack widths with high precision. The eyepiece of microscope is equipped with a linear scale called graticule and enables the measurement of any planar dimensions. The microscope is provided with a knob to focus on the crack, and the eyepiece can be rotated 360° to align the graticule perpendicular to the crack to measure crack widths. The measuring range of the crack microscope is 0 to 2.5 mm; the 2.5 mm measuring scale is divided into divisions of 0.25 mm, which are subdivided further into divisions of 0.025 mm. Figures 3.5(a) and (b) show the crack microscope and graticule of the eye piece, respectively.



(a)



(b)

Figure 3.4: (a) Crack microscope and (b) Graticule

### 3.6 Test procedure

Within thirty minutes after the contact between water and cement during mixing, the concrete specimens were cast, placed, finished and shifted to the environmental chamber. In the chamber, the specimens were exposed to a temperature of  $42 \pm 1^\circ\text{C}$ , relative humidity of  $35 \pm 5\%$  and air velocity of  $4.5 \pm 0.5$  m/s. The specimens were inspected every 30 minutes for signs of cracking, and the crack initiation times were noted. Specimens were exposed to these conditions for 24 hours. Also, pans filled with concrete and water were placed beside the specimen to monitor moisture loss. These pans were weighed at regular intervals of 30 minutes for a period of 4 hours.

After 24 hours, the specimens were removed from the environmental chamber and allowed to cool for 24 hours, after which the residual crack dimensions were determined.

For determining the crack area, crack widths were measured using the crack microscope at regular intervals of 10 mm along the crack length, and the crack length was measured using a thread. 10 mm intervals were marked on along the crack with the help of markings on the thread as shown in Figures 3.6 and 3.7.



Figure 3.5: Measurement of crack width and length



Figure 3.6: Closer view of marked thread

### **3.7 Fresh properties of concrete - experimental methods**

The fresh properties determined were slump, unit weight and final setting time of concrete. Slump and unit weight were measured in accordance with ASTM C143-12 (Standard test method for slump of hydraulic cement concrete) and ASTM C138-14 (Standard test method for density, yield and air content of concrete), respectively. The final setting of concrete was determined as per IS 8142-1976 (Method of test for determining setting time of concrete by penetration resistance).

For determining the final setting time of concrete, it was wet-sieved on to a non-absorptive surface through 4.75 mm sieve. The mortar thus obtained was thoroughly remixed and placed in a watertight container (of  $150 \times 150 \times 150$  mm) in three layers. Each layer was consolidated by rodding with a tamping rod to remove entrapped air. The mortar was filled at least 10 mm below the top edge of the container to facilitate collection and removal of bleed water, and also to avoid contact between the mortar and protective covering. Prior to the penetration measurements, the bleed water accumulated at the surface was removed using a syringe after tilting the container by placing a block under one side of it. Penetration tests were made at hourly intervals after 4 hours from initial contact of cement with water. Depending on the degree of hardening of the mortar, the appropriate needle was inserted in the penetration resistance apparatus and brought into contact with the surface. Force was gradually and uniformly applied on the handle. The force required to produce a 25 mm penetration and the time of application (measured as elapsed time, from initial contact of cement with water) were recorded. Penetration resistance is calculated using the bearing area of the needle. The final setting time is defined as the time elapsed to attain a penetration resistance of  $26.97 \text{ N/mm}^2$ .

### **3.8 Experimental methods for hardened properties of concrete**

#### **3.8.1 Compressive strength**

Compressive strength of all the mixtures was determined using a 3 MN capacity Controls testing machine. Figure 3.8(a) shows the machine and Figure 3.8(b) shows the close-up view of the loading frame. Concrete cubes of 100 mm size were tested at 1, 3, 7, 14 and 28 days. Three cubes were tested at each age, at a loading rate of 2289 N/s, in accordance with IS 516 - 1959 (Methods of tests for strength of concrete).



(a)



(b)

Figure 3.7: Compression test setup (a) testing machine and (b) Close-up view

### 3.8.2 Flexural toughness

The most important characteristic of incorporating fibres in concrete is the enhancement in the flexural response of the concrete. This mechanical property of fibre reinforced concrete differs significantly from that of unreinforced concrete. In general, it is widely accepted that incorporation of fibres improves the resistance to crack growth and ductility. However, the improvement in flexural toughness of concrete at fibre dosages required to mitigate plastic shrinkage cracking remains a question. In order to determine this, three point flexural beam tests were carried out.

Fibre reinforced concrete prisms were tested at the age of 28 days in 1 MN closed-loop servo-controlled Controls testing system, under constant deflection rate. Specimens were tested in a simply supported configuration with a span of 450 mm, and subjected to third-point loading, as shown in the Figure 3.9. It was made sure that in all the cases the loading direction was perpendicular to the direction of casting so as to nullify the unconservative bias that may arise due to the settlement of fibres. Deflections were measured using two Linear Variable Displacement Transducers (LVDTs) of 1 micron accuracy. LVDTs were fixed on either side at mid-height of the specimens using yoke frames. These yokes were clamped to the specimen by screw heads as shown in Figure 3.9. LVDTs were made to rest on the S shaped brackets that were glued to the top surface of the specimen. The deflection measurement setup used in the study conforms to ASTM C1609-12 (Standard test method for flexural

performance of fibre reinforced concrete) and JSCE–SF4 (Method of tests for flexural strength and flexural toughness of steel fibre reinforced concrete).



Figure 3.8: Third point loading test configuration

Initially, tests were started under load control with a constant load rate of 100 N/s. After attaining 20% of the estimated peak load, the control variable is switched to displacement, and the test is done at a constant rate of 0.5 m/s. Tests were stopped when either the load carrying capacity drops to 3 kN or failure of the specimen occurs. The control parameters of closed loop control were decided based on previous experience and the testing machine characteristics. A minimum of six prisms were tested for each fibre concrete for determining the flexural parameters.

The load deflection curves were obtained for each specimen and consequently various flexural parameters, namely, flexural strength, equivalent flexural strength and equivalent flexural strength ratio, were calculated.

### 3.8.2.1 Flexural strength

For the simply supported three point loading configuration, the expression for flexural strength ( $f_{ct}$ ) is:

$$f_{ct} = \frac{Pl}{bd^2} \quad 3.1$$

where P is the first peak load in N, and l, b and d are span length, width and depth of the specimen in mm, respectively.

### 3.8.2.2 Equivalent flexural strength

The equivalent flexural strength ( $f_{e,n}$ ) is the representative measure of the toughness of the fibre concrete, and gives the average strength up to a specified deflection. It is calculated using the average load ( $P_{e,n}$ ) from the expression:

$$P_{e,n} = \frac{T_{e,n}}{\delta_n} \quad 3.2$$

yielding,

$$f_{e,n} = \frac{P_{e,n} \times l}{bd^2} \quad 3.3$$

where  $T_{e,n}$  is the area under the curve up to the deflection  $\delta_n = l/n$ , and  $n$  denotes the deflection limit; normally,  $n = 150$  and  $300$  (i.e., for a span of  $450$ , the deflections of  $3$  and  $1.5$  mm, respectively).

### 3.8.2.3 Equivalent flexural strength ratio

Equivalent Flexural Strength Ratio ( $R_{e,n}$ ) is the ratio between the mean equivalent flexural strength ( $f_{me,n}$ ) and the mean flexural strength ( $f_{mct}$ ) at a specified deflection, given as:

$$R_{e,n} = \frac{f_{me,n} \times 100}{f_{mct}} \quad 3.4$$

## 3.9 Summary

This chapter outlines the properties of all the materials, mix proportioning, and the mixing procedure used for the study. It also describes the various test procedures used for the determination of fresh and hardened properties of concrete. In addition, the methodology and configuration adopted for the assessment of the plastic shrinkage cracking were discussed comprehensively.

## **CHAPTER 4**

# **INFLUENCE OF SUPPLEMENTARY CEMENTITIOUS MATERIALS ON THE PLASTIC SHRINKAGE CRACKING OF CONCRETE**

### **4.1 Introduction**

Supplementary cementitious materials (SCMs) are being extensively used in concrete either as a replacement for portland cement or in blended cements. The use of blended cements and SCMs in concrete is being promoted for producing better performance, as well as for environmental concerns (i.e., reduction of carbon footprint of cement and better exploitation of the clinker). Incorporation of SCMs in concrete or usage of blended cements usually modifies the properties of concrete in both fresh and hardened states, compared to the use of only ordinary portland cement. Generally, these materials retard the setting of concrete, bleeding and early-age strength. When concretes with these materials are used in structures with extensive surface areas, such as pavements, slabs, bridge decks, tunnel linings, etc., there is a serious concern for plastic shrinkage cracking, especially in hot and dry conditions. Such premature surface cracks may accelerate the ingress of harmful agents, and impair the durability and serviceability of the structures.

For studying the influence of supplementary cementitious material and blended cements on plastic shrinkage cracking, the mixes mentioned in the previous chapter were assessed. Three mixes, CM, FA15 and FA30, having slumps of 100 – 120 mm, without superplasticizer, and four other mixes, PPC, SG15, SG30, and PSC mixes, each with an appropriate dosage of superplasticizer added to attain the desired slump range, were tested. The effect of the addition of the superplasticizer in the mixes PPC, SG15, SG30 and PSC on plastic shrinkage cracking was assessed by comparing the results with tests of identical concretes without the incorporation of superplasticizer.

This chapter reports the experimental results of the concrete mixtures investigated in the study. The influence of supplementary cementitious materials and blended cements on plastic shrinkage cracking of concrete was analyzed based on the results obtained. Other properties such as workability, fresh unit weight, final setting

time and compressive strength were also evaluated. Finally, the discussion of the results and the summary of the results are presented.

## 4.2 Fresh and hardened properties of concrete

### 4.2.1 Workability

The slump data for all the mixes are given in Table 4.1. The replacement of fly ash for ordinary portland cement (OPC) did not affect the workability of the concrete. On the other hand, the use of blended cements (PPC and PSC) and the combination of OPC and slag reduced the workability significantly. Hence, in these mixes, superplasticizer had to be used for attaining the target slump, as mentioned earlier. The dosages of superplasticizer required for the respective mixes were fixed based on trials, and are reported in Table 4.1. Blended cements and slag being finer than OPC had higher water demand (see Chapter 3), leading to the lower workability of concrete.

### 4.2.2 Fresh unit weight

Fresh unit weights of various concrete mixes are summarized in Table 4.1. It can be seen that the unit weight decreases slightly as OPC is replaced with fly ash whereas the unit weights of the other mixes are similar. The decrease in the fresh unit weight in case of fly ash mixes is due to the difference between the densities of the fly ash and OPC. The density of the fly ash is less than the density of OPC. Hence, weight replacement of these low density material for OPC with fly ash slightly increases the paste volume fraction (see Figure 4.1) in concrete and decreases the fresh unit weight.

Table 4.1: Fresh properties of concrete

Mix ID	Fresh unit weight (kg/m <sup>3</sup> )	Dosage of SP (% of binder content)	Slump (mm)
CM	2445	0	100-120
PPC	2425	0.20	100-120
PSC	2420	0.32	100-120
FA15	2415	0	100-120
FA30	2390	0	100-120
SG15	2430	0.23	100-120
SG30	2420	0.38	100-120
PPC*	2425	0	30-50
PSC*	2420	0	30-50
SG15*	2430	0	30-50
SG30*	2420	0	30-50

Note: \*without superplasticizer

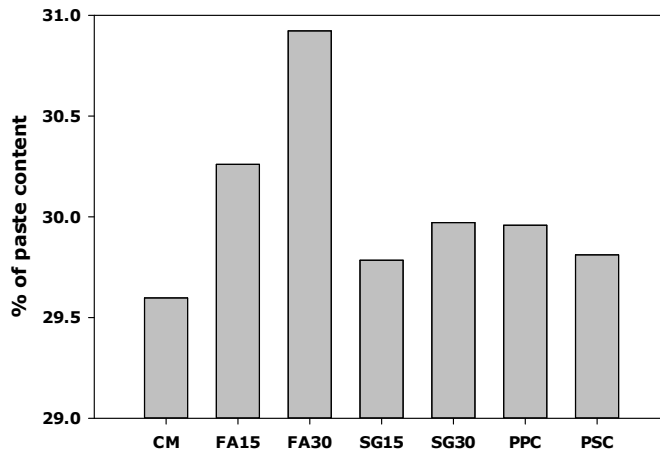


Figure 4.1: Paste content in various mixes

#### 4.2.3 Final setting times

The final setting times from three trials on each of the concrete mixes with slumps of 100-120 mm are shown in Figure 4.2 and Table 4.2. From the results, it is clear that the setting was retarded in all the mixes, relative to control mix. The maximum retardation was observed in the FA30, SG30 and PSC concretes. In these cases, the final setting time was about an hour longer than that of the control mix. The observed increase in final setting time can be attributed to the slow rate of hydration. These results are in agreement with the findings reported by Brooks et al. (2000), Marthong and Agrawal (2012), and Siddique and Bennacer (2012).

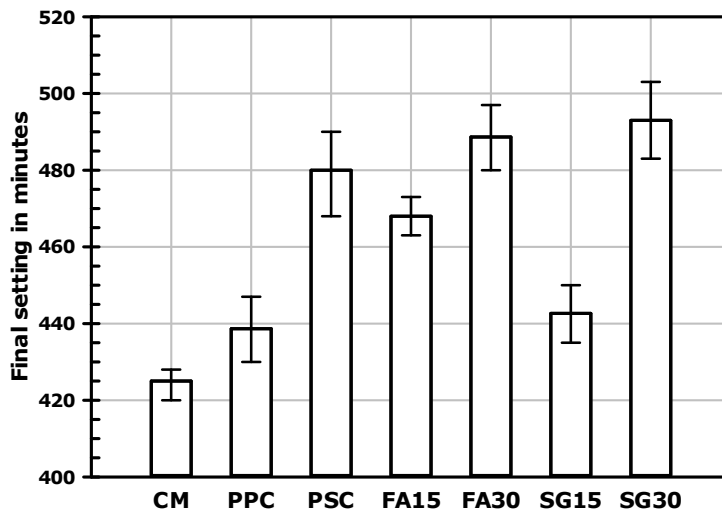


Figure 4.2: Final setting time of concretes

Table 4.2: Final setting times: average and standard deviation

Mix ID	Average final setting time (min)	S.D	CoV (%)
CM	425	4.4	1.0
PPC	440	8.5	1.9
PSC	480	11.1	2.3
FA15	470	5.0	1.1
FA30	490	8.5	1.7
SG15	440	7.5	1.7
SG30	495	10.0	2.0

S.D and CoV – standard deviation and coefficient of variation for 3 trials

#### 4.2.4 Compressive strength

The compressive strength data for all the concrete mixtures are given in Table 4.3, and the average compressive strengths are plotted against age in Figures 4.3 to 4.5. From Figure 4.3, it can be seen that the commercially-available blended cements PPC and PSC resulted in lower strength at all the ages, relative to the control mix, as expected. At 28 days, the compressive strength of control mix was 45.5 MPa whereas the compressive strength of PPC and PPC mixes were 39.9 and 31.2 MPa, respectively. Figures 4.4 and 4.5 show the variation in strength development due to the incorporation of fly ash and slag at replacement levels of 15% and 30%, respectively. It is evident that the compressive strength declined at all ages with the increase in fly ash and slag dosage, with a stronger effect in the case of fly ash; at 28 days, the decrease in compressive strength at 30% replacement of fly ash and slag are 21% and 12%, respectively.

The results obtained in this work confirm the conclusions of Siddique (2004), Mittal et al. (2008), Marthong and Agrawal (2012), and Dhanya (2015), who reported that the incorporation of Indian fly ashes (that are coarser than cement) reduces the compressive strength of concrete. Similarly, researchers such as Siddique (2012), Qiang (2013), and Dhanya (2015) have concluded that the replacement of cement with Indian slag reduces the early compressive strength of concrete.

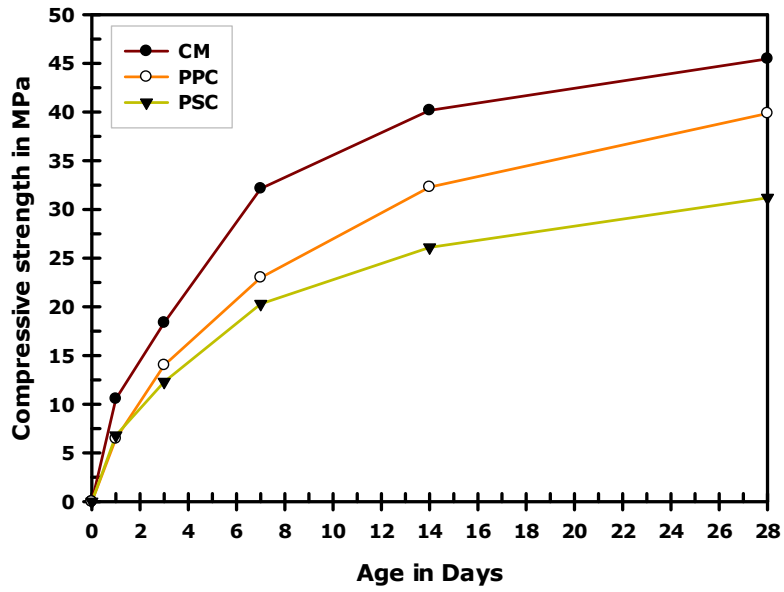


Figure 4.3: Compressive strength development for three different cements

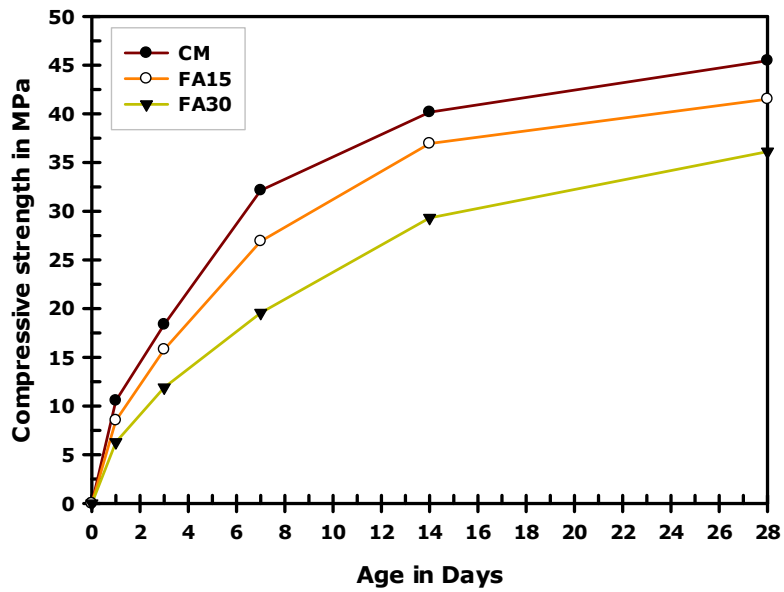


Figure 4.4: Compressive strength development for fly ash concretes

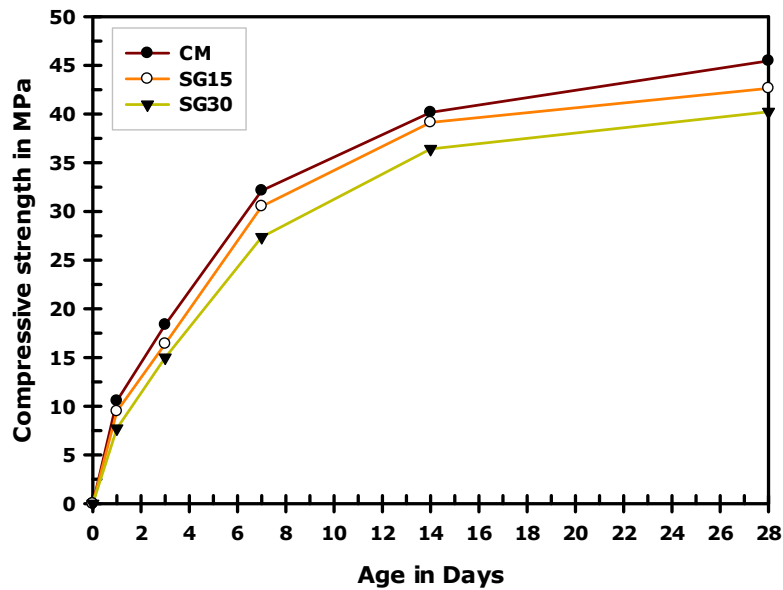


Figure 4.5: Compressive strength development for slag concretes

Table 4.3: Compressive strengths at various ages

Mix ID	Compressive strength (MPa)									
	1 day		3 days		7 days		14 days		28 days	
	Mean	S.D	Mean	S.D	Mean	S.D	Mean	S.D	Mean	S.D
CM	10.5	0.2	18.4	0.4	32.1	1.6	40.2	1.2	45.5	1.2
PPC	6.5	0.2	14.1	0.3	23.0	0.5	32.3	0.8	39.9	1.5
PSC	6.8	0.1	12.3	0.2	20.3	0.7	26.1	0.5	31.2	0.4
FA15	8.5	0.7	15.8	0.4	26.9	2.1	37.0	1.1	41.5	1.9
FA30	6.3	0.5	11.9	0.5	19.6	0.3	29.3	0.5	36.1	1.5
SG15	9.5	0.3	16.4	0.1	30.5	0.4	39.1	1.5	42.6	0.4
SG30	7.7	0.1	15.1	0.2	27.4	0.5	36.4	0.4	40.2	0.6

Note: S.D – standard deviation for 3 specimens

### 4.3 Plastic shrinkage results

Figures 4.6 to 4.12 show the images of the surfaces of the specimens with plastic shrinkage cracking. It can be observed that, in all the cases, the cracks are formed at the middle of the specimen, i.e. above the stress riser; they are initiated above the centre of the stress riser and propagate towards the ends. In concretes with lower cracking potential (i.e., CM, FA15 and FA30), cracking does not extend over the entire width of the specimen whereas in the others the crack covers the width of the specimen. The crack data for all the concretes investigated is summarized in Table 4.4.



Figure 4.6: Plastic shrinkage cracking in CM

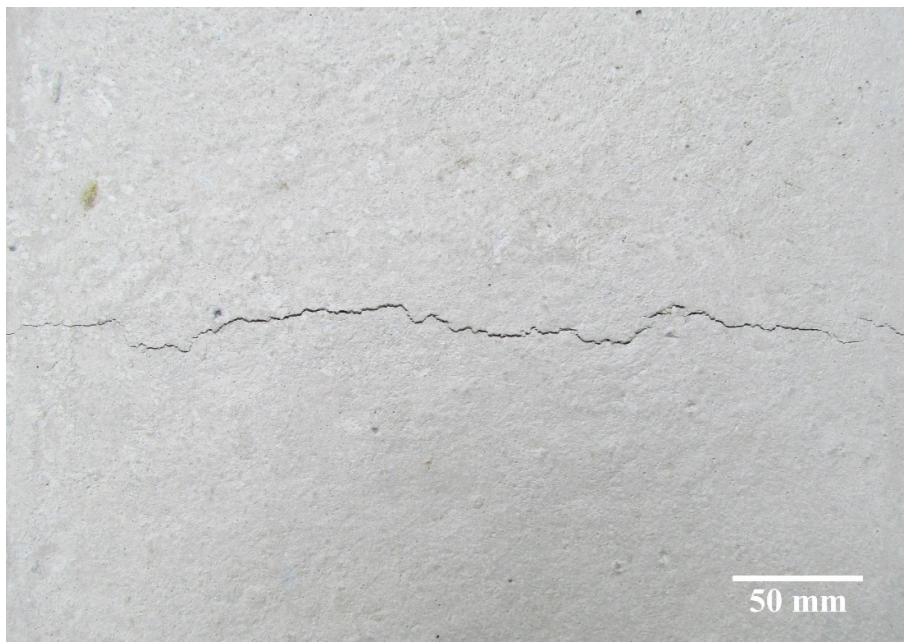


Figure 4.7: Plastic shrinkage cracking in PPC

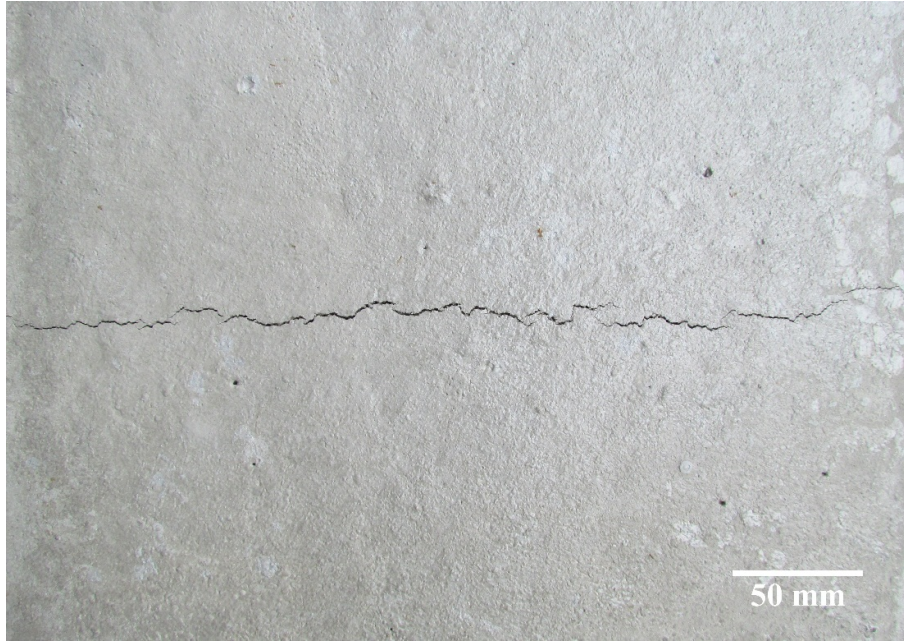


Figure 4.8: Plastic shrinkage cracking in PSC



Figure 4.9: Plastic shrinkage cracking in FA15



Figure 4.10: Plastic shrinkage cracking in FA30

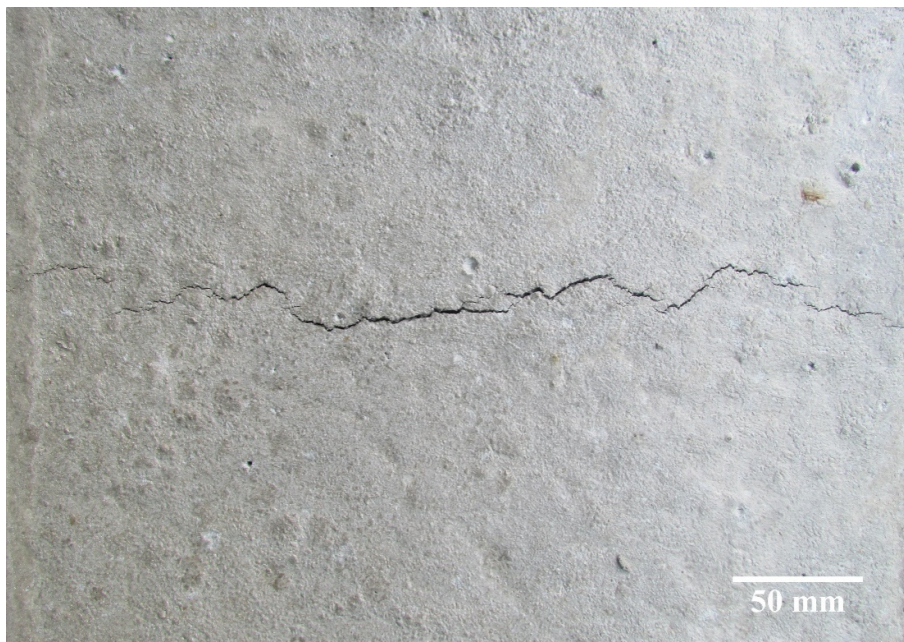


Figure 4.11: Plastic shrinkage cracking in SG15

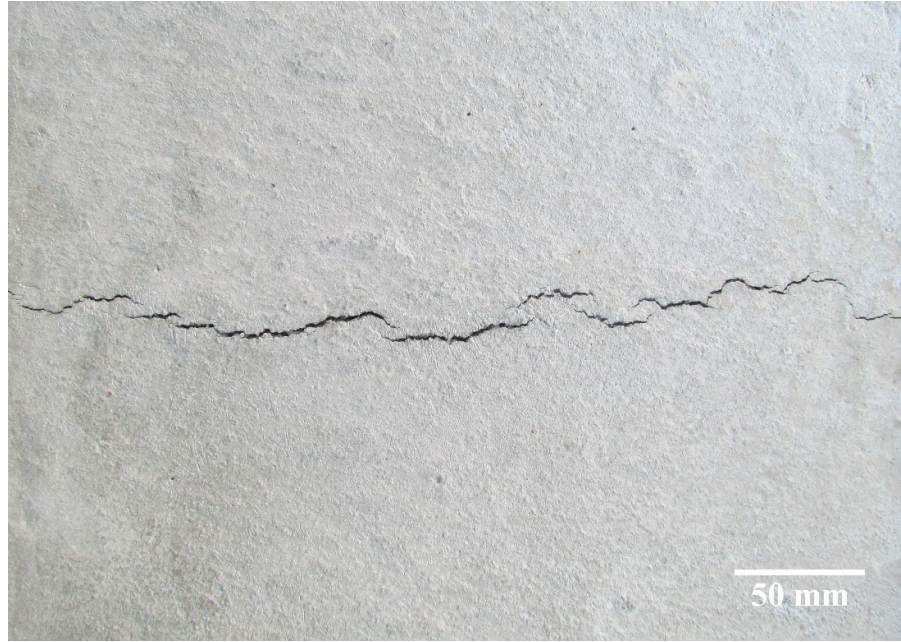


Figure 4.12: Plastic shrinkage cracking in SG30

Table 4.4: Summary of test results

Mix ID	Crack initiation time (min)	Crack properties				% increase in crack area	% increase in mean crack width
		Crack area (mm <sup>2</sup> )	Crack length (mm)	Max. crack width (mm)	Mean crack width (mm)		
CM	207	97	263	0.68	0.37	-	-
PPC	172	223	425	1.12	0.53	129	42
PSC	192	278	399	1.27	0.70	185	88
FA15	180	121	303	0.93	0.40	24	7
FA30	167	138	333	1.03	0.42	42	12
SG15	197	225	427	1.25	0.53	132	42
SG30	183	402	444	1.73	0.91	313	144

#### 4.3.1 Influence of blended cements on plastic shrinkage cracking

The cracking data for the concretes with the three different cements are presented in Figures 4.13 to 4.16. The results indicate that the minimum crack area was observed in case of the control mix and the crack areas were higher for the blended cements. The average crack area in control mix was 100 mm<sup>2</sup> while in the cases of PPC and PSC, it increased to 220 mm<sup>2</sup> and 280 mm<sup>2</sup>, respectively. The maximum crack width in the control mix was 0.6-0.7 mm while in the case of concrete with blended cements, the crack widths were in order of 1.0 to 1.4 mm. From Figure 4.13, it can be

noted that, compared to the control mix, the mean crack width increased by 41% and 88% in PPC and PSC, respectively. Moreover, the cracks were initiated earlier in the concretes with blended cements than in the control mix (see Figure 4.16).

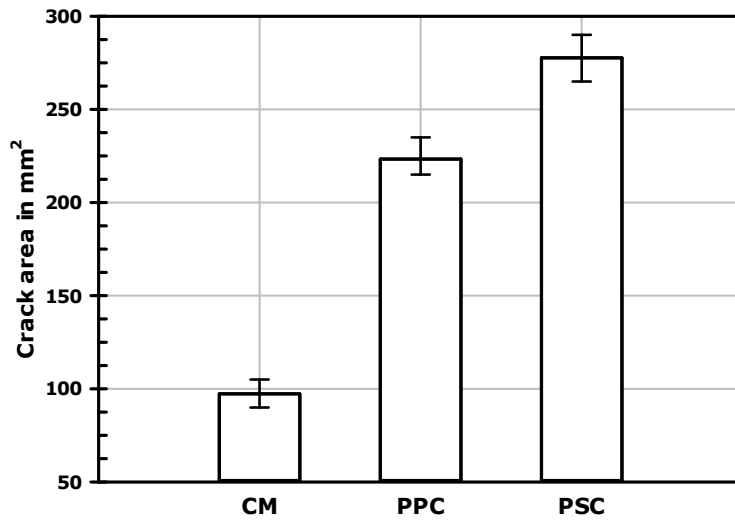


Figure 4.13: Crack area of concretes with different cements

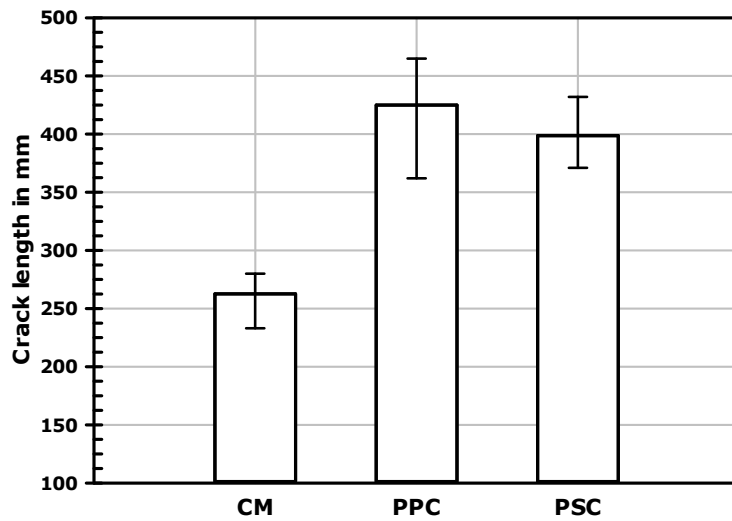


Figure 4.14: Crack length of concretes with different cements

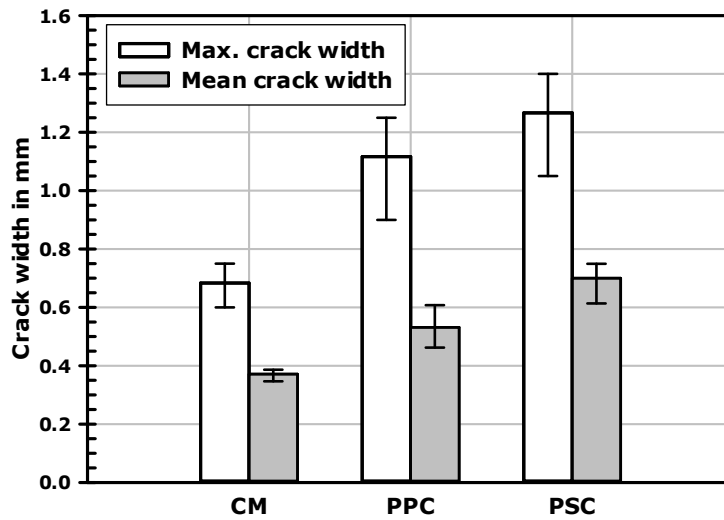


Figure 4.15: Crack width of concretes with three different cements

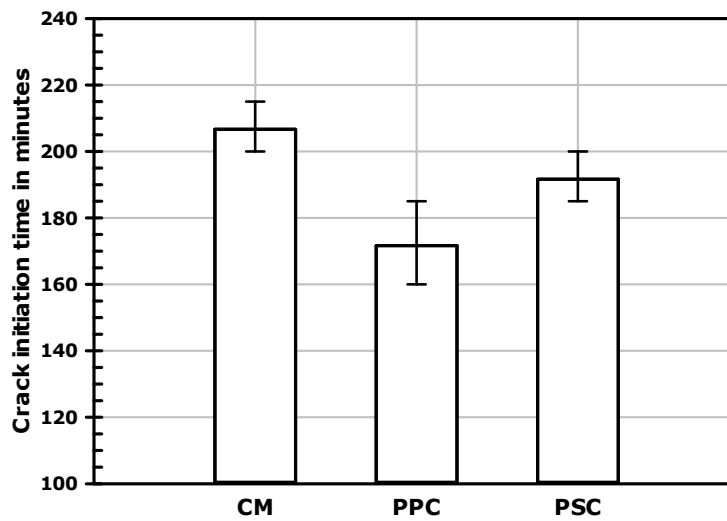


Figure 4.16: Crack initiation time of concretes with three different cements

### 4.3.2 Influence of fly ash on plastic shrinkage cracking

Figures 4.17 to 4.20 show the crack area, crack length, maximum crack width, mean crack width and crack initiation time for the concretes incorporating fly ash, respectively. Increases in crack area, crack length and maximum crack width were observed with incorporation of fly ash; the crack area, length and maximum width were increased by 42%, 27% and 51%, for 30% replacement. Also, the mean crack width increased slightly by 7% and 12% at replacement levels of 15% and 30%,

respectively. The cracks were initiated 30 minutes earlier in these mixes compared to the control mix.

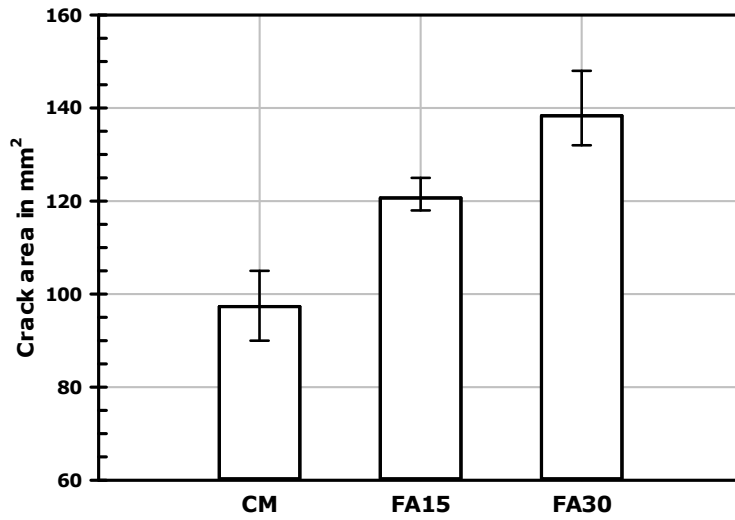


Figure 4.17: Crack area of concretes at different replacement levels of fly ash

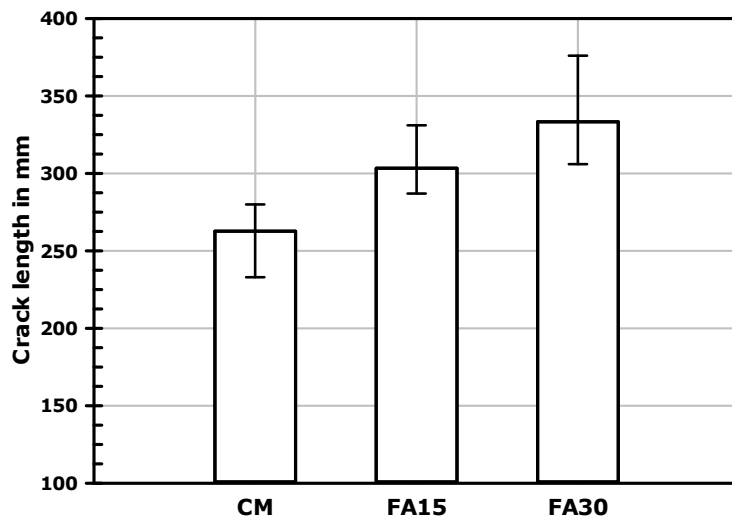


Figure 4.18: Crack length of concretes at different replacement levels of fly ash

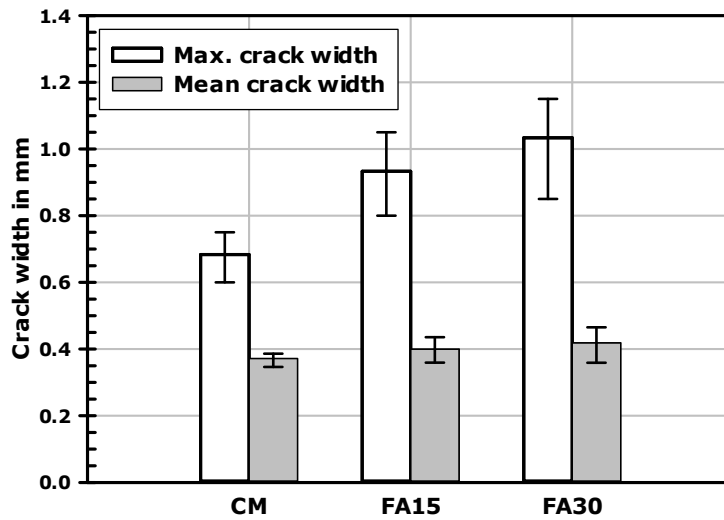


Figure 4.19: Crack width of concretes at different replacement levels of fly ash

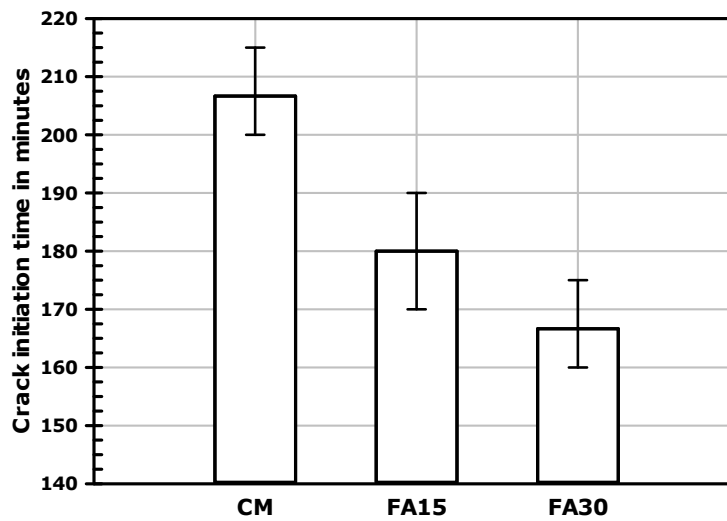


Figure 4.20: Crack initiation of concretes at different replacement levels of fly ash

### 4.3.3 Influence of slag on plastic shrinkage cracking

The overall data including crack area, crack length, maximum crack width, mean crack width and crack initiation time for the mixes with slag are presented in Figures 4.21 to 4.24, respectively. Figures 4.21 and 4.23 clearly indicate that the incorporation of slag resulted in a significant increase in both crack area and maximum crack width, relative to the control mix. The crack area in the control mix was 100 mm<sup>2</sup>, and increased, at the replacement levels of 15% and 30%, to 225 mm<sup>2</sup> and 400 mm<sup>2</sup>,

respectively. This was also accompanied by a significant increase in the maximum crack width. At 30% replacement level, the maximum crack width observed was 1.9 mm while in the control mix, the maximum crack width was in the order of 0.6-0.7 mm. Moreover, from [Figure 4.23](#), it can be illustrated that, relative to control mix, the mean crack width increased by 40% and 140% in the SG15 and SG30 mixes, respectively. The crack initiation times are plotted in Figure 4.24. It can be observed that the time for the first crack was lower in these mixes.

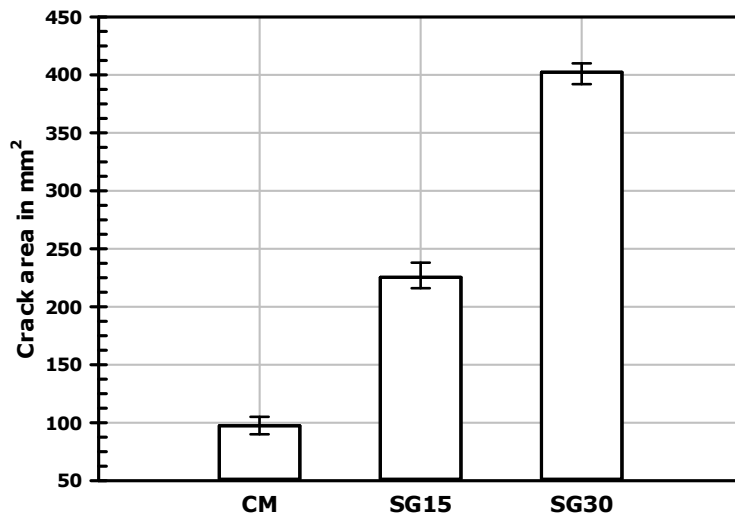


Figure 4.21: Crack area of concretes at different replacement levels of slag

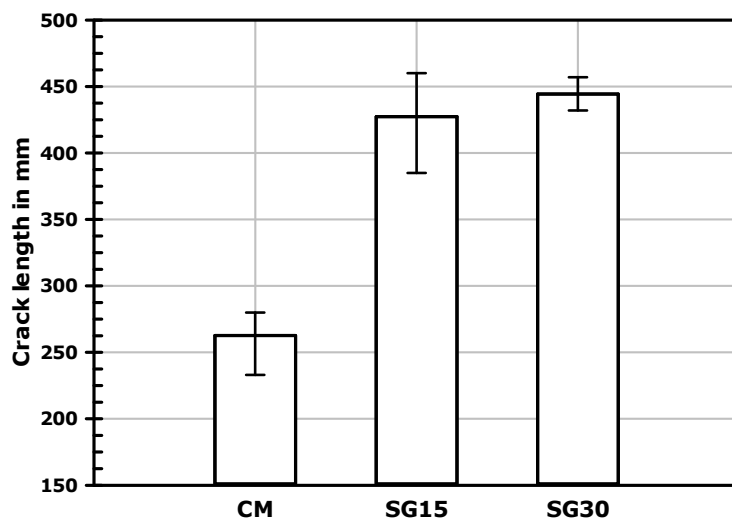


Figure 4.22: Crack length of concretes at different replacement levels of slag

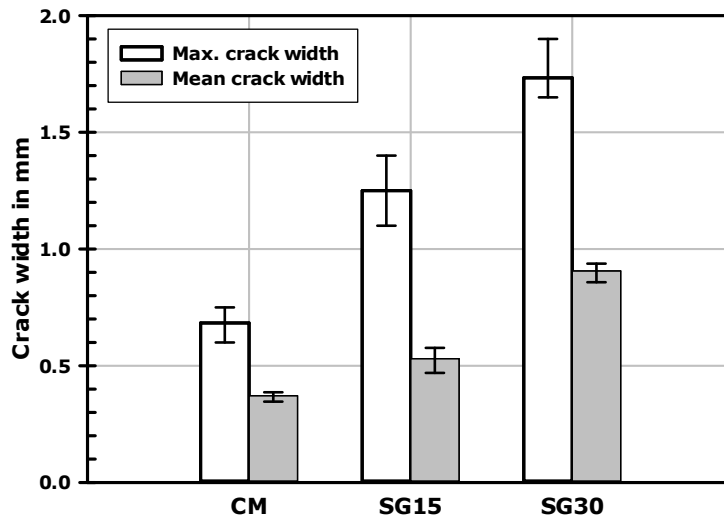


Figure 4.23: Crack width of concretes at different replacement levels of slag

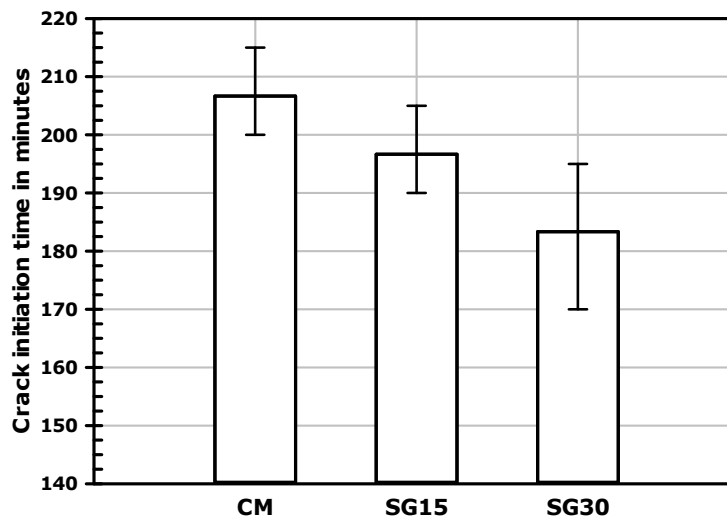


Figure 4.24: Crack initiation of concretes at different replacement levels of slag

#### 4.3.4 Influence of superplasticizer on plastic shrinkage

The plastic shrinkage cracking results of the concrete mixes in which superplasticizer was used are summarized in Figures 4.25 to 4.29. At the dosage of superplasticizer incorporated, a marginal decrease in crack area and length was observed in all the concretes with the superplasticizer, inspite of having a much higher slump. In addition, the maximum and mean crack widths decreased slightly, compared to the concretes without superplasticizer. Moreover, the crack initiation was delayed for

these concretes with the use of superplasticizer. Previous studies by Cabrera et al. (1992) and Al-Amoudi et al. (2005) have also reported that superplasticizers could have a beneficial effect in reducing plastic shrinkage cracking.

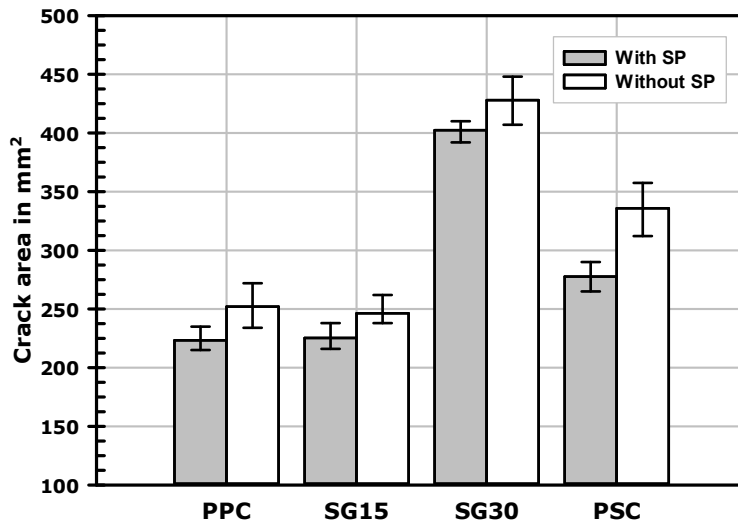


Figure 4.25: Crack area of concretes with and without superplasticizer

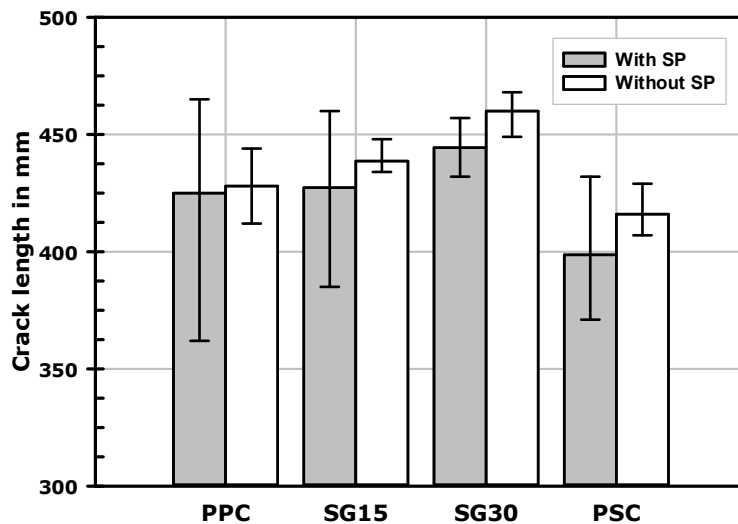


Figure 4.26: Crack length of concretes with and without superplasticizer

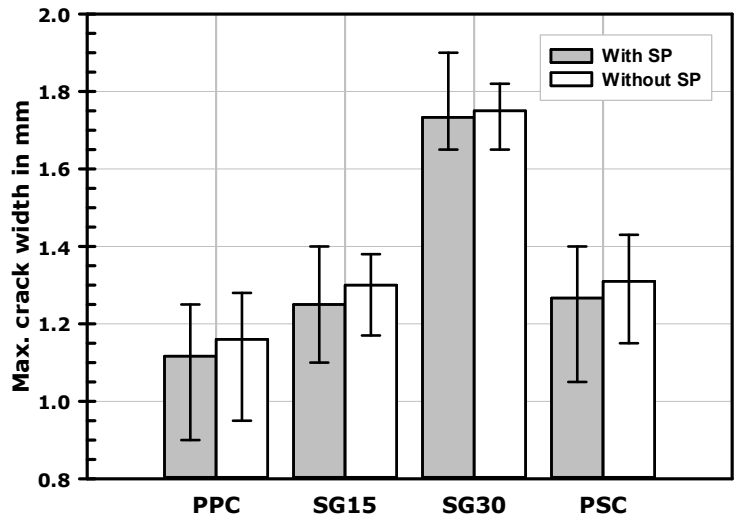


Figure 4.27: Maximum crack width of concretes with and without superplasticizer

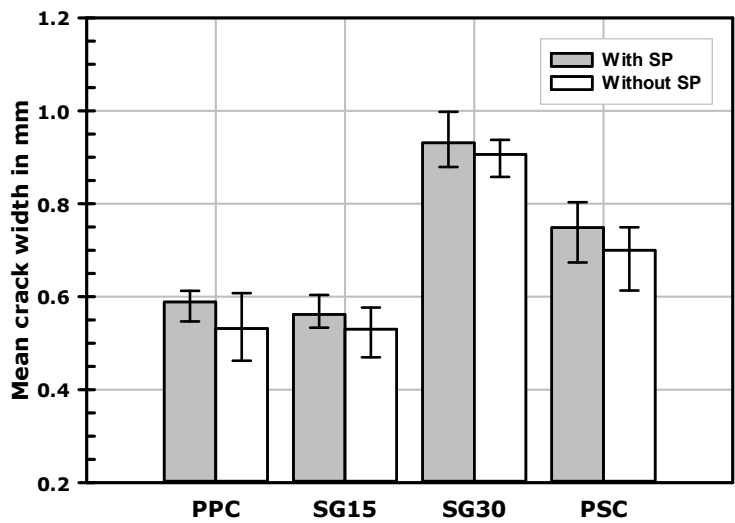


Figure 4.28: Mean crack width of concretes with and without superplasticizer

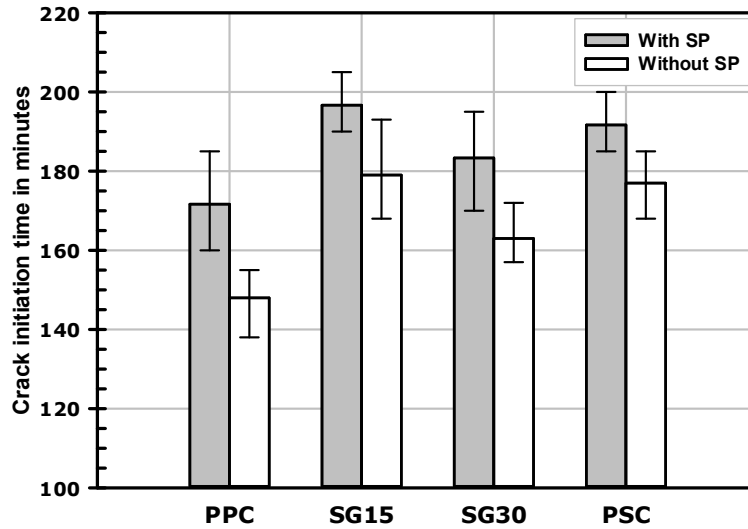


Figure 4.29: Crack initiation time of concretes with and without superplasticizer

#### 4.4 Evaporation rates

Figure 4.30 shows the cumulative rate of evaporation over four hours for various concretes having a slump of 100-120 mm, determined by measuring the change in weight of the pans filled with concrete and water. The straight line shows the rate of evaporation from the free water surface, corresponding to an average of about 0.90 kg/m<sup>2</sup>/hr. It can be seen that the rate of moisture loss from the concrete was initially equal to that of water and later decreases gradually with time. The rate of evaporation from all the concretes was similar, with no significant variation observed due to the replacement of cement with SCMs or blended cements. The intention was to assess the evaporation rates on uncracked surfaces, mainly to represent the severity of the environment and to compare the effects on different concretes.

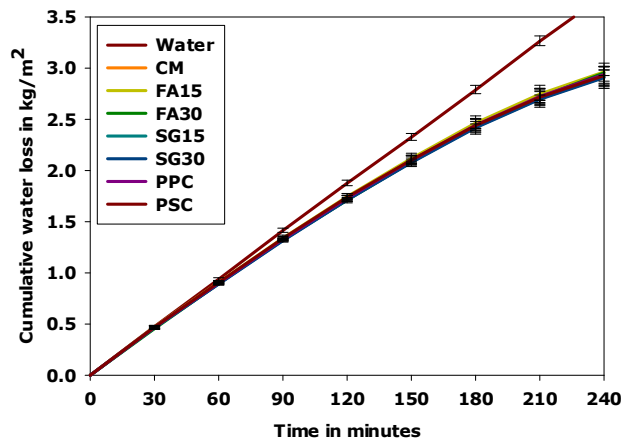


Figure 4.30: Cumulative rate of evaporation of various concretes

## 4.5 Capillary pressure

The main driving force that leads to plastic shrinkage cracking in cementitious systems is the build-up of the capillary pressure in the pore liquid of the system, generated by the menisci at the surface of the concrete. This capillary pressure tends to pull the solid particles together and subsequently cause shrinkage. Hence, the maximum capillary pressure generated in the system reflects the amount of shrinkage that can occur in the system. The maximum capillary pressure ( $P_{max}$ ) generated in the system was calculated using the expression shown below, and the values obtained are presented in the Table 4.5.

$$P_{max} = \frac{0.001 \gamma \cdot S}{w/b} \quad 4.1$$

where,  $\gamma$  [N/m] is the surface tension of the pore liquid,  $S$  [m<sup>2</sup>/kg] is the specific surface area of the binder and  $w/b$  is the water-binder ratio. Eqn. 4.1 has been obtained by modifying Powers expression (Powers, 1960) by substituting the cement by binder. For the calculation of maximum capillary pressure in case of CM, PSC and PPC, specific surface area values of the corresponding cements obtained from Blaine's air permeability were used. For the SCM mixes (FA15, FA30, SG15, SG30), the specific surface areas were calculated from the individual specific surface areas of OPC, FA and SG, based on the replacement levels of SCMs for cement. The calculated specific surface areas of all the binders are given in Table 4.5 along with the calculated variation (i.e., increase or decrease) in the maximum capillary pressure. The surface tension of water was assumed to be 0.07 N/m (at 42 C).

Table 4.5: Maximum capillary for various concretes

Mix ID	S (m <sup>2</sup> /kg)	P <sub>max</sub> (kPa)	% variation
CM	340	43.3	-
FA30	321	40.8	-5.7
FA15	330	42.0	-2.9
SG15	353	44.9	3.7
PPC	365	46.5	7.4
SG30	366	46.5	7.5
PSC	370	47.1	8.8

The maximum capillary pressure for various concretes ranges from 40.8 to 47.1 kPa. These values agree well with the values measured by Mora et al. (2008) and

Saliba et al. (2011). The replacement of fly ash for OPC decreases the specific surface of the binder and in turn slightly decreases the maximum capillary pressure. The decrease in the maximum capillary pressure for 30% replacement of fly ash was 5.7% compared to CM. On the other hand, the replacement of slag and blended cements increase the specific surface area and consequently increase the maximum capillary pressure. Compared to CM, the maximum increase in the capillary pressure was 8.8% and was observed in case of PSC. These slight variations in the maximum capillary pressure can be considered as insignificant to influence the plastic shrinkage cracking.

#### **4.6 Discussion**

The study of the influence of SCMs and blended cements on plastic shrinkage cracking clearly demonstrates that the potential for cracking increases with the replacement of SCMs and blended cements. From the investigations, it was noticed that the rate of evaporation, capillary pressure and paste content were similar for all the concretes investigated. Consequently, the variables that affect the alteration in the plastic shrinkage cracking potential are setting time, early age strength and bleeding characteristics, all of which can change with the binder composition. As mentioned earlier, the replacement of SCMs and blended cements for OPC retard the setting of concretes and affect the early age strength. From Table 4.3, it is clear that the one-day strength decreases gradually with an increase in the dosage of the SCMs. With the replacement of 30% cement by fly ash and slag, the decreases in one-day strength were 40% and 27%, respectively. Similarly, the replacement of OPC by blended cements reduced the one-day strength by 35%. Consequently, the rate of strength gain at early ages can be a reason for the increase in the cracking observed due to the replacement of OPC with SCMs and blended cements.

In all the concretes investigated, plastic shrinkage cracks were initiated earlier in the concretes with SCMs, relative to CM. This can be attributed to the reduction in the bleeding capacity of the concretes with the replacement of the SCMs or blended cements for OPC, which was observed visually. As a result, in hot and dry conditions, the rate of evaporation can exceed the rate of bleeding earlier in the concretes with SCMs, leading to earlier cracking compared to concretes without SCMs. This implies that curing of concretes with SCMs should be initiated earlier than for concretes with only OPC.

It was seen that the incorporation of the superplasticizer had a beneficial effect in reducing plastic shrinkage cracking and prolonging the onset of cracking. This could be attributed to the fact that superplasticizers reduce the surface tension and contribute to reducing the capillary pressure.

#### **4.7 Summary**

This chapter reports the results of the influence of supplementary cementitious materials and blended cements on plastic shrinkage cracking, and also on fresh and hardened properties of concrete. Specifically, this chapter illustrates the following:

- The use of blended cements (PPC and PSC) and the combination of OPC and slag significantly reduced the workability while the replacement of fly ash for OPC did not affect the workability of the concrete.
- The weight replacement of fly ash for OPC slightly reduced the unit weight of concrete due to variation in densities of fly ash and OPC, and in rest of the cases the unit weights were similar.
- The incorporation of SCMs and blended cements in concrete retard setting and slightly reduce the rate of development of the strength.
- The risk of plastic shrinkage cracking increases with the replacement of SCMs and blended cements for OPC. The intensity of cracking increases with the increase in the replacement levels.
- The rate of evaporation and maximum capillary pressure calculated from Power's equation were similar for all the concretes with no significant variation due to the incorporation of SCMs or blended cements in concrete.

## CHAPTER 5

### INFLUENCE OF FIBRES ON PLASTIC SHRINKAGE CRACKING OF CONCRETE

#### 5.1 Introduction

Incorporation of fibres at low dosages is expected to provide benefits while the concrete is still in plastic state and also to enhance some of the properties at hardened state. In some structures, like slabs on grades, pavements, screeds, tunnel linings, bridge decks etc., it is advantageous to add fibres as secondary reinforcement to control cracking at early ages. In this chapter, the contribution of fibres in reducing the plastic shrinkage cracking potential of concrete is assessed. First, the performance assessment of the fibres is presented, including the determination of fresh and hardened properties of the fibre reinforced concrete. The fresh properties include workability and fresh unit weight while the hardened properties include compressive strength and flexural toughness. Next, the plastic shrinkage results of the concretes with fibres are presented and discussed.

#### 5.2 Assessment of the fibre performance in fresh and hardened concrete

For assessing the performance of the fibres, five types of fibres were incorporated into the control mixes at the dosages recommended by the corresponding supplier. The fresh and hardened properties of the fibre reinforced concretes were determined. Slumps of all the mixes were in the range of 100-120 mm. The notation used to refer to the 5 mixes is given in Table 5.1, along with the superplasticizer dosage used.

Table 5.1: Experimental matrix for investigation with control mix

Mix ID	Slump without superplasticizer (mm)	Slump with superplasticizer (mm)	Dosage of superplasticizer for target slump (% of binder content)	Fresh unit weight (kg/m <sup>3</sup> )
CM-PAN	30-50	100-120	0.20	2445
CM-GLS	30-50	100-120	0.25	2445
CM-PP	30-50	100-120	0.30	2450
CM-PE	30-50	100-120	0.30	2450
CM-ST	30-50	100-120	0.25	2450

### **5.2.1 Workability and fresh unit weight**

Considerable reduction in the workability of the concrete was observed with the incorporation of the fibres in the concrete. For instance, the slump of control mix was 100-120 mm, and dropped to 30-50 mm with the addition of fibres. Therefore, superplasticizer had to be incorporated or its dosage had to be increased for attaining the target slump. The dosage of superplasticizer for each mix was fixed based on trials, and the values obtained are provided in Table 5.1. The reason for the reduction in slump with addition of fibres is due to the network that forms within the concrete, increasing the viscosity of the concrete and reducing slump. Recent studies by Jiang et al. (2014), and Söylev and Özturan (2014) also reported the decrease in the workability due to incorporation of short fibres.

Incorporation of fibres in concrete did not show any effect on the fresh unit weight of the concrete. This is mainly due to the low dosage of fibres that were incorporated.

### **5.2.2 Compressive strength**

Figure 5.1 and Table 5.2 show the compressive strength results of the control mix reinforced with different types of fibres. A marginal enhancement in compressive strength was observed for all fibres compared to plain control. Among the five types of fibres, steel fibres contributed to the highest compressive strength while the glass fibres gave the lowest compressive strength. At 28 days, the increase in the strength in case of CM-ST was about 7% compared to plain control mix. The increases in strength at 28 days for GLS, PAN, PP and PE fibres were 1% 3%, 5% and 6%, respectively. Previous studies by Wongtanakitcharoen (2005), Sivakumar and Santhanam (2007), and Jiang (2014) also observed similar marginal improvements (<6%) in compressive strength at fibre dosages of  $\leq 0.1\%$  volume fraction.

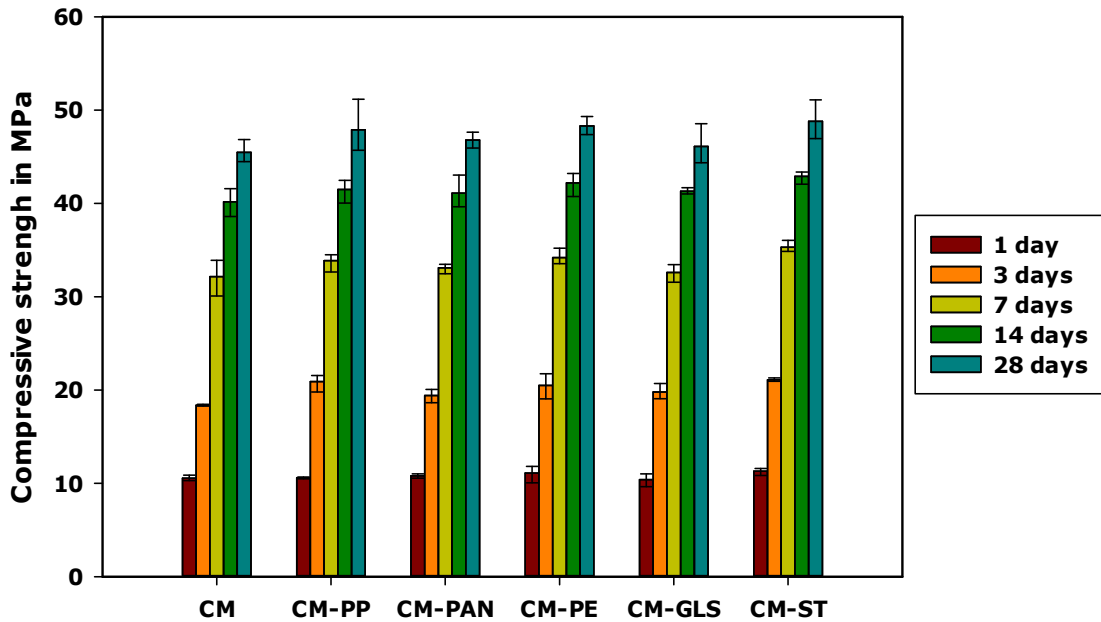


Figure 5.1: Compressive strength of various fibres with control mix

Table 5.2: Compressive strengths of fibre reinforced concrete at various ages

Mix ID	Compressive strength (MPa)									
	1 day		3 days		7 days		14 days		28 days	
	Mean	S.D	Mean	S.D	Mean	S.D	Mean	S.D	Mean	S.D
CM	10.5	0.2	18.4	0.1	32.1	1.6	40.2	1.2	45.5	1.2
CM-PP	10.6	0.1	20.9	0.8	33.9	0.9	41.5	1.1	47.9	2.9
CM-PAN	10.8	0.2	19.4	0.6	33.1	0.4	41.1	1.4	46.8	0.9
CM-PE	11.1	0.8	20.5	1.1	34.2	0.7	42.2	1.1	48.3	1.0
CM-GLS	10.4	0.6	19.8	0.7	32.6	0.8	41.3	0.3	46.1	2.2
CM-ST	11.3	0.3	21.1	0.1	35.3	0.5	42.9	0.6	48.8	2.1

S.D – standard deviation for 3 specimens

### 5.2.3 Flexural response

Typical load deflection curves based on the average deflection from two LVDTs for all the fibres are shown in Figure 5.2. It can be seen that the PE fibre gives a higher peak load whereas the steel fibre gives much better load-carrying capacity at larger displacements. In Figure 5.3, the same curves are shown up to a deflection of 300 micron. It is evident that the plain concrete demonstrates relatively brittle behaviour, with the load carrying capacity decreasing rapidly with increase in deflection. The steel fibres showed a significant influence in the post-peak behaviour

while the influence of synthetic fibres was nominal. In the following sections, flexural strength and toughness parameters of concretes with different fibres are compared.

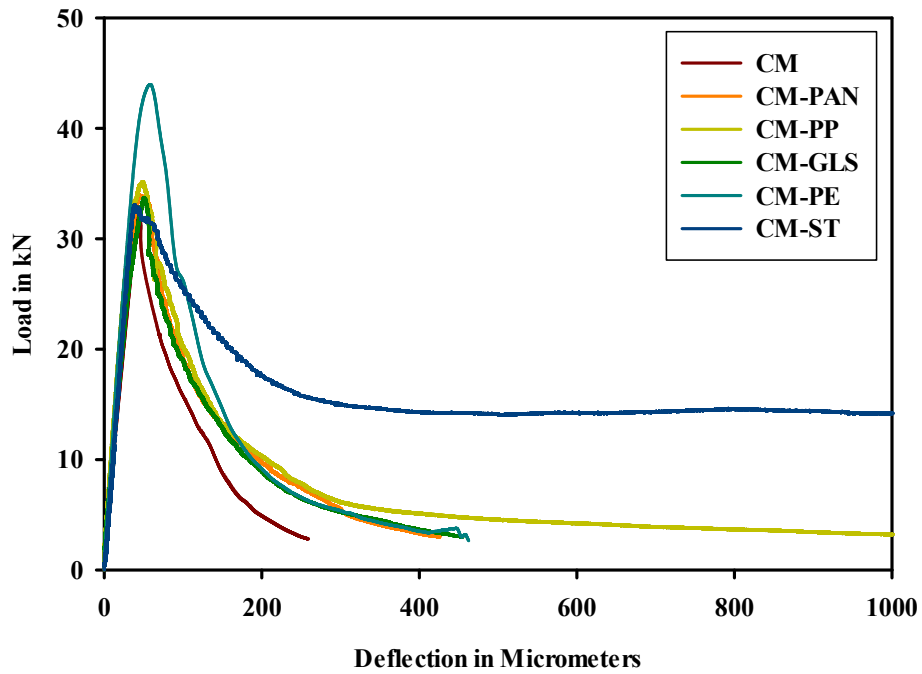


Figure 5.2: Typical load deflection curves of various fibre reinforced concretes

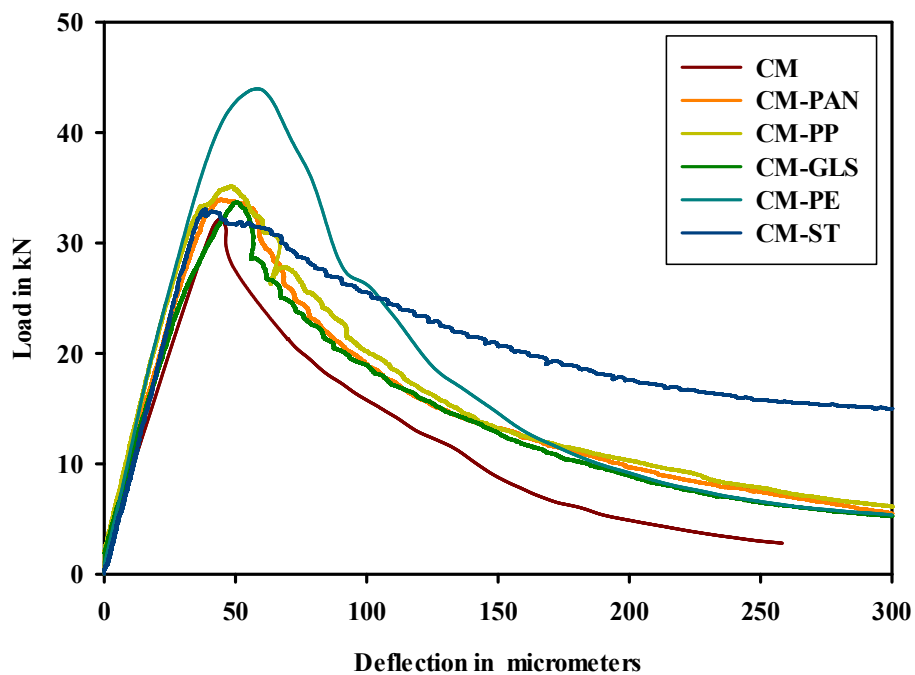


Figure 5.3: Typical load deflection curves up to 300 micron deflection

### 5.2.3.1 Flexural Strength

The results of flexural strength tests are presented in Table 5.3. It can be seen that the effect of incorporation of fibres on flexural strength was negligible, except in case of polyester fibre; the increase in flexural strength due to addition of polyester fibre compared to plain concrete was about 1.3 MPa while in the cases of other fibres the increase was only about 0.2 to 0.3 MPa. Interestingly, polyester fibres did not contribute considerably to the post-peak region although they increase the peak load carrying capacity.

### 5.2.3.2 Toughness parameters

From the load-deflection curves, toughness indices, namely two equivalent flexural strengths ( $f_{e,300}$  and  $f_{e,150}$ ) and two equivalent flexural strength ratios ( $R_{e,300}$  and  $R_{e,150}$ ), were calculated for all the concretes at deflection limits  $n = 300$  and  $150$ . The summary of the calculated toughness indices are presented in Table 5.3. As expected, the addition of fibres slightly affected the post-peak softening response of the concrete by bridging across the cracks and eliminating sudden brittle fracture. The steel fibre reinforced concrete showed highest values for all the toughness parameters, reflecting the significant improvement in the post-peak load carrying capacity. Among the synthetic fibres, polypropylene fibres showed better performance. Comparison of the two equivalent flexural strengths show that the  $f_{e,300}$  and  $f_{e,150}$  are approximately equal in case of steel fibres, indicating pseudo-ductile behaviour; however, in case of synthetic fibres,  $f_{e,150}$  values were lower compared to  $f_{e,300}$ , exhibiting softening-type response.

The equivalent flexural strength ratios reflect the percentage of flexural strength retained by the concrete after cracking. As expected, steel fibres showed strength retention of about 46% and 42% at deflection limits of 1.5 mm and 3 mm, respectively, reflecting the marginal decrease in load carrying capacity as the crack widens. Among synthetic fibres, polypropylene fibres showed the highest retention of flexural strength at both the deflection limits. However, the  $R_{e,150}$  values of all the synthetic fibres are much lower than  $R_{e,300}$  indicating the significant drop in strength retention capacity. In addition, it was observed that the variation in toughness parameters was highest for glass and PAN fibres, with coefficients of variation of about 20%, while polypropylene and steel fibres showed the least variation. This

could be due to the lower dosages used in the cases of PAN and glass fibres compared to the other cases.

Table 5.3: Toughness parameters of various fibres

Mix ID	$f_{ct}$		$f_{e,300}$		$f_{e,150}$		$R_{e,300}$		$R_{e,150}$	
	Mean (MPa)	CoV (%)	Mean (MPa)	CoV (%)	Mean (MPa)	CoV (%)	Mean (%)	CoV (%)	Mean (%)	CoV (%)
CM	4.2	7.6	0.3	12.8	0.02	12.8	8.3	10.9	4.2	10.9
CM-PP	4.5	7.5	0.8	8.0	0.03	8.0	17	11.9	8.5	11.9
CM-PAN	4.4	6.8	0.5	19.3	0.05	19.3	11.6	19.9	5.8	19.9
CM-PE	5.4	9.8	0.5	18.2	0.05	18.1	13.1	8.9	6.6	8.9
CM-GLS	4.4	6.7	0.5	21.3	0.05	21.3	11.3	23.8	5.7	23.8
CM-ST	4.5	9.0	2.1	12.2	1.9	11	46	13.2	42	10.0

CoV- coefficient of variation of 6 samples

### 5.3 Influence of fibres in mitigating plastic shrinkage cracking in the control mix

#### 5.3.1 Performance of fibres

All the fibres were assessed for their efficiency in mitigating plastic shrinkage cracking at the dosage recommended by the corresponding supplier. The addition of fibres in concrete, even at low volume fractions, has a significant influence on plastic shrinkage cracking. In the restrained plastic shrinkage tests, all the fibres completely eliminated cracking in CM implying good performance.

#### 5.3.2 Evaporation rates

Figure 5.4 shows the results of the rate of evaporation of various fibres with control mix. The straight line gives the average rate of evaporation of water, corresponding to about 0.90 kg/m<sup>2</sup>/hr. The rate of moisture loss from the concrete was initially equal to the rate of evaporation of water and decreases gradually with time. It can be observed that the rates of evaporation in fibre reinforced concretes were less compared to plain concrete. The coefficient of variation being high among the evaporation rates of fibre reinforced concretes, fibres were not compared individually for their influence on evaporation. Figure 5.5 show the effect of all the fibres on evaporation, where the error bar at each interval of CM-Fibres represents the maximum and minimum values of cumulative rate of evaporation considering all the fibres. Mora et al. (2001) and

Wang et al. (2002) also observed reduction in cumulative loss of water with the incorporation of fibres. The reduction in cumulative loss of water can be due to the absorption of the water, blocking of the bleed channel and increasing the tortuosity of the flow path by the fibres (Wang et al., 2002).

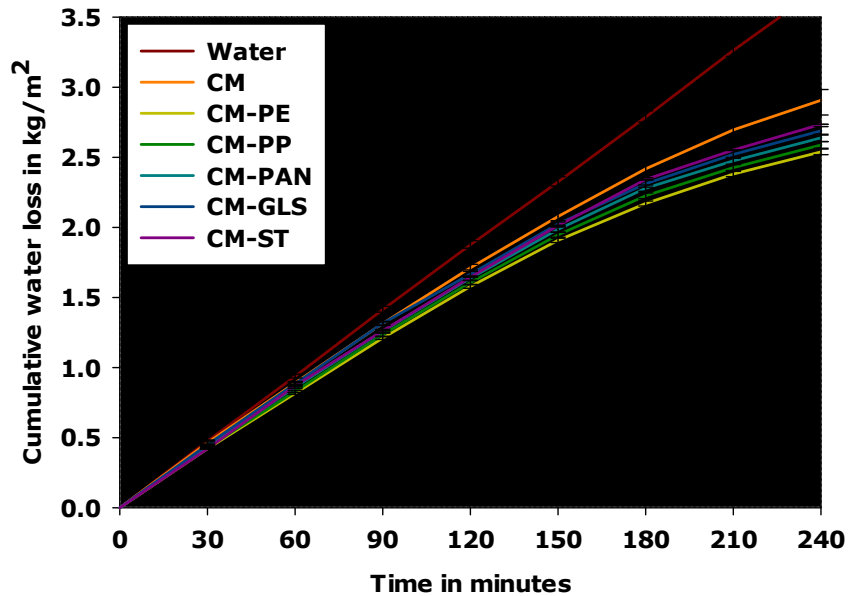


Figure 5.4: Cumulative rate of evaporation of various fibres with control mix

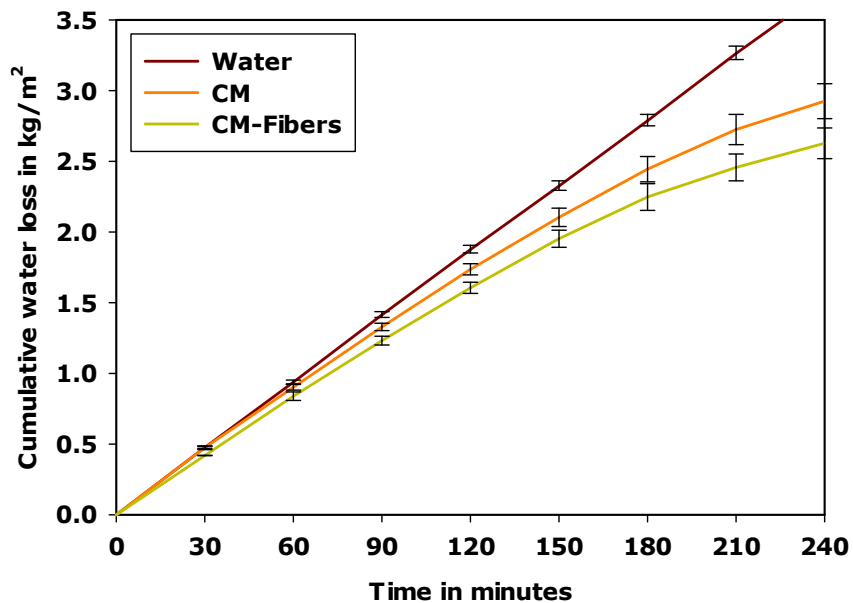


Figure 5.5: Cumulative rate of evaporation of different concretes

#### 5.4 Influence of fibres in mitigating plastic shrinkage cracking in mixes with 30% replacement of cement by SCMs

Since all the fibres were able to completely eliminate cracking in the control mix, they were assessed in more drastic conditions with the concretes with SCMs. The five types of fibres were incorporated in the two mixes with highest replacement levels of slag (SG30) and fly ash (FA30), for assessing their performance. Even in this case, the slump of all the mixes was in the range of 100–120 mm. The notation used to refer to the next set of mixes is given in Table 5.4, along with the superplasticizer dosage used.

Table 5.4: Experimental matrix for investigation with SCM mixes

Mix ID	Slump without superplasticizer (mm)	Slump with superplasticizer (mm)	Dosage of superplasticizer for target slump (% of binder content)
FA30-PAN	30-50	100-120	0.20
FA30-GLS	30-50	100-120	0.25
FA30-PP	30-50	100-120	0.30
FA30-PE	30-50	100-120	0.30
FA30-ST	30-50	100-120	0.25
SG30-PAN	0-20	100-120	0.60
SG30-GLS	0-20	100-120	0.50
SG30-PP	0-20	100-120	0.70
SG30-PE	0-20	100-120	0.80
SG30-ST	0-20	100-120	0.50

##### 5.4.1 Performance of fibres

The presence of fibres in concrete has a substantial influence in mitigating plastic shrinkage cracking. The results of the mixes are summarized in Table 5.5. Out of the 10 combinations, 8 of the mixes did not crack while SF30-PAN and SF30-GLS exhibited some cracking. Figure 5.6 and 5.7 show the cracks on the surface of SF30-PAN and SF30-GLS, respectively. The results indicate that the PAN and GLS fibres were beneficial in reducing the severity of cracking with SF30 mix, though they failed to completely mitigate cracking. Cracks originate at the centre of the specimen but failed to propagate completely along the width of the specimen, reflecting the reduced

potential for plastic shrinkage cracking. The crack initiation was delayed by 40 minutes in these two mixes compared to the plain mix.

Table 5.5: Summary of the results

Mix ID	Crack initiation time (min)	Crack properties				Percentage reduction in crack area	Percentage reduction in mean width
		Crack length (mm)	Max. width (mm)	Mean crack width (mm)	Crack area (mm <sup>2</sup> )		
SG30	183	444	1.73	0.91	402	-	-
FA30-PAN	Did not crack					100	100
FA30-GLS						100	100
FA30-PP						100	100
FA30-PE						100	100
FA30-ST						100	100
SG30-PP						100	100
SG30-PE						100	100
SG30-ST						100	100
SG30-PAN						225	365
SG30-GLS	230	240	0.52	0.23	55	86	75

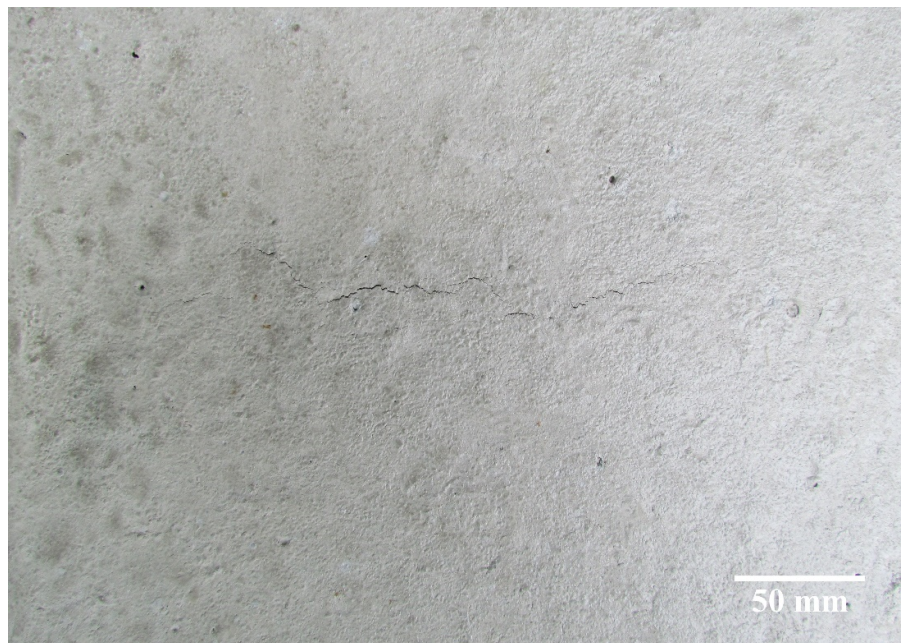


Figure 5.6: Plastic shrinkage crack in SG30-PAN

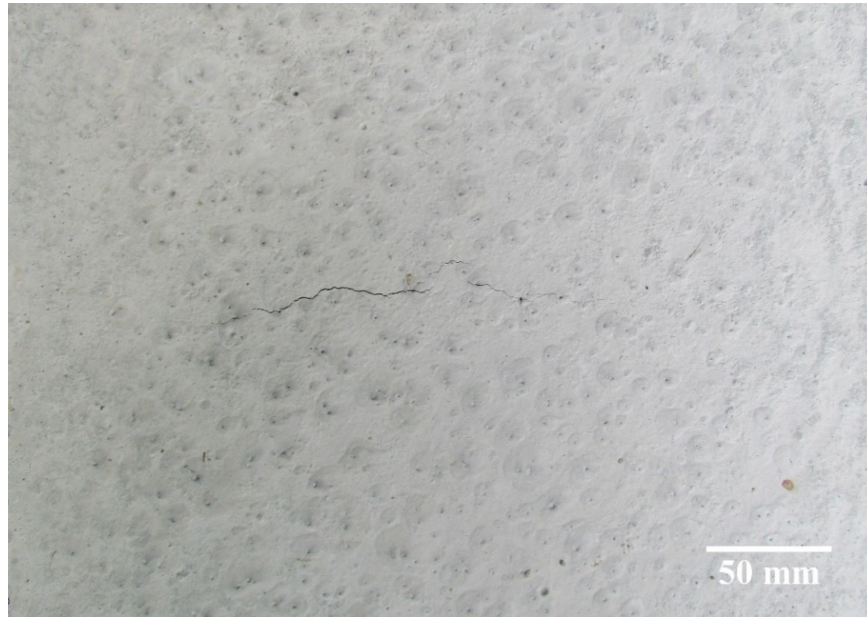


Figure 5.7: Plastic shrinkage crack in SG30-GLS

#### 5.4.2 Evaporation rates

Figure 5.8 show the effect of fibres on the cumulative rate of evaporation in CM and the mixes with 30% replacement of cement by SCMs. From the previous chapter, it was seen that the replacement of SCMs for OPC did not the affect the rate of evaporation of concrete. Hence, it can be concluded that the effect observed with the incorporation fibres in the concretes with the SCMs is the same as in CM.

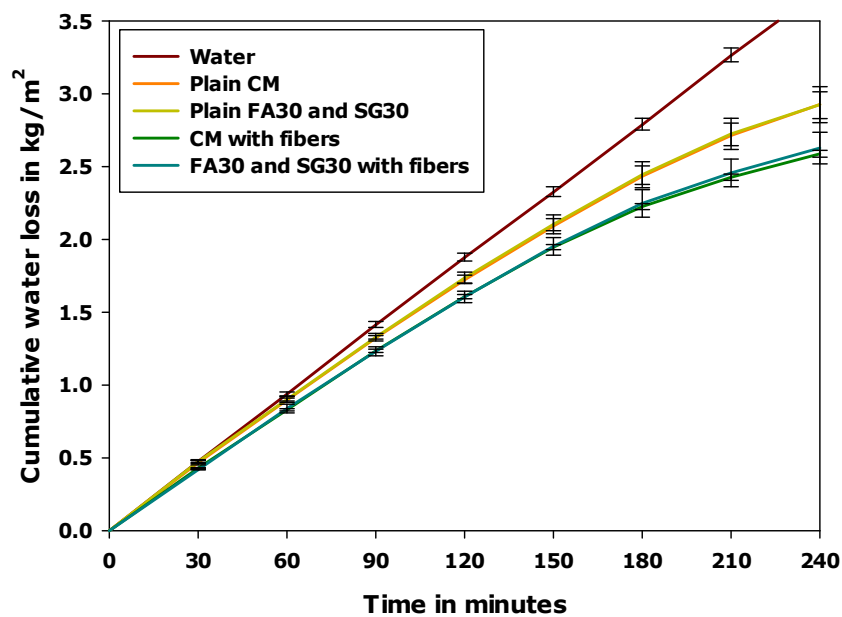


Figure 5.8: Cumulative rate of evaporation of concretes with and without fibres

## 5.5 Influence of fibres in mitigating plastic shrinkage cracking at higher dosages

From the previous investigation, it is seen that the recommended dosage of PAN and GLS fibres could not eliminate cracking with SG30 mix. Hence, both the fibres were tested at a higher fibre dosage of  $1.2 \text{ kg/m}^3$  with the same mix. Table 5.6 shows the dosage of superplasticizer incorporated for the higher fibre dosage for attaining the target slump of 100–120 mm along with the notations used. Figure 5.9 shows the cumulative rate of evaporation of fibre reinforced concrete (FRC) at different fibre dosage. It can be seen that the evaporation decreased slightly with the increase in the dosage of the fibres. At  $1.2 \text{ kg/m}^3$  dosage, the PAN and GLS fibres completely eliminate cracking, indicating that the recommended fibre dosage should be increased to get a performance comparable to the PE and PP fibres at  $0.9 \text{ kg/m}^3$  dosage.

Table 5.6: Experimental matrix for investigation at higher dosage of fibres

Mix ID	Slump without superplasticizer (mm)	Slump with superplasticizer (mm)	Dosage of superplasticizer for target slump (% of binder content)
SG30-PAN+	0-10	100-120	0.70
SG30-GLS+	0-10	100-120	0.60

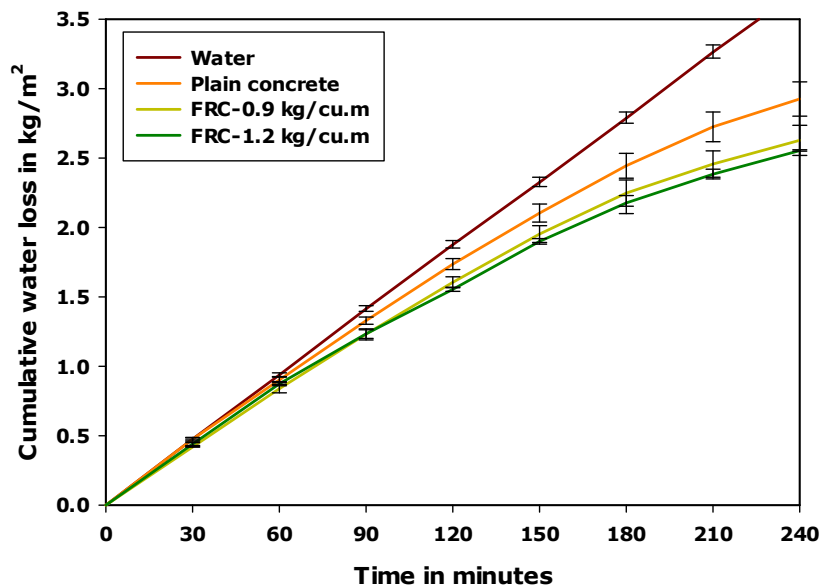


Figure 5.9: Cumulative rate of evaporation of concrete with different fibre dosages

## 5.6 Discussion

Wang et al. (2002) reported that the incorporation of fibres in concrete induces large size pores at the interface between the cement paste and fibre due to the accumulation of water underneath the fibres. These large pores makes the interface porous and reduce the maximum capillary pressure generated, providing a partial benefit for reducing plastic shrinkage cracking. Moreover, the incorporation of low volume short fibres in concrete reinforces the entire concrete mass with a random network. The distributed fibres increase the crack resistance of the concrete by reducing the stress concentration at micro-crack tips and absorbing the energy generated due to shrinkage stresses of the specimen (Xie, 2011). Furthermore, Qi et al. (2003) experimentally demonstrated that the presence of fibres in concrete reduces the amount of differential plastic settlement that can occur over the internal obstacles (i.e., over reinforcing bars or at locations of change in section height), and contributes to reduce plastic shrinkage cracking. These are the factors that together mitigate plastic shrinkage cracking, with the incorporation of fibres in concrete.

At the recommended dosages, all the fibres completely eliminated cracking in the control mix. The performance of the fibres in the SG30 mix was also good, except that the dosages of the PAN and GLS have to be increased beyond the recommended dosage for the cracking to be eliminated. The improvement in the performance at higher dosage can be attributed to the increase in the number of fibres.

## 5.7 Summary

This chapter reports the results of the effect of fibres in mitigating plastic shrinkage cracking, and also on the fresh and hardened properties of the concrete. Specifically, this chapter illustrates the following:

- Addition of low volumes of short fibres reduced the workability of concrete.
- The compressive strength of the fibre reinforced concretes increased marginally compared to the control mix. The maximum enhancement in compressive strength was 7% (in case of CM-ST).
- Compared to plain concrete, steel fibre reinforced concrete showed a significant improvement on the flexural response of the concrete. On the other hand, the effect of the synthetic fibres was nominal.

- Incorporation of fibres in concrete reduced the moisture loss from concrete and attributed in controlling plastic shrinkage cracking.
- Fibres significantly contributed in mitigating plastic shrinkage cracking. Among the synthetic fibres evaluated at the dosages recommended by the suppliers, polyester and polypropylene performed better than glass and polyacrylonitrile.
- For mitigating cracking using glass and polyacrylonitrile fibres in SG30 mix, higher dosage of these fibres had to be incorporated.

## CHAPTER 6

# MITIGATION OF PLASTIC SHRINKAGE CRACKING USING SHRINKAGE REDUCING ADMIXTURES

### 6.1 Introduction

Modern high performance concretes with relatively low water-binder ratio and admixtures are highly susceptible to plastic shrinkage cracking. This problem remains a serious concern especially for structures with extensive surface areas, such as pavements, slabs, bridge decks, tunnel linings, etc. Several approaches have been followed to address this problem in the field applications. Some of the approaches are reducing the paste content, increasing aggregate content, use of shrinkage compensating cement, use of fibres, etc. A novel approach to address this problem was the advent of the shrinkage reducing admixture (SRA). Over the past decades, extensive studies have been conducted on the effects of using SRAs on the hardened concrete. However, there are limited studies on its influence on plastic shrinkage cracking. Recent studies by Lura et al. (2007), Mora et al. (2009), Saliba et al. (2011), and Leemann et al. (2014) have shown that SRAs can play a useful role in controlling plastic shrinkage cracking.

In this chapter, four SRAs have been evaluated for their efficiency in controlling plastic shrinkage cracking. In Chapter 4, it was seen that the mix SG30 was most prone to plastic shrinkage cracking, and hence, for this study, it is considered as the reference mix. The chapter also reports the fresh properties and compressive strengths of the concretes with the different SRAs.

### 6.2 Fresh and Hardened Properties of Concrete

#### 6.2.1 Workability

Table 6.1 shows the dosage of superplasticizer required for attaining the target slump of 100–120 mm. Incorporation of SRA showed some plasticizing effect due to reduction in surface tension of the water, which resulted in the increase of the slump. The effect was evident at dosage of 2% while it was not significant at dosage of 1%. Hence at dosage of 2%, the amount of superplasticizer required to attain the target

slump was slightly reduced relative to the same mix without shrinkage reducing admixture.

Table 6.1: Superplasticizer dosage and unit weight

Mix ID	Dosage of SP (%)	Fresh unit weight (kg/m <sup>3</sup> )
SG30	0.41	2420
SG30-BM-1%	0.40	2425
SG30-BT-1%	0.40	2420
SG30-GE-1%	0.39	2415
SG30-CS-1%	0.40	2420
SG30-BM-2%	0.33	2425
SG30-BT-2%	0.30	2415
SG30-GE-2%	0.31	2425
SG30-CS-2%	0.32	2420

### 6.2.2 Fresh Unit Weight

As mentioned earlier, fresh unit weight was determined as per ASTM C138-14 for all the mixes with shrinkage reducing admixtures. The results of fresh unit weight are presented in Table 6.1. The results indicate that the incorporation of shrinkage reducing admixture has practically no effect on the unit weight of concrete.

### 6.2.3 Compressive Strength

The effect of the incorporation of SRA on the compressive strength is shown in Figure 6.1 and the data are presented in Table 6.2. It can be seen that the concretes containing SRAs exhibited lower compressive strength at all the ages, compared to the reference mix (SG30). At the dosage of 2%, the decrease in 1-day strength was more significant; the reduction in compressive strength at the dosages of 1% and 2% were between 16-19% and 30-35%, respectively. Among different SRAs evaluated, CS showed the lowest compressive strength at all the ages and at both the dosages. At 28 days, the reduction in compressive strength in SG30-CS at dosages of 1% and 2% was 7 and 11%, respectively. The loss in compressive strength has mainly been attributed to the effect of SRA on the hydration process (Rajabipour, 2008). The incorporation of SRA is said to reduce the polarity of mixing water and depress the affinity of alkalis to dissolve and ionize in the mixing water. As a result, the pore fluid with SRA contains lower concentration of alkali ions relative to the pore fluid without

SRA. This affects the rate of cement hydration, and contributes to retardation in hydration and strength development of concrete containing SRA (Rajabipour, 2008). The reduction in compressive strength with incorporation of SRA also conforms to the observations made by previous researchers, such as Roncero et al. (2003), Quangphu et al. (2008), Mora et al. (2009), and Saliba et al. (2011).

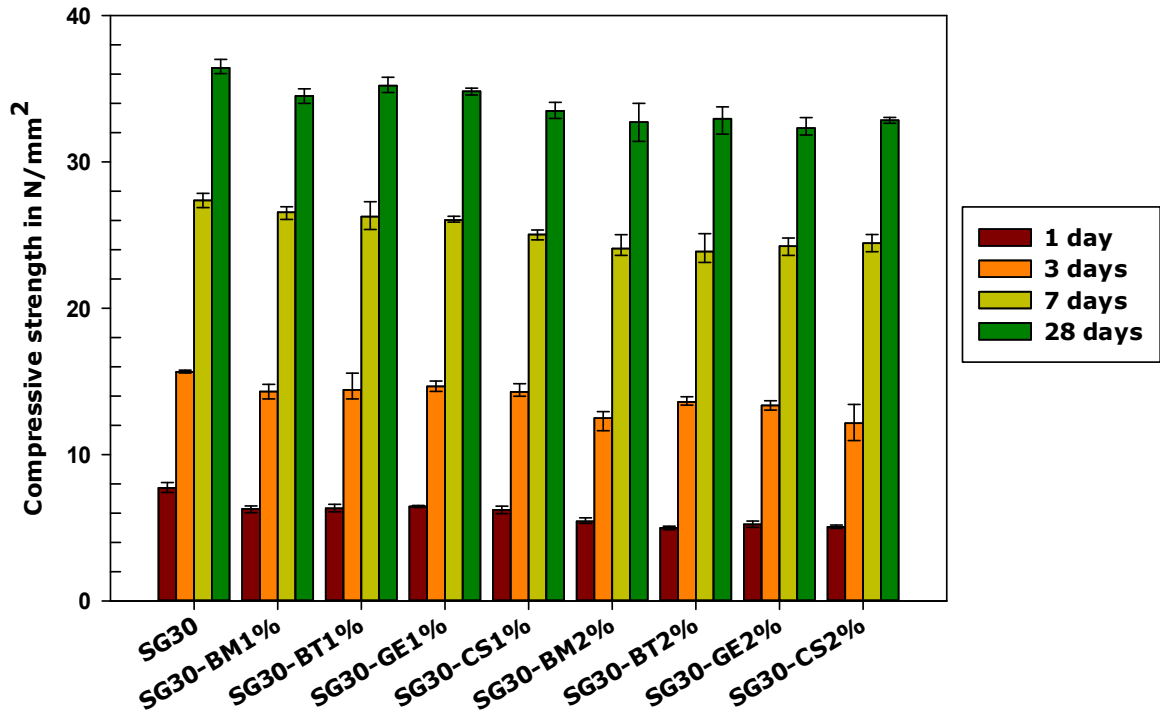


Figure 6.1: Compressive strengths of concrete with SRAs

Table 6.2: Compressive strength results

Mix ID	Compressive strength (MPa)									
	1 day		3 days		7 days		14 days		28 days	
	Mean	S.D	Mean	S.D	Mean	S.D	Mean	S.D	Mean	S.D
SG30	7.7	0.3	15.6	0.1	27.4	0.4	36.4	0.4	41.2	0.6
SG30-BT1%	6.3	0.2	14.3	0.4	26.6	0.4	34.5	0.4	39.9	0.7
SG30-BM1%	6.3	0.2	14.4	0.8	26.3	0.8	35.2	0.4	39.6	0.2
SG30-GE1%	6.5	0.1	14.7	0.3	26.0	0.2	34.8	0.2	40.3	0.8
SG30-CS1%	6.2	0.2	14.3	0.4	25.0	0.3	33.5	0.4	38.3	0.8
SG30-BT2%	5.4	0.2	12.5	0.6	24.1	0.7	32.7	1.1	38.1	0.7
SG30-BM2%	5.0	0.1	13.6	0.3	23.9	0.9	32.9	0.8	38.3	1.4
SG30-GE2%	5.2	0.2	13.4	0.3	24.2	0.5	33.0	0.5	37.1	1.2
SG30-CS2%	5.1	0.1	12.1	1.0	24.4	0.5	32.8	0.2	36.6	0.8

### 6.3 Evaporation rates

The results obtained for the rate of evaporation are shown in Figure 6.2. The straight line gives the average rate of evaporation of water as  $0.90 \text{ kg/m}^2/\text{hr}$ . In the first hour, the rate of moisture loss from of all the concretes appear to be similar but later the SRAs reduce the rate of moisture loss from the concrete. The variation among the evaporation rates of concretes with SRAs being high, the values for the SRAs are not compared individually for their influence on rate of evaporation. However, the data for all the SRAs are plotted collectively for two different dosages as SG30-SRAs-1% and SG30-SRAs-2%, as shown in Figure 6.3, where the error bar in each case represents the maximum and minimum rates of evaporation. It can be noticed that the increase in dosage of SRA from 1 to 2% slightly lowers the rate of evaporation, which confirms the observations of Lura et al. (2007).

Generally, the capillary pressure generated by the menisci at the surface of the concrete cause shrinkage. As a consequence, the pore fluid will be drawn to the surface. Higher the pressure generated, the more fluid is drawn out of the porous network to evaporate from the surface. In the concretes with SRA, the capillary pressure generated will be lower compared to the concrete without SRA due to modification of surface tension, which subsequently decreases the rate of evaporation (Lura et al. 2007).

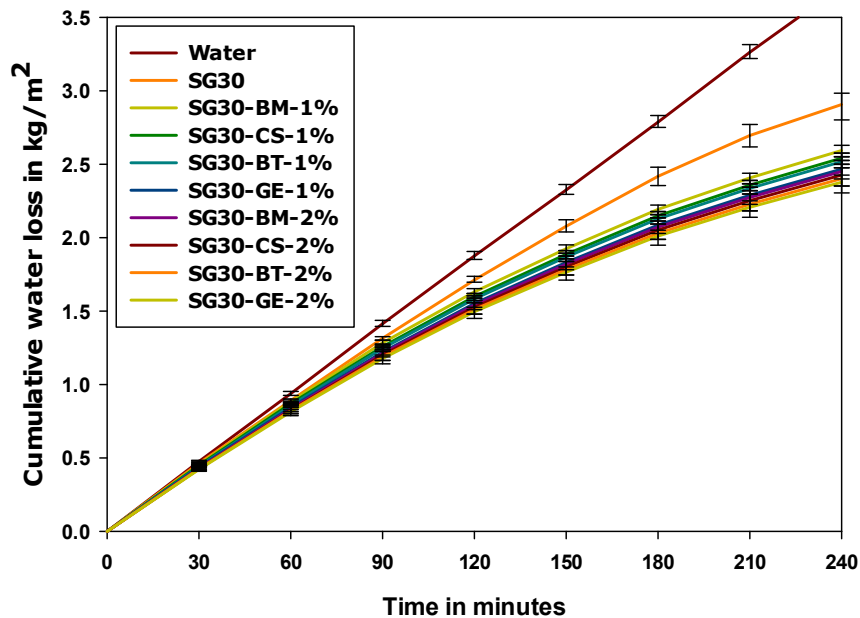


Figure 6.2: Evaporation rates of SG30 with various SRAs

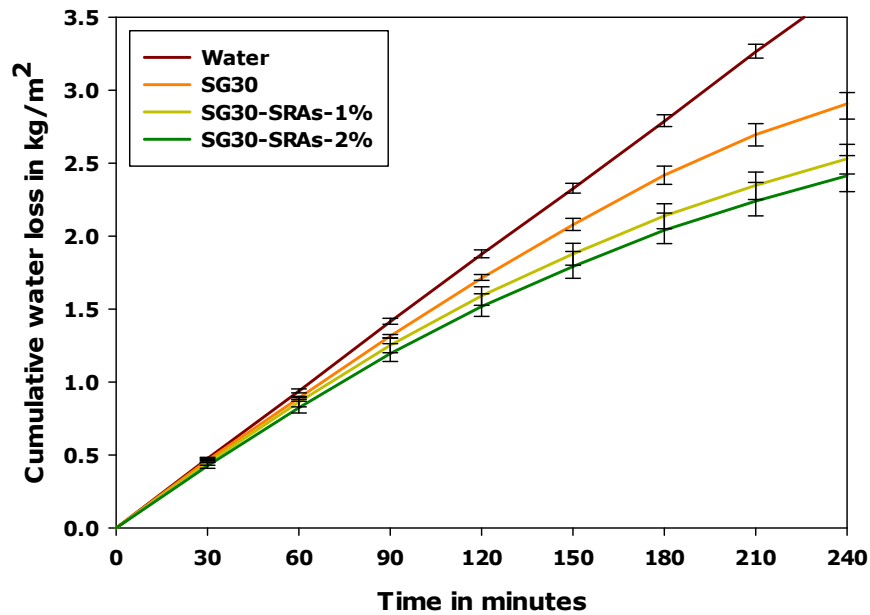


Figure 6.3: Evaporation rates of SG30 with various SRAs

#### 6.4 Influence of Shrinkage Reducing Admixtures on Plastic Shrinkage Cracking

Table 6.3 summarizes the plastic shrinkage results of concretes with SRAs. Incorporation of shrinkage reducing admixtures in the concrete contributed to controlling plastic shrinkage cracking. It is evident from the results that at an SRA dosage of 1%, all the concretes exhibited cracking, though the intensity of cracking is lower compared to that in the reference concrete (i.e., SG30). The reduction in crack area by the SRAs BM, CS, BT and GE were 44%, 52%, 61% and 65%, respectively. The maximum crack width of 1.65-1.90 mm in SG30 was reduced to 0.7-1.0 mm with the incorporation of 1% of SRA. Consequently, the mean crack widths and crack lengths also decreased. At the SRA dosage of 2%, concretes SG30-BM and SG30-CS exhibited cracking while SG30-BT and SG30-GE did not show any cracking, indicating much better performance. Moreover, the crack initiation times in all the concretes increased by about 20-30 minutes with the incorporation of SRAs.

Table 6.3: Summary of test results

Mix ID	Crack initiation time (min)	Crack properties				Reduction in crack area (%)	Reduction in mean width (%)
		Length (mm)	Max. width (mm)	Mean width (mm)	Crack area (mm <sup>2</sup> )		
SG30	185	444	1.73	0.91	402	-	-
SG30-BM-1%	205	439	1.02	0.52	227	44	43
SG30-CS-1%	210	382	0.83	0.50	193	52	45
SG30-BT-1%	205	359	0.70	0.44	158	61	51
SG30-GE-1%	220	380	0.77	0.37	142	65	59
SG30-BM-2%	215	378	0.88	0.40	152	62	55
SG30-CS-2%	210	377	0.70	0.36	135	67	61
SG30-BT-2%	Did not crack					100	100
SG30-GE-2%						100	100

## 6.5 Discussion

Incorporation of the SRA in concrete was successful in controlling plastic shrinkage cracking. At a dosage of 2%, two glycol-based shrinkage reducing admixtures (BT & GE) completely eliminated cracking while the other two did not perform as well, though there is a reduction of cracking in all the cases. This reiterates the fact that commercial SRAs can differ significantly in performance though they are of the same generic chemical family, confirming the findings of Mora et al. (2000). The reduction in cracking can be mainly attributed to the decrease in the surface tension of the pore fluid in concrete. This, consequently, abates the rate of moisture loss from the concrete (see Figure 6.2), and reduces the maximum and rate of development of the capillary pressure in concrete. Subsequently, the onset of cracking under harsh conditions is prolonged and plastic shrinkage cracking of concrete can be mitigated. In contrast to the substantial benefits of SRAs, a shortcoming is that the SRA reduces the strength of concrete (see Figure 6.1).

## 6.6 Summary

This chapter reports the effect of SRAs in controlling plastic shrinkage cracking, and also on the fresh and hardened properties of concrete. Specifically, the results illustrate the following:

- Incorporation of SRAs in concrete showed some plasticizing effect and enhanced the workability of concrete, which was more evident at a dosage of 2%.
- Compared to the control mix, the compressive strength of concretes with SRAs reduced significantly at early ages. However, at later ages, the reduction in compressive strength was less.
- SRAs showed a positive effect in controlling plastic shrinkage cracking, at a dosage of 1%. At a dosage of 2%, two SRAs (BT and GE) completely eliminated cracking in the tests while the other two did not perform as well, though they decreased the crack area by more than 60%
- The cumulative rate of evaporation of the concretes with SRAs decreased substantially compared to the control mix and contributed to mitigating plastic shrinkage cracking.

## CHAPTER 7

# MITIGATION OF PLASTIC SHRINKAGE CRACKING USING CURING COMPOUNDS

### 7.1 Introduction

The most effective method to control plastic shrinkage cracking is to reduce the evaporation of moisture from the plastic concrete surface immediately after it is cast. Some of the conventional methods for reducing evaporation include spraying water, covering with wet burlap or plastic sheet, fogging, etc. These methods prevent or compensate the loss of water from the freshly placed concrete and create a humid environment in the vicinity to improve cracking-resistance. However, it is recognized that considerable difficulties arise in assessing the correct time to apply these methods on the freshly placed concrete surface. Improper and untimely application of these methods can severely affect the concrete. Also, at some construction sites, water is seldom available, and trucking water is expensive and difficult to supervise. Furthermore, sheet or wet burlap covers becomes cost prohibitive due to the large quantity of material required to cover the entire surface cast in a day. The most economical and feasible way to overcome this problem is to use curing compounds. Generally, curing compounds are sprayed on the finished concrete as soon as the final trowelling is completed in case of mixtures with no bleed water or immediately after the water sheen disappears. These compounds form a protective membrane on the surface of fresh concrete, and inhibit the loss of mix water from the concrete and control early age cracking due to shrinkage. A suitable curing compound can be capable of maintaining 95% of the original moisture content in a concrete mix. Curing compounds are preferred as they completely eliminate the follow-up or supervision, the use of troublesome covering and expensive or scarce water (Fattuhi 1986; Choi et al. 2012).

A variety of different generic curing compounds are available in the market, some of them are acrylic-based, wax-based, resin-based, water-based, bitumen-based, etc. The efficiency of the curing compounds can be highly variable and can reduce considerably with the increase in temperature and the decrease in humidity. In

addition, there is a dearth of information on the effectiveness of the curing compounds in reducing plastic shrinkage cracking and evaporation from the surface of fresh concrete.

In this chapter, four different commercially-available curing compounds were evaluated for their efficiency in mitigating plastic shrinkage cracking. The chapter also describes the procedure adopted for evaluation and presents a discussion of results.

## 7.2 Experimental procedure

To determine the efficacy of different curing compounds in controlling plastic shrinkage cracking, a similar approach as described in ASTM C1579 was followed. The mix with highest potential for cracking, i.e. SG30, was selected as the reference mix for the study. The specimen is placed in the environmental chamber soon after casting. 90 minutes later (i.e., after the sheen disappears), the specimen is removed from the chamber and the curing compound is sprayed, and then the specimen is kept back in the chamber. The curing compound is sprayed with the help of a compressed air-operated gun (see Figure 7.1) at an application rate of 5 m<sup>2</sup>/l.



Figure 7.1 Application of curing compound

For estimating the rate of evaporation, three stainless steel pans were used. One pan was used to measure the evaporation of water while the other two were used to measure the moisture loss from concrete with and without curing compound. When the specimen was removed for application of curing compound, the pan with concrete was also removed and weighed, and the curing compound was applied on its surface at the same rate as that of specimen. The pan was reweighed immediately after

application and then placed back in the chamber. These pans were weighed at regular intervals of 30 minutes to measure the change in weight.

### 7.3 Evaporation rates

Evaporation results are presented in the form of cumulative water lost per unit area as a function of time. The results indicate that the amount of water evaporating from fresh concrete is reduced after the application of curing compound. This was demonstrated by the significant reduction in the slope of the curves shown in the Figure 7.2. It is interesting to note that the moisture loss from the concrete decreased immediately after the application of the curing compound. A recent study by Nahata et al. (2014) also observed such reduction in the moisture loss with the application of the curing compounds. However, the effectiveness of the compounds varied significantly. It can be also seen that two curing compounds, AR and MR, were more efficient in reducing the rate of evaporation than WX and WA, which can be mainly attributed to their higher water vapour resistance (i.e., reluctance of the material to allow water vapour pass through).

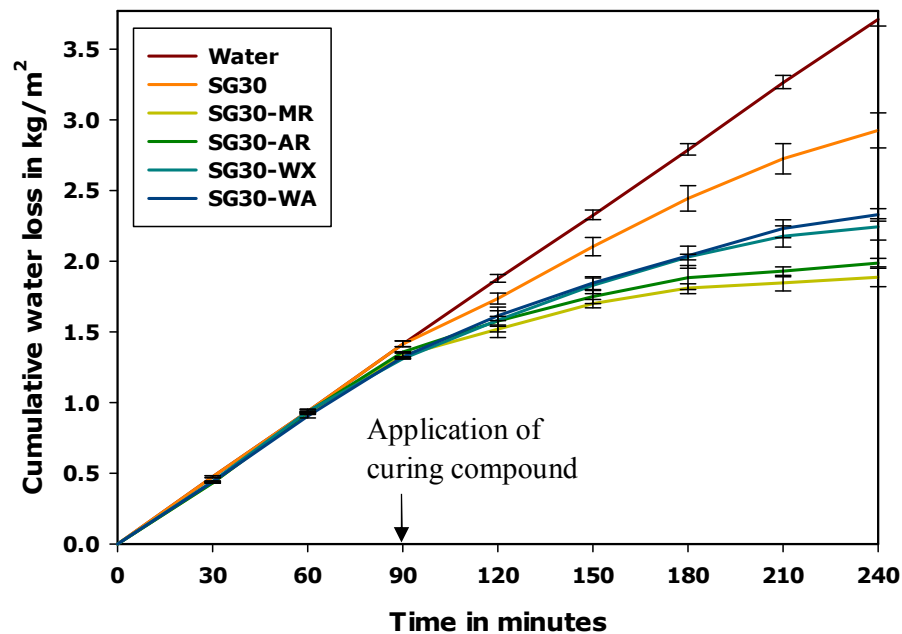


Figure 7.2: Cumulative rate of evaporation of SG30 with various curing compounds

#### 7.4 Influence of curing compounds on plastic shrinkage cracking

When the concrete was tested with the curing compounds, the specimens with two compounds AR and MR did not exhibit any cracking, indicating better performance, while the other two specimens with the compounds WX and WA exhibited cracking (see Figure 7.3). This can be attributed to the higher efficacy of AR and MR in limiting the evaporation of water. The crack data is summarized in Table 7.1. It can be seen that at the temperature of 43°C, i.e. at testing conditions, the compounds WA and WX were able to reduce crack area by 44% and 29%, respectively. Additionally, the maximum and mean crack widths also reduced. The reduction in the mean crack width in SG30-WX and SG30-WA were 22% and 40%, respectively. Moreover, the crack initiation times were delayed by 40 minutes for these concretes with the application of curing compounds.

Table 7.1: Summary of test results

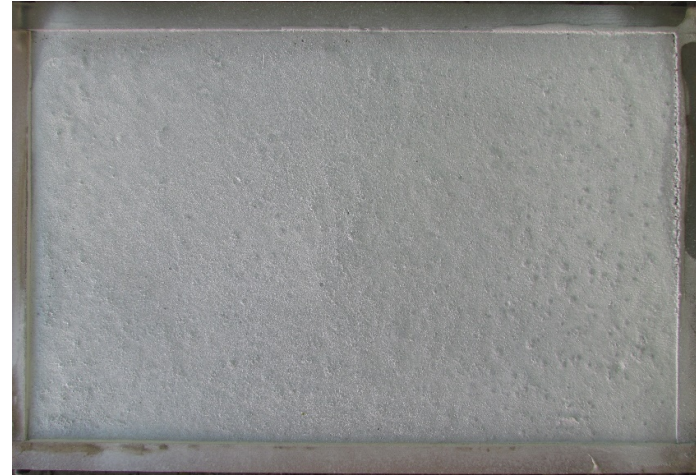
Mix ID	Crack initiation time (min)	Crack properties				Reduction in crack area (%)	Reduction in mean width (%)
		Length (mm)	Max. width (mm)	Mean width (mm)	Crack area (mm <sup>2</sup> )		
SG30	185	444	1.73	0.91	402	-	-
SG30-WX	225	406	1.00	0.71	287	29	22
SG30-WA	235	413	0.73	0.55	227	44	40
SG30-MR	Did not crack					100	100
SG30-AR						100	100

#### 7.5 Discussion

From the results, it is evident that the curing compounds can help in mitigating plastic shrinkage cracking. However, the efficiencies of curing compounds are not all the same and can vary significantly. Out of the four compounds tested, MR and AR completely eliminated cracking while WX and WA did not perform as well. The elimination of cracking or reduction in the intensity of cracking with the application of the curing compounds was mainly due to the reduction in the evaporation loss from the concrete. As the efficiency of the curing compounds varies significantly, it is important to choose an economical curing compound that can be effective at the prevailing site conditions.



(a)



(b)



(c)



(d)

Figure 7.3: Plastic shrinkage test with curing compounds: (a) MR, (b) AR, (c) WA and (d) WX

## **7.6 Summary**

This chapter reports the results of the efficacy of the curing compounds in controlling plastic shrinkage cracking. Among the four compounds tested, two compounds (MR and AR) completely eliminated cracking by drastically reducing the moisture loss from the surface of the concrete. On the other hand, the other two compounds were less efficient in reducing moisture loss and, consequently, were only able to reduce cracking and not eliminate it completely.

## CHAPTER 8

### CONCLUSIONS AND SCOPE FOR FURTHER STUDIES

#### 8.1 Introduction

This study investigated the influence of mineral admixtures on plastic shrinkage cracking and the efficacy of the commercially available solutions for controlling plastic shrinkage cracking. The standard ASTM-C1579 was adopted as the basis for the investigation. This chapter highlights the significant conclusions drawn from the present study and suggests the scope for further studies.

#### 8.2 General conclusions

The replacement of the supplementary cementitious materials (SCMs) and blended cements for ordinary portland cement (OPC) increased the risk of plastic shrinkage of cracking by retarding the setting and reducing the rate of development of the strength. Consequently, the intensity of cracking increased with the increase in the replacement levels of the SCMs. Additionally, cracks were initiated earlier in the mixes with SCMs, relative to the control mix due to the reduction in the bleeding capacity of the concrete. The incorporation of the superplasticizer had a beneficial effect in slightly reducing plastic shrinkage cracking and prolonging the onset of cracking. The use of plastic shrinkage mitigating ingredients, such as fibres, shrinkage reducing admixtures (SRA) and curing compounds, were helpful in combating plastic shrinkage cracking. However, the recommended dosages by the supplier may or may not completely mitigate plastic shrinkage cracking in all the concretes. Depending on the shrinkage potential of the concrete, the dosage of the shrinkage mitigating ingredients may have to be increased for controlling plastic shrinkage cracking.

#### 8.3 Specific conclusions

##### 8.3.1 Workability

- The replacement of fly ash for ordinary portland cement (OPC) did not affect the workability of the concrete. On the other hand, the use of blended cements (PPC

and PSC) and the combination of OPC and slag reduced the workability significantly.

- Considerable reduction in the workability of the concrete was observed with the incorporation of the fibres in the concrete. The slump of control mix was 100-120 mm, and dropped to 30-50 mm with the addition of fibres in concrete.
- Incorporation of SRA showed some plasticizing effect and resulted in the increase of the slump. The effect was evident at dosage of 2% while it was not significant at dosage of 1%.

### **8.3.2 Fresh unit weight**

- The unit weight decreases slightly as OPC is replaced with SCMs or blended cements. The decrease in the unit weight is due to the differences in the densities of OPC, SCMs and blended cements.
- Incorporation of fibres and shrinkage reducing admixtures into concrete did not have any effect on the fresh unit weight of the concrete.

### **8.3.3 Compressive strength**

- The commercially-available blended cements PPC and PSC resulted in lower strength at all the ages, relative to the control mix. The blended cements (PPC and PSC) reduced the compressive strength by 35% and 12-30% at the ages of 1 day and 28 days, respectively.
- The compressive strength declined at all ages with an increase in fly ash and slag dosage, with a stronger effect in the case of fly ash. At 1 day, the decrease in compressive strength at 30% replacement of fly ash and slag were 40% and 27%, respectively. Similarly at 28 days, the reduction in compressive strength at 30% replacement of fly ash and slag were 21% and 12%, respectively.
- A marginal enhancement in compressive strength was observed for all fibres compared to control mix. The maximum enhancement in compressive strength was only 7% (in case of CM-ST).
- The concretes containing SRAs exhibited lower compressive strength at all the ages compared to the reference mix (SG30). At the dosage of 1%, the decrease in early-age strength ( $\leq 3$  days) was marginal while at a dosage of 2% the reduction was significant. The reduction in one day compressive strength at the dosages of

1% and 2% were between 16-19% and 30-35%, respectively. However, at later ages, the reduction was less than 11% compared to the reference mix.

#### **8.3.4 Flexural response**

- The plain concrete demonstrated relatively brittle behavior, with the load carrying capacity decreasing rapidly with increase in deflection. The steel fibres showed a significant influence in the post-peak behavior while the influence of synthetic fibres was nominal.
- The effect of incorporation of fibres on flexural strength was negligible, except in case of polyester fibres; the increase in flexural strength due to addition of polyester fibres compared to plain concrete was about 1.3 MPa while in the cases of other fibres the increase was about 0.2 to 0.3 MPa.
- Steel fibres showed highest strength retention of about 46% and 42% at deflection limits of 1.5 mm and 3 mm, respectively. Among the synthetic fibres, polypropylene fibres showed the highest retention of flexural strength at both the deflection limits.

#### **8.3.5 Influence of SCMs on plastic shrinkage cracking**

- The risk of plastic shrinkage cracking increased with the replacement of SCMs and blended cements for OPC. The intensity of cracking increased with the increase in the replacement levels.
- Replacement of PPC and PSC for OPC increased the crack area from 100 mm<sup>2</sup> to 220 mm<sup>2</sup> and 280 mm<sup>2</sup>, respectively. Similarly, the crack length, maximum crack width and mean crack width also increased substantially.
- Increases in crack area, crack length and maximum crack width were observed with incorporation of fly ash; the crack area, length and maximum width were increased by 42%, 27% and 51%, for 30% replacement. Also, the mean crack width increased slightly by 7% and 12% at replacement levels of 15% and 30%, respectively.
- A significant increase in potential for cracking was observed, relative to control mix, with the replacement of slag. At a replacement level of 30%, the crack area increased by 4 times, the maximum crack width increased from 0.6-0.7 mm to 1.9 mm and the mean crack width increased by 140%.

- A marginal decrease in crack area and length was observed in all the concretes that incorporated a superplasticizer inspite of having a much higher slump. In addition, the maximum and mean crack widths decreased slightly, compared to the concretes without superplasticizer.
- Plastic shrinkage cracks were initiated earlier in the concretes with SCMs and blended cements, relative to OPC. This implies that curing of concretes with SCMs should be initiated earlier than for concretes with only OPC.
- The rate of evaporation and maximum capillary pressure calculated from Power's equation were similar for all the concretes with no significant variation due to the incorporation of SCMs or blended cements in concrete. The significant reduction in the early-age strength was found to be the main reason for the increase in cracking.

### **8.3.6 Mitigation of cracking using shrinkage reducing components**

#### **8.3.6.1 Fibres**

- At the recommended dosage, all fibres completely eliminated cracking in the OPC concrete implying good performance. However, when incorporated in the mix with 30% replacement by slag (SG30), the steel, polyester and polypropylene fibres completely eliminated cracking while the glass and polyacrylonitrile fibres exhibited some cracking. Though they failed to completely mitigate cracking, the results indicate that the PAN and GLS fibres were beneficial in reducing the severity of cracking with the SG30 mix.
- For mitigating cracking, using glass and polyacrylonitrile fibres in the SG30 mix, higher dosage of fibres had to be incorporated than that recommended by the manufacturer.
- The reduction in cumulative loss of water from the concrete as well as the bridging of the cracks that could develop in the fresh concrete were found to be the reasons for the significant influence in plastic shrinkage cracking potential.

#### **8.3.6.2 Shrinkage reducing admixtures**

- Incorporation of shrinkage reducing admixtures in the concrete also contributed significantly in controlling plastic shrinkage cracking.

- At dosage rate of 1%, all the SRAs exhibited cracking, however, the intensity of cracking reduced compared to the reference concrete (i.e., SG30). The reduction in crack area by the SRAs BM, CS, BT and GE were 44%, 52%, 61% and 65%, respectively. The maximum crack width of 1.65-1.9 mm in SG30 was reduced to 0.7-1.0 mm. Also, the mean crack widths and crack lengths decreased.
- At the dosage of 2%, SG30-BM and SG30-CS exhibited cracking while the SG30-BT and SG30-GE concretes did not show any cracking, indicating much better performance.
- The crack initiation times in all the concretes were increased by about 20-30 minutes with the incorporation of SRAs.
- Also, in concretes with shrinkage reducing admixtures, the reduction in cumulative loss of water from the concrete was found to be the prime reasons for the significant influence in plastic shrinkage cracking.

#### **8.3.6.3 Curing compounds**

- Among the four compounds tested, two compounds (AR and MR) completely eliminated cracking while the other two compounds (WA and WX) exhibited cracking.
- The compounds WA and WX reduced the crack area by 44% and 29%, respectively. The maximum and mean crack widths also reduced substantially. The reduction in the mean crack width in case of SG30-WX and SG30-WA was 22% and 40%, respectively.
- The elimination of cracking or reduction in intensity of cracking with the application of the curing compounds was mainly due to the reduction in the evaporation loss from the concrete.

#### **8.4 Scope for further studies**

- In this thesis capillary pressure was calculated based on the Power's expression and was found to be almost similar for various concretes investigated. However, it would be interesting to measure the capillary pressure that is generated in concrete using a tensiometer and check whether it is conforming to the equation.
- The bleeding characteristics of concretes had a significant influence on the crack initiation time of the concrete. The mixes with relatively high bleeding capacity

were less prone to plastic shrinkage cracking. Hence, the bleeding of the concretes can be measured and correlated with the results obtained.

- The influence of water-cement ratio, binder content, aggregate content, temperature and humidity, chemical admixtures and different levels of restraint on plastic shrinkage cracking can be investigated.

## REFERENCES

- ACI Committee 232, Use of Fly Ash in Concrete (ACI 232.2R-03), American Concrete Institute, Farmington Hills, Mich., 34 p.
- ACI Committee 233, Slag Cement in Concrete and Mortar (ACI 233R-03), American Concrete Institute, Farmington Hills, Mich., 19 p.
- ACI Committee 305, Hot Weather Concreting (ACI 305R-10), American Concrete Institute, Farmington Hills, Mich., 20 p.
- ASTM Standard Designation C1069-12, Standard test method for flexural performance of fibre reinforced concrete, West Conshohocken, Pennsylvania, USA.
- ASTM Standard Designation C138-14, Standard test method for density (unit weight), yield and air content (gravimetric) of concrete, West Conshohocken, Pennsylvania, USA.
- ASTM Standard Designation C143-12, Standard test method for slump of hydraulic cement concrete, West Conshohocken, Pennsylvania, USA.
- ASTM Standard Designation C1579-13, Standard test method for evaluating plastic shrinkage cracking of restrained fibre reinforced concrete, West Conshohocken, Pennsylvania, USA.
- Al-Amoudi, O.S.B., Abiola, T.O. & Maslehuddin, M., 2006. Effect of superplasticizer on plastic shrinkage of plain and silica fume cement concretes. *Construction and Building Materials*, 20(9), pp. 642–647.
- Al-Gahtani, A.S., 2010. Effect of curing methods on properties of plain and blended cement concretes. *Construction and Building Materials*, 24(3), pp. 308–314.
- Almusallam, A.A., Maslehuddin, M. & Khan, M.M., 1998. Effect of mix proportions on plastic shrinkage cracking of concrete in hot environments. *Construction and Building Materials*, 6 (6-7), pp. 353–358.
- Balaguru, P., 1994. Contribution of fibres to crack reduction of cement composites during the initial and final setting period. *ACI Materials Journal*, 91(3), pp. 280–288.
- Banthia, N., Azzabi, M., & Pigeon, M., 1993. Restraint shrinkage cracking in fibre reinforced cementitious composites. *Materials and Structures*, 26(161), pp. 405–413.
- Banthia, N., Yan, C. & Mindess, S., 1996. Restraint shrinkage cracking in fibre reinforced concrete: a novel test technique. *Cement and Concrete Research*, 26(1), pp. 9-14.
- Banthia, N. & Yan, C., 2000. Shrinkage Cracking in Polyolefin Fibre-Reinforced Concrete. *ACI Materials Journal*, 97(4), pp. 432-437.

- Banthia, N. & Gupta, R., 2006. Influence of polypropylene fibre geometry on plastic shrinkage cracking in concrete. *Cement and Concrete Research*, 36(7), pp. 1263–1267.
- Banthia, N. & Gupta, R., 2007. Test method for evaluation of plastic shrinkage cracking in fibre-reinforced cementitious materials. *Experimental Techniques*, 31(6), pp. 44-48.
- Banthia, N. & Gupta, R., 2009. Plastic shrinkage cracking in cementitious repairs and overlays. *Materials and Structures*, 42, pp. 567–579.
- Bayasi, Z. & McIntyre, M., 2003. Application of Fibrillated Polypropylene Fibres for Restraint of Plastic Shrinkage Cracking in Silica Fume Concrete. *ACI Materials Journal*, 99(4), pp. 337–344.
- Berke, N.S. & Dallaire, M.P., 1994. The effect of low addition rates of polypropylene fibres on plastic shrinkage cracking and mechanical properties of concrete. in: *Fibre reinforced concrete: Development and innovations*; ACI SP-142-2, American Concrete Institute, pp. 19–41.
- Bentz, D.P., Geiker, M.R. & Hansen, K.K., 2001. Shrinkage-reducing admixtures and early-age desiccation in cement pastes and mortars. *Cement and Concrete Research*, 31(7), pp. 1075–1085.
- Bloom, R., & Bentur, A., 1995. Free and restrained shrinkage of normal and high strength concrete. *ACI Materials Journal*, 92(2), pp. 211-217.
- Boghossian, E. & Wegner, L.D., 2008. Use of flax fibres to reduce plastic shrinkage cracking in concrete. *Cement and Concrete Composites*, 30(10), pp.929–937.
- Boshoff, W.P., Combrinck, R., & Maritz, J., 2012. A model for the prediction of plastic shrinkage cracking in concrete. *Concrete Repair, Rehabilitation and Retrofitting III – Alexander et al. (Eds)*, Taylor & Francis Group, London, pp. 402-47.
- Brooks, J.J., Megat Johari, M.A. & Mazloom, M., 2000. Effect of admixtures on setting times of high strength concrete. *Cement and Concrete Composites*, 22, pp. 293–301.
- Cabrera, J.G., Cusens, A.R., & Wang, B.Y., 1992. Effect of superplasticizers on the plastic shrinkage of concrete. *Magazine of Concrete Research*, 44(160), pp. 149- 155.
- Choi, S., Yeon, J.H. & Won, M.C., 2012. Improvements of curing operations for Portland cement concrete pavement. *Construction and Building Materials*, 35, pp. 597–604.
- Cohen, M.D., Olek, J. & Dolch, W.L., 1990. Mechanism of plastic shrinkage cracking. *Cement and Concrete Research*, 20(1), pp. 103-119.

Combrinck, R., 2012. Plastic shrinkage cracking in conventional and low volume fibre reinforced concrete. MSc Thesis, Stellenbosch University, South Africa.

Combrick, R. & Boshoff, W.P., 2012. Influence of restraint on the early age cracking of concrete with and without fibres. In: Joaquim Barros et al. (Eds), BEFIB2012 – Fibre reinforced concrete, UM, Guimarães.

Dahl, P. A., 1989. Influence of fibre reinforcement on plastic shrinkage cracking,” proceeding of international conference on recent development on fibre reinforced cement and concrete. Cardiff, UK, pp. 435-441.

Dias, W.P.S.Ã., 2003. Influence of mix and environment on plastic shrinkage cracking. Magazine of Concrete Research, 55(4), pp. 385–394.

Dhanya, B.S., 2015. Study of the influence of supplementary cementitious materials on the durability properties of concrete. Ph.D thesis, IIT Madras, India.

Eren, O. & Marar, K., 2010. Effect of steel fibres on plastic shrinkage cracking of normal and high strength concretes. Materials Research, 13(2), pp. 135-141.

Fattuhi, N. I., 1986. Curing compounds for fresh and hardened concrete. Building and environment, 21(2), pp. 119-125.

Filho, R.D. & Sanjuan, M.A., 1999. Effect of low modulus sisal and polypropylene fibre on the free and restrained shrinkage of mortars at early age. Cement and Concrete Research, 29(10), pp. 1597–604.

Folliard, K.J.& Berke, N.S., 1997. Properties of high-performance concrete containing shrinkage-reducing admixture. Cement and Concrete Research, 27(9), pp. 1357–1364.

Gettu, R. & Roncero, J., 2005. On the long-term response of concrete with a shrinkage reducing admixture. In: R.K. Dhir, P.C. Hewlett and M.D. Newlands (Eds.), Admixtures – Enhancing Concrete Performance (Proc. Intl. Conf., Dundee, UK), Thomas Telford, London, pp. 209–216.

Ghoddousi, P., Raiss, A.M. & Parhizkar, T., 2007. A comparison between plastic shrinkage of concrete containing silica fume and the normal concrete. International Journal of Civil Engineering, 5(4), pp.266–273.

Gupta, R., Banthia, N. & Dyer, P., 2006. Field application and monitoring of crack resistant fibre-reinforced concrete overlays. ACI Spring 2006 and Fall 2006 Conventions, pp. 123–137.

He, X.& Peng, D., 2011. Experimental study on crack resistance property of fresh polypropylene fibre concrete. Internal Conference on Multimedia Technology, Hangzhou, China, pp. 1064-1069.

- Hover, K.C., 2006. Evaporation of Water from Concrete Surfaces. *ACI Materials Journal*, 103(5), pp.384–389.
- Indian Standard Designation, IS 10262-2009, Concrete mix proportioning-Guidelines, Bureau of Indian Standards, New Delhi, India.
- Indian Standard Designation, IS 12269-1987, Specification for 53 grade ordinary portland cement, Bureau of Indian Standards, New Delhi, India.
- Indian Standard Designation, IS 1489 Part 1-1991, Portland pozzolana cement-Specification, Bureau of Indian Standards, New Delhi, India.
- Indian Standard Designation, IS 3812-1981, Specification for flyash for use as pozzolana and admixture, Bureau of Indian Standards, New Delhi, India.
- Indian Standard Designation, IS 383-1970, Specification for coarse and fine aggregate from natural source for concrete, Bureau of Indian Standards, New Delhi, India.
- Indian Standard Designation, IS 455-1989, Portland slag cement-Specification, Bureau of Indian Standards, New Delhi, India.
- Indian Standard Designation, IS 516-1959, Methods of tests for strength of concrete, Bureau of Indian Standards, New Delhi, India.
- Indian Standard Designation, IS 8142-1976, Method of test for determining setting time of concrete by penetration resistance, Bureau of Indian Standards, New Delhi, India.
- Indian Road Congress Special Publication, IRC SP: 62-2014, Guidelines for design and construction of cement concrete pavements for low volume roads, New Delhi, India.
- Jiang, C., Fan, K., Wu, F. & Chen, D., 2014. Experimental study on the mechanical properties and microstructure of chopped basalt fibre reinforced concrete. *Materials and Design*, 58, pp. 187–193.
- Japan Society of Civil Engineers Designation, JSCE SF4-1984, Method of tests for flexural strength and flexural toughness of steel fibre reinforced concrete, Japan.
- Johari, M.A., Brooks, J.J., Kabir, S. & Rivard, P., 2011. Influence of supplementary cementitious materials on engineering properties of high strength concrete. *Construction and Building Materials*, 25(5), pp. 2639–2648.
- Kraai, P.P., 1985. A proposed test to determine the cracking potential due to drying shrinkage of concrete. *Concrete Construction*, 30(9), pp. 775-778.

- Leemann, A., Nygaard, P. & Lura, P., 2014. Impact of admixtures on the plastic shrinkage cracking of self-compacting concrete. *Cement and Concrete Composites*, 46, pp. 1–7.
- Leitch, W., 1957. Plastic shrinkage. *ACI Journal Proceedings*, 28(8), pp. 797–802.
- Lura, P., Mazzotta, G.B., Rajabipour, F., & Weiss J., 2006. Evaporation, settlement, temperature evolution, and development of plastic shrinkage cracks in mortars with shrinkage-reducing admixtures. In: *Proceedings of the international RILEM-JCI seminar on concrete durability and service life planning (ConcreteLife006)*, Ein-Bokek, Israel, pp. 203–213.
- Lura, P., Pease, B.J., Mazzotta, G., Rajabipour, F., & Weiss, J., 2007. Influence of shrinkage-reducing admixtures on development of plastic shrinkage cracks. *ACI Materials Journal*, 104(2), pp. 187–194.
- Mangat, P.S. & Azari, M.M., 1990. Plastic shrinkage of steel fibre reinforced concrete. *Materials and structures*, 23, pp. 186-195.
- Marthong, C. & Agarwal, T.P., 2012. Effect of flyash additive on concrete properties. *International Journal of Engineering Research and Applications*, 2(4), pp. 1986-1991.
- Maslehuddin, M., Ibrahim, M., Shameem, M., Ali, M.R. & Al-Mehthel, M.H., 2013. Effect of curing methods on shrinkage and corrosion resistance of concrete. *Construction and Building Materials*, 41, pp. 634-641.
- Mehta, P.K. & Monteiro, P.J.M., 2006. *Concrete – microstructure, properties, and materials*. 3rd ed. New York: McGraw-Hill, 659 p.
- Menzel, C.A., 1954. Causes and prevention of crack development in plastic concrete. *Proceedings of the Portland Cement Association, Annual Meeting*, pp. 130-136.
- Mittal, A., Kaisare, M.B. & Shetty, R., 2005. Experimental study on use of fly ash in concrete, Tarapur Atomic Power Project 3&4, Nuclear Power Corporation of India Ltd.
- Mora-Ruacho, J., Martín, M.A., Gettu, R. & Aguado, A., 2000. Study of plastic shrinkage cracking in concrete and the influence of fibres and a shrinkage reducing admixture, in: V.M. Malhotra (Ed.), *Proc. Fifth CANMET/ACI Intl Conf on Durability of Concrete (Barcelona, Spain), Supplementary Papers*, pp. 469–483.
- Mora, J., Gettu, R., Olazábal, C. & Martín, M.A., 2001. Study of plastic shrinkage cracking in concrete due to high rates of evaporation. *Concrete under severe conditions: environment and loading (Intl. Conf., Vancouver)*, Eds. N.Banthia, K.Sakai and O.E.Gjørsv, University of British Columbia, Vancouver, Canada, pp. 1425-1432.

- Mora, J., Gettu, R., Olazábal, C., Martín, M.A. & Aguado, A., 2002. Effect of the incorporation of fibres on the plastic shrinkage of concrete. *Sendero (Chihuahua, Mexico)*, No. 2, pp. 22-34.
- Mora, J., Aguado, A. & Gettu, R., 2003. The influence of shrinkage reducing admixtures on plastic shrinkage. *Materials and Construction*, 53(271-272), pp. 71-80.
- Mora-Ruacho, J., Gettu, R. & Aguado, A., 2009. Influence of shrinkage-reducing admixtures on the reduction of plastic shrinkage cracking in concrete. *Cement and Concrete Research*, 39(3), pp. 141–146.
- Naaman, A.E., Wongtanakitcharoen, T. & Hauser, G., 2005. Influence of different fibres on plastic shrinkage cracking of concrete. *Cement and Concrete Research*, 36(7), pp. 1263–1267.
- Nabil, B., Aissa, A. & Aguida, B.I., 2011. Use of a new approach (design of experiments method) to study different procedures to avoid plastic shrinkage cracking of concrete in hot climates. *Journal of Advanced Concrete Technology*, 9(2), pp. 149-157.
- Nahata, Y., Kholia, N. & Tank, T.G., 2014. Effect of Curing Methods on Efficiency of Curing of Cement Mortar. *APCBEE Procedia* 9, pp. 222-229.
- Najm, H. & Balaguru, P., 2003. Effect of Large-Diameter Polymeric Fibres on Shrinkage Cracking of Cement Composites. *ACI Materilas Journal*, 99(4), pp. 345–351.
- Newlands, M.D., Paine, K.A., Vemuri, N.A. & Dhir, R.K., 2008. A linear test method for determining early-age shrinkage of concrete. *Magazine of Concrete Research*, 60(10), pp. 747-757.
- Padron, I. & Zollo, R. F., 1990. Effect of synthetic fibres on volume stability and cracking of portland cement concrete and mortar. *ACI Materials Journal*, 87(4), pp. 327-332.
- Paillere, A. M., Buil, M. & Serrano, J. J., 1989. Effect of fibre addition on the autogeneous shrinkage of silica fume concrete. *ACI Materials Journal*, 86(2), pp. 139-144.
- Pelisser, F., Santos Neto, A.B.S., Rovere, H.L. & Pinto, R.C.A., 2010. Effect of the addition of synthetic fibres to concrete thin slabs on plastic shrinkage cracking. *Construction and Building Materials*, 24(11), pp. 2171–2176.
- Peyton, S., 2006. Curing practices to reduce plastic shrinkage in concrete bridge decks. MS thesis, University of Arkansas, USA.

- Powers, T.C., 1960. Physical properties of cement paste and concrete. Proceedings of the Fourth International Symposium on the Chemistry of Cement, Washington, D.C., pp. 577-608.
- Qi, C., Weiss, J. & Olek, J., 2003. Characterization of plastic shrinkage cracking in fibre reinforced concrete using image analysis and a modified Weibull function. *Materials and Structures*, 36(260), pp. 386–395.
- Qi, C., 2003. Quantitative assessment of plastic shrinkage cracking and its impact on the corrosion of steel reinforcement. Ph.D. thesis, Purdue University, USA.
- Qi, C., Weiss, J. & Olek, J., 2005. Assessing the settlement of fresh concrete using a non-contact laser profiling approach. International Conference on Construction Materials: ConMat'05, Vancouver, Canada.
- Qiang, W., Peiyu, Y., Jianwei, Y. & Bo, Z., 2013. Influence of steel slag on mechanical properties and durability of concrete. *Construction and Building Materials*, 47, pp. 1414–1420.
- Quangphu, N., Linhua, J., Jiaping, L., Qian, T. & Tienquan, D., 2008. Influence of shrinkage-reducing admixture on drying shrinkage and mechanical properties of high-performance concrete. *Water Science and Engineering*, 1(4), pp. 67-74.
- Rajabipour, F., Sant, G. & Weiss, J., 2008. Interactions between shrinkage reducing admixtures (SRA) and cement paste's pore solution. *Cement and Concrete Research*, 38, pp. 606–615.
- Roncero, J., Gettu, R., & Martín, M.A., 2003. Evaluation of the influence of a shrinkage reducing admixture on the microstructure and long-term behavior of concrete, in: V.M. Malhotra (Ed.), Proc. Seventh CANMET/ACI Intl. Conf. on Superplasticizers and Other Chemical Admixtures in Concrete (Berlin), Supplementary papers, pp. 207–226.
- Rongbing, B. & Jian, S., 2005. Synthesis and evaluation of shrinkage-reducing admixture for cementitious materials. *Cement and Concrete Research*, 35(3), pp. 445–448.
- Saliba, J., Rozière, E., Grondin, F. & Loukili, A., 2011. Influence of shrinkage-reducing admixtures on plastic and long-term shrinkage. *Cement and Concrete Composites*, 33(2), pp.209–217.
- Samman, T.A., Mirza, W.H. & Wafa, F.F., 1996. Plastic shrinkage cracking of normal and high-strength concrete: a comparative study. *ACI Materials Journal*, 93(1), pp. 36–40.
- Sanjuán, M.A. & Moragues, A., 1994. A testing method for measuring plastic shrinkage in polypropylene fibre reinforced mortars. *Materials Letters* 21, pp. 239–246.

- Sanjuán, M.A. & Moragues, A., 1997. Polypropylene-fibre-reinforced mortar mixes: optimization to control plastic shrinkage. *Composites Science and Technology*, 51, pp. 655-660.
- Shaeles, C. A. & Hover, K.C., 1988. Influence of mix proportions and construction operations on plastic shrinkage cracking in thin slabs. *ACI Materials Journal*, 85(6), pp.495–504.
- Shah, S.P., Karaguler, M.E. & Sarigaphuti, M., 1993. Effects of Shrinkage-Reducing Admixtures on Restrained Shrinkage Cracking of Concrete. *ACI Materials Journal*, 89(3), pp. 289–295.
- Siddique, R., 2004. Performance characteristics of high-volume Class F fly ash concrete. *Cement and Concrete Research*, 34, pp. 487 – 493
- Siddique, R. & Bennacer, R., 2012. Use of iron and steel industry by-product (GGBS) in cement paste and mortar. *Resources, Conservation and Recycling*, 69, pp. 29-34.
- Sivakumar, A. & Santhanam, M., 2007. A quantitative study on the plastic shrinkage cracking in high strength hybrid fibre reinforced concrete. *Cement and Concrete Composites*, 29(7), pp.575–581.
- Slowik, V., Schmidt, M. & Fritzsich, R., 2008. Capillary pressure in fresh cement-based materials and identification of the air entry value. *Cement and Concrete Composites*, 30(7), pp. 557–565.
- Soroushian, P., Mirza, F. & Alhozaimy, A., 1995. Plastic Shrinkage Cracking of Polypropylene Fibre Reinforced Concrete. *ACI Materials Journal*, 92(5), pp. 553–560.
- Soroushian, P. & Ravanbakhsh, S., 1999. Control of plastic shrinkage cracking with specialty cellulose fibres, *ACI Materials Journal*, 95(4), pp. 429–435.
- Söylev, T.A. & Özturan, T., 2014. Durability, physical and mechanical properties of fibre-reinforced concretes at low-volume fraction. *Construction and Building Materials*, 73, pp. 67–75
- Turcry, P. & Loukili, A., 2006. A evaluation of plastic shrinkage cracking of self-consolidating concrete. *ACI Materials Journal*, 103(4), pp. 272–279.
- Uno, P.J., 1998. Plastic shrinkage cracking and evaporation formulas. *ACI Materials Journal*, 95(4), pp.365–375.
- U.S. Department of Transportation, Guide for curing of cement concrete pavements-2006, Georgetown Pike, USA.
- Wang, K., Shah, S.P. & Phuaksuk, P., 2002. Plastic shrinkage cracking in concrete materials – Influence of fly ash and fibres. *ACI Materials Journal*, 98(6), pp. 458–464.

- Weiss, J., Shah, S.P. & Yang, W., 1998. Shrinkage cracking of restrained concrete slabs. *Journal of Engineering Mechanics*, 124(7), pp.765–774.
- Weyers, R.E., Conway, J.C. & Cady, P.D., 1982. Photoelastic analysis of rigid inclusions in fresh concrete. *Cement and Concrete Research*, 12(4), pp. 475–484.
- Wittmann, F.H., 1976. On the action of capillary pressure on fresh concrete. *Cement and Concrete Research*, 6(1), pp. 49–56.
- Wongtanakitcharoen, T., 2005. Effect of randomly distributed fibres on plastic shrinkage cracking of cement composites. Ph.D. thesis, University of Michigan, USA.
- Wongtanakitcharoen, T. & Naaman, A.E., 2006. Unrestrained early age shrinkage of concrete with polypropylene, PVA, and carbon fibres. *Materials and Structures*, 40(3), pp. 289–300.
- Xie, X.S., Tian, F. & Hong, Y.H., 2011. Experimental investigation into the impact of polypropylene fibres and SRA on the early crack resistance of concrete. *Advanced Materials Research*, 194-196, pp. 858–864.
- Yokoyama, K., Hiraishi, S., Kasai, Y. & Kishitani, K., 1996. Experimental study of shrinkage and cracking of flowing concrete at early ages, *JCA Proc. Cem. Concr.* 50, pp. 588–593.

## **APPENDIX A**

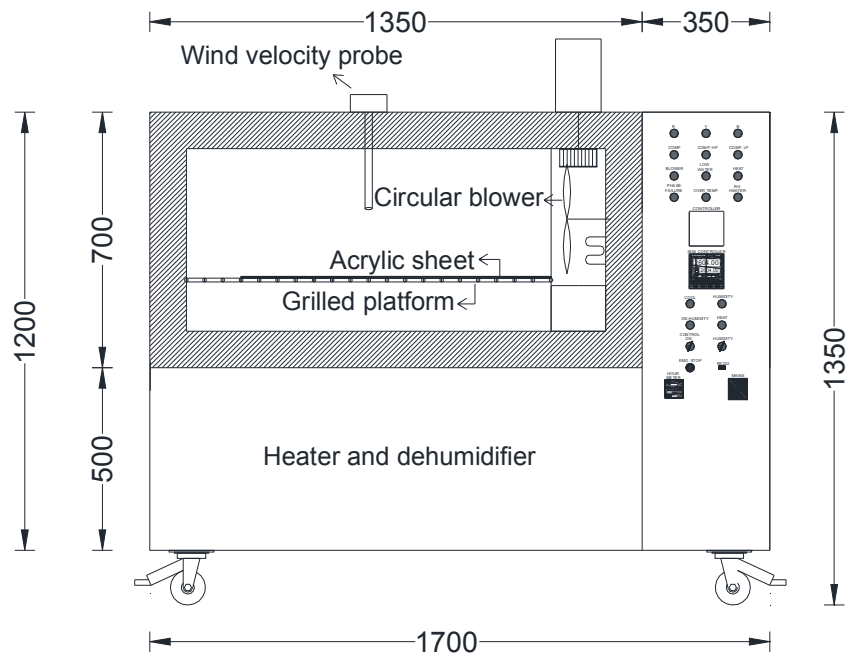
### **DESIGN AND PERFORMANCE ASSESSMENT OF THE ENVIRONMENTAL CHAMBER**

#### **A.1. Introduction**

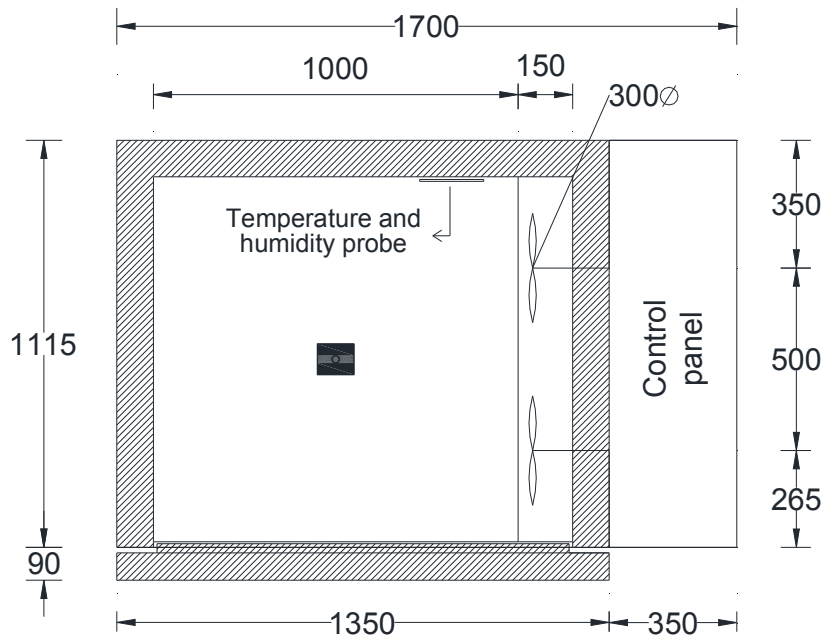
An environmental chamber was specially designed as per the guidelines in the standard ASTM C-1579 to stimulate specific environmental conditions with high evaporation that is conducive to initiate plastic shrinkage cracking. The technical specifications, design, problems encountered as well as the performance of the environmental chamber are presented in this appendix.

#### **A.2. First design of the climatic chamber**

The schematic design of the environmental chamber is shown in the Figure A.1 while the technical specifications are provided in Table A.1. The environmental chamber is specially designed for conditioning 500 litres of volume space, to the programmed temperature, relative humidity and air velocity values with highly reliable accuracy and control. Temperature and relative humidity are electrically controlled by a heating system, refrigeration unit and humidifier system. Air is continuously circulated in the chamber to monitor the comparison of the set values and the air is treated if necessary. The two circular blowers can be set at variable speeds for an equivalent air speed over the surface of the specimen. In addition the chamber is equipped with sensors to accurately measure the temperature, relative humidity and air velocity that prevail in the chamber. The current values including the set values are displayed in the control panel. The conditioned volume space creates ideal conditions to expose the sample and test its performance at different climatic conditions.



FRONT VIEW



TOP VIEW

Figure A.1 Schematic layout of the first design of the chamber

Table A.1 Specifications of environmental chamber

Dimensions (internal)	1000 × 1000 × 500 mm
Temperature range	Ambient to +50°C
Humidity range	30% RH to 60% RH
Air Velocity Range	2 to 5 m/s
Temperature measurement accuracy	+/- 0.1°C
Humidity measurement accuracy	+/- 1%
Air Velocity measurement accuracy	+/- 0.3 m/s
Heating system	Inconel sheathed type heating element was used
Refrigeration Unit	Single stage Copeland air cooled condenser system with compressor, condensing unit, and CFC free refrigeration gas were used
Humidifier system	Air atomizers for humidification of the entire chamber, warm water vapour generator with heating system, over-heat safety system, vapour storage tank with blowing system were used in the chamber Dry air compressor of 3-4bar pressure was used for precise low humidity control
Construction	The chamber exterior was fabricated from 16SWG MS powder coated material and the interior with a 16SWG SS304

### A.3. Problems encountered with the first design

After the chamber was designed as per the specifications, the performance of the chamber was assessed by measuring the temperature, relative humidity and air velocity using a Digital Air/Temp/ RH Meter (see Figure A.2). The temperature and relative humidity were precisely maintained to the set values on the other hand air velocities were not uniform and varied significantly at a particular position. Hence, the non-uniformity or turbulence of the air flow in the chamber was the main problem encountered after the first design. Since the blowers were circular, the ascending conical front of air from blowers were over lapping at the center of the chamber and there was no clear defined path of air flow at the corners (blow side) of the chamber as illustrated in Figure A.3. The overlapping of the air fronts led to the non-uniformity of the air flow in the chamber.

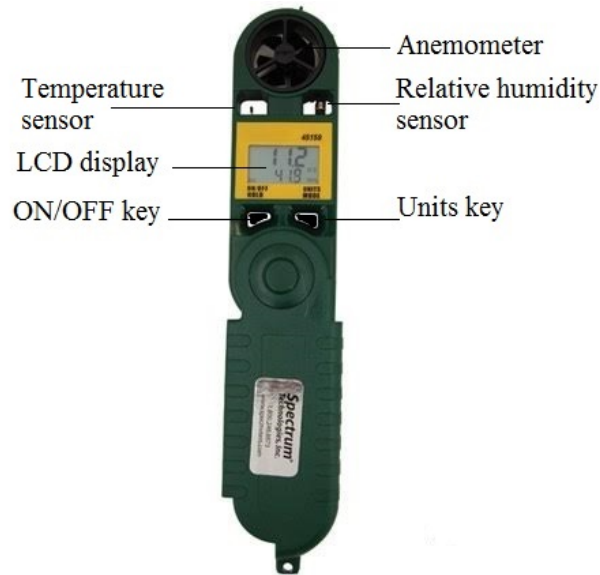


Figure A.2 Digital Air/Temp/ RH Meter

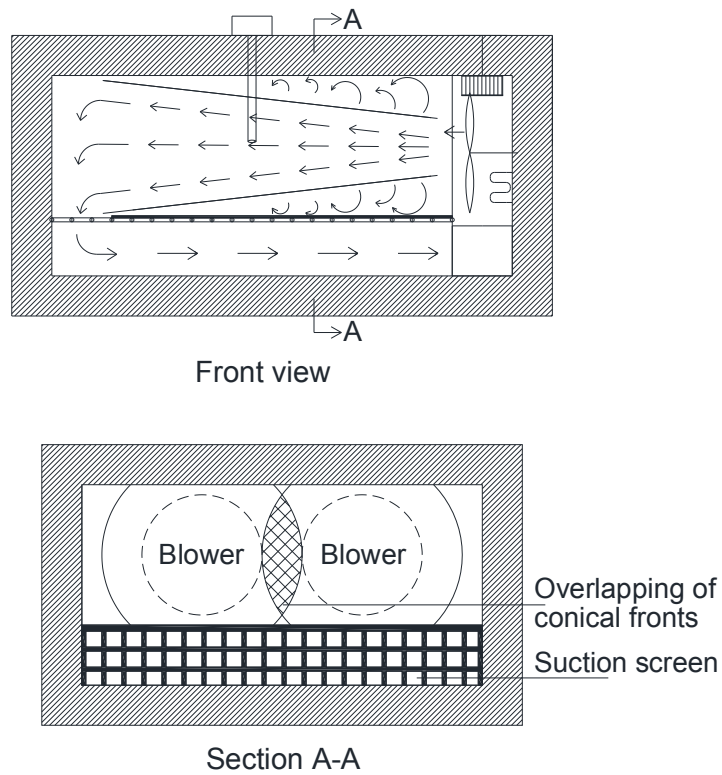


Figure A.3 Air flow pattern

#### A.4. Modified design of the chamber

To achieve the uniform circulation of air over the specimen and in the chamber, the circular blower was replaced with a horizontal blower. For the modification of the

chamber, additional work space was occupied and the internal dimensions reduced to 770×1000×500 mm. The modified layout of the chamber is shown in the Figure A.4. After the modification, the air flow was laminar and the air velocities were reasonably similar.

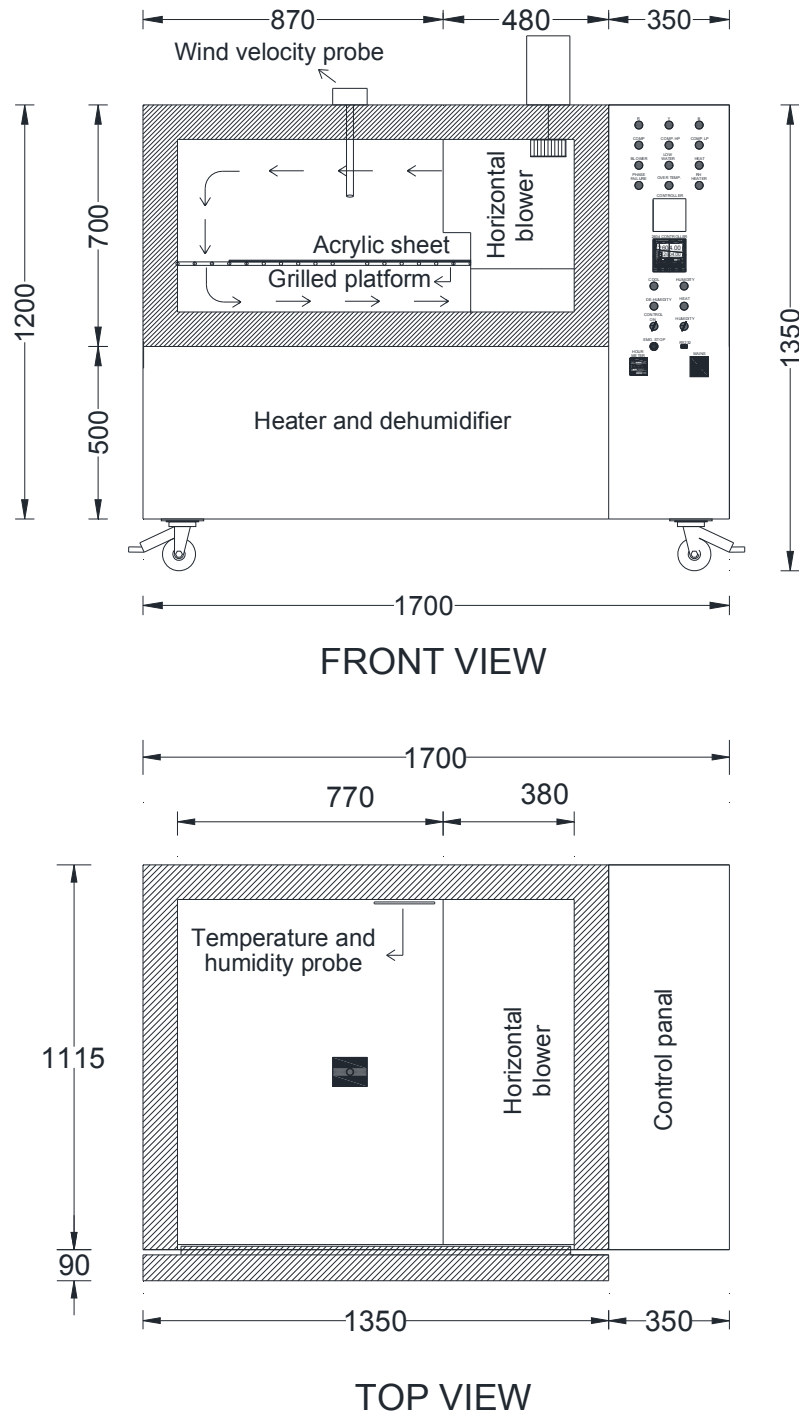


Figure A.4 Modified layout of the chamber

### A.5. Performance evaluation of the chamber

To assess the performance of the chamber, 12 different positions (see Figure A.5) were selected in the chamber and the temperature, relative humidity and air velocity were measured using the Digital Air/Temp/ RH Meter. Out of 12 positions selected, 6 positions were on the blow side and the rest on the suction side. Evaporation rate of the water was also monitored at these places using a circular pan of 220 mm diameter. On the blow side, the positions were selected such that the surface of the monitoring pan exactly represents the surface of the specimen. For achieving this, pans were placed at a height of 120 mm so that the surface of the pans will be at a height of 160 mm, which is the height of the plastic shrinkage mould. While on the suction side the position was at the surface of the chamber. The temperature, relative humidity and the air velocity at which the chamber was evaluated for its performance were 42°C, 40% and 4 m/s, respectively. All the parameters measured at these positions are shown in Table A.2.

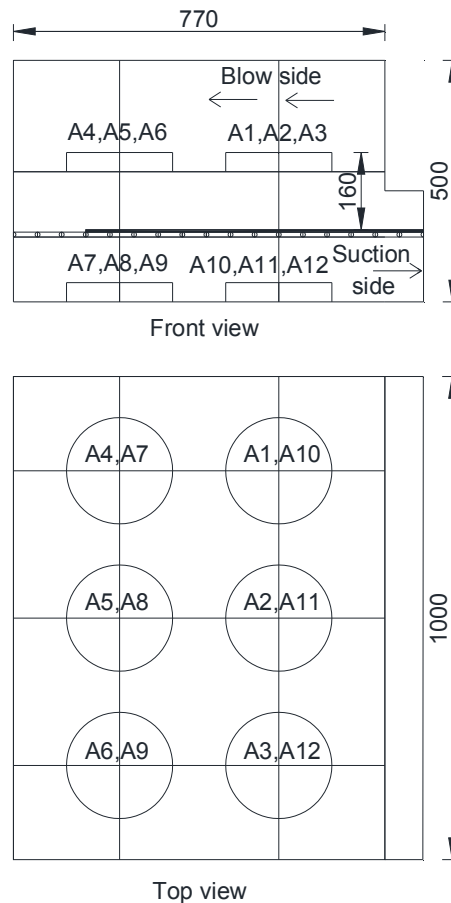


Figure A.5 Positions selected for the evaluation

Table A.2 Summary of the measured parameters

Position	Temperature (°C)	Relative humidity (%)	Air velocity (m/s)	Evaporation rate (kg/hr/m <sup>2</sup> )
A1	41.9	40.8	3.6	0.82
A2	41.8	40.0	3.5	0.81
A3	41.9	39.9	3.6	0.85
A4	42.2	41.1	3.3	0.80
A5	41.8	39.8	3.2	0.78
A6	41.8	40.0	3.1	0.77
A7	42.1	41.2	2.9	0.74
A8	41.9	41.8	2.8	0.73
A9	42.0	40.1	2.8	0.72
A10	41.8	39.6	2.7	0.70
A11	41.9	40.9	2.8	0.69
A12	42.1	41.0	2.6	0.68

It can be seen that the temperature and relative humidity were precisely maintained and were in the range of  $42\pm 0.2^{\circ}\text{C}$  and  $40\pm 2\%$ , respectively. The air velocity at the blow side (A1, A2 and A3) was  $3.5\pm 0.2$  m/s and gradually decreased to  $2.6\pm 0.2$  m/s at the suction side (A10, A11 and A12). This was due to the flow of air from the high pressure side (blow side) to the low pressure side (suction side). The rate of evaporation was in the range of  $0.75\pm 0.1$  kg/hr/m<sup>2</sup>.